

EFFECTIVE STRESS PATHS IN A SENSITIVE CLAY

by

PETER MICHAEL BYRNE

B. E., University College Dublin, Ireland, 1959

A THESIS SUBMITTED IN PARTIAL FULFILMENT OF
THE REQUIREMENTS FOR THE DEGREE OF

M. A. Sc.

in the Department

of

Civil Engineering

We accept this thesis as conforming to the
required standard

THE UNIVERSITY OF BRITISH COLUMBIA

April, 1966

In presenting this thesis in partial fulfilment of the requirements for an advanced degree at the University of British Columbia, I agree that the Library shall make it freely available for reference and study. I further agree that permission for extensive copying of this thesis for scholarly purposes may be granted by the Head of my Department or by his representatives. It is understood that copying or publication of this thesis for financial gain shall not be allowed without my written permission.

Department of Civil Engineering

The University of British Columbia
Vancouver 8, Canada

Date May 12, 1966

ABSTRACT

Results of drained and undrained triaxial compressions tests on a sensitive clay are presented in this thesis. Contours of water content from both drained and undrained tests are compared, and it appears that for the clay tested, there is not a unique relationship between effective stresses and water content as found by Rendulic and Henkel for remolded soil. The Roscoe concept of a state boundary surface, which is similar to the Rendulic concept is examined, and it also does not hold for the clay tested.

The Roscoe energy equation is applied to the results of all tests and it appears to hold quite well. It indicates that for a soil which is yielding there is only one fundamental strength parameter, M , which is independent of both strain and strain rate.

Methods of predicting stress-strain relationships are examined. The Roscoe method, which is based on the existence of a state boundary surface is not strictly applicable, but does yield results which are of the same order as the measured relationships. The Landanyi method does not appear to apply to the clay tested.

A method for predicting residual pore pressures and or permeability in drained triaxial tests is derived. This enabled allowances to be made for the effect of residual pore pressures in drained tests. However, it is felt that the method may have more application in the examination of soil structure, since a comparison of the permeability of samples at the same void ratio and temperature yields a measure of structural difference.

TABLE OF CONTENTS

		PAGE
CHAPTER 1	INTRODUCTION	1
	1.1 Purpose	1
	1.2 Scope	2
CHAPTER 2	REVIEW OF LITERATURE	4
	2.1 Review of Literature	4
	2.2 Discussion	21
CHAPTER 3	MACROSCOPIC COMPONENTS OF SHEAR STRENGTH	24
CHAPTER 4	TESTING PROCEDURES	30
	4.1 Description of soil tested	30
	4.2 Field sampling and storing of block samples	35
	4.3 Description of test equipment	35
	4.4 Testing technique	47
CHAPTER 5	DISCUSSION OF TESTING TECHNIQUE	56
	5.1 Introduction	56
	5.2 Non-uniform stress and strain	56
	5.3 Non-uniform pore pressures in undrained tests	59
	5.4 Residual pore pressures in drained tests	61
	5.5 Pore pressure measuring devices	62
	5.6 Rate of testing	64
	5.7 Pore pressures resulting from secondary effects	67
	5.8 Membrane leakage	70
	5.9 Ram Friction	71
CHAPTER 6	RESIDUAL PORE PRESSURES IN DRAINED TESTS	73
	6.1 Introduction	73

	PAGE
CHAPTER 6.2 Method 1	75
6.3 Method 2	76
CHAPTER 7 TEST RESULTS	85
7.1 Introduction	85
7.2 Characteristics of Haney clay	86
7.3 Comparison of contours of water content from drained and undrained tests	96
7.4 Energy corrections	107
7.5 Examination of methods for predicting stress-strain relations	115
7.6 Effect of strain rate on drained tests	122
CHAPTER 8 CONCLUSIONS AND SUGGESTIONS FOR FURTHER RESEARCH	125
8.1 Conclusions	125
8.2 Suggestions for further research	126
LIST OF SYMBOLS	128
LIST OF REFERENCES	131
APPENDIX I	135
APPENDIX II	142

LIST OF TABLES

		PAGE
TABLE I	PHYSICAL PROPERTIES OF HANEY CLAY	31
TABLE II	CHEMICAL PROPERTIES OF HANEY CLAY	34

LIST OF FIGURES

Figure		Page
1.	Rendulic Graphical Representation of Stresses in Triaxial Tests	5
2.	Contours of Water Content for Normally Consolidated London Clay	8
3.	Stress Water Content Relations for Normally Consolidated Weald Clay	10
4.	Roscoe et al. Yield Surface	12
5.	Roscoe et al. energy balance	16
6.	Method of Determining Stress-Strain Relationships for Kaolin	18
7.	Strength Parameters	26
8.	Grain Size Distribution Curve for Haney Clay	32
9.	Standard Consolidation curve for Haney Clay	33
10.	Block Samples of Haney Clay at Site	36
11.	Triaxial Cell and Chamber Pressure System	37
12.	Drainage and Pore Pressure Measuring System	38
13.	Test Equipment	39
14.	Sample Trimming Equipment	48
15.	Sample in Place on Triaxial Base	48
16.	Sample During Shear	53
17.	Build-Up in Pore Pressure After Consolidation Haney Clay	69
18.	Illustration of Method for Determining Drainage Rate During Shearing	79
19.	Relationship Between Void Ratio and Permeability During Drained Shearing of Haney Clay	80
20.	Relationship Between Measured Residual Pore Pressure and Shear Strain in Drained Tests	82
21.	Comparison of Measured and Calculated Residual Pore Pressures in Drained Tests	82

Figure		Page
22.	Relationship Between Water Content and Logarithm of Isotropic Consolidation Pressure, Haney Clay	87
23.	Relationship Between Undrained Strength and Isotropic Consolidation Pressure, Haney Clay	89
24.	Stress-Strain Relationships for Undrained Tests on Haney Clay	91
25.	Principal Stress Ratio Versus Strain for Undrained Tests on Haney Clay	91
26.	Relationship Between Pore Pressure and Strain for Undrained Tests on Haney Clay	92
27.	Pore Pressure Parameter A Versus Strain for Haney Clay	92
28.	Stress-Strain Relationships for Drained Tests on Haney Clay	94
29.	Calculated Residual Pore Pressure Vs. Strain for Consolidated Drained Tests on Haney Clay	95
30.	Effect of Residual Excess Pore Pressure on the Principal Stress Ratio Vs. Shear Strain Relation, Test S-13	97
31.	Relationships Between Principal Stress Ratio and Strain from Drained Tests on Haney Clay	97
32.	Comparison of Principal Stress Ratio Vs. Strain Relationships from Drained and Undrained Tests on Haney Clay	98
33.	Comparison of Contours of Water Content from Drained and Undrained Tests on Haney Clay	99
34.	Effective Stress Paths from Consolidated Undrained Tests on Haney Clay	100
35.	Effective Stress Paths and Contours of Water Content from Drained Tests	101
36.	State Boundary Surface from Undrained Tests on Haney Clay (Burland Plot)	104
37.	State Boundary Surface from Drained Tests on Haney Clay (Burland Plot)	105

Figure		Page
38.	Comparison of State Boundary Surfaces from Drained and Undrained Tests on Haney Clay	106
39.	Relationships Between Mean Normal Stress and Water Content for Haney Clay	109
40.	Corrected and Uncorrected Stress Paths from Undrained Tests on Haney Clay (Roscoe et al. Energy Eq.)	111
41.	Corrected and Uncorrected Stress Paths from Drained Tests on Haney Clay (Roscoe et al. Energy Eq.)	112
42.	Roscoe M Parameter Versus Strain, Haney Clay	113
43.	Contours of Water Content and Strain from Undrained Tests on Haney Clay	117
44.	Comparison of Measured and Calculated Stress-Strain Relations for Drained Tests on Haney Clay	119
45.	Comparison of Theoretical and Experimental State Boundary Surfaces (Burland Plot)	121
46.	Effect of Strain Rate on the Stress-strain Relations for Drained Tests on Haney Clay	123
47.	Effect of Strain Rate on the Principal Stress Ratio Vs. Strain Relations for Drained Tests on Haney Clay	124
48.	Effect of Strain Rate on the Water Content Vs. Strain Relations for Drained Tests on Haney Clay.	124
49.	Diagrams Showing Assumptions of Method 1	136
50.	Stress-Strain Characteristics of Haney Clay	138
51.	Relationship Between Coefficient of Consolidation and Effective Stress for Haney Clay	140

ACKNOWLEDGEMENT

The investigation reported herein has been supported by funds provided by the National Research Council of Canada. These funds also included financial support for the writer. Grateful appreciation is expressed for this assistance without which the graduate studies and this thesis could not have been accomplished.

The writer wishes to express his thanks to Dr. W. D. Liam Finn and to Professor N. D. Nathan for their guidance and constructive criticism during the preparation of this thesis.

Drained tests results were obtained by Mr. T. J. Hirst with whom the task of developing suitable test equipment was shared.

Dr. E. H. Gardner, Department of Soil Science kindly supplied data on the chemical properties of the clay tested.

The technical assistance supplied by the staff of the Civil Engineer Department is gratefully acknowledged.

CHAPTER 1

PURPOSE AND SCOPE

1.1 Purpose

Rendulic (1936, 1937) and Henkel (1958, 1959, 1960) have shown that a unique relationship exists between effective stresses and water content, or void ratio, for both drained and undrained triaxial tests on saturated remolded isotropically consolidated clay. The prime purpose of this testing program was to determine if a similar relationship exists for a sensitive undisturbed clay. A secondary purpose was to compare the behaviour of the clay with that predicted by Roscoe and Schofield (1963) for an idealized "Wet-Clay" and in particular to compare stress-strain relations.

Most problems involving the design of earth structures are concerned with either stability or settlement of a soil mass. In stability analysis, the structure is analyzed to insure that the sum of the resisting forces on any potential failure surface is greater than the sum of the driving forces. No attempt is made to determine the magnitude of the deformations. The resisting forces are determined from strength tests on the soil. It is generally agreed that for most soils, the strength in terms of effective stresses is practically independent of the type of triaxial test performed, drained or undrained. However, for sensitive soils there is some disagreement on this. The testing program was undertaken jointly by Mr. T. J. Hirst and the writer. Hirst (1966) discusses the strength envelopes obtained from drained and undrained tests.

Settlement analyses are concerned with the magnitude of

deformations. For many structures, such as foundations, it is important that these be limited. Deformations are caused by volumetric strains due to changes in void ratio and by shear strains due to distortion. If there is a unique relationship between stresses and water content or void ratio that is independent of stress path, then the volumetric strain can be calculated for any stress path which lies between a drained and undrained path. The shear strains, however, are very much dependent on stress path. Poorooshasb and Roscoe (1963) determined a relationship between volumetric and shear strains for normally loaded remolded clay and from their theory, it is possible to estimate the shear strains for any stress path. A state boundary or yield surface is a fundamental part of their theory and this only exists if there is a unique relationship between stresses and water content.

It is realized that stress-strain relations and contours of water content may be dependent on strain rate, therefore, drained and undrained tests were performed at the same rate. Additional drained tests were performed at slower rates which allowed the effect of strain rate on drained relations to be examined.

1.2 Scope

A review of pertinent literature is presented in Chapter 2. A discussion of macroscopic components of shear resistance is presented in Chapter 3. The clay tested, test equipment and testing technique are discussed in Chapters 4 and 5. Residual pore pressures of some magnitude are always present in drained tests. A method for predicting these pore pressures is presented

in Chapter 6. The results from drained and undrained triaxial compression tests on Haney clay are presented and discussed in Chapter 7. Conclusions and suggestions for further research are presented in Chapter 8.

CHAPTER 2

REVIEW OF LITERATURE

2.1 Review of Literature

Basic experimental relations between triaxial stress conditions, water content, and pore-water pressure for normally consolidated clays were first established by Rendulic (1936, 1937). He performed both drained and undrained compression and extension tests on saturated remolded Vienna clay. Test specimens were drained by a central core of sand and mica mixture, and pore-water pressures were those existing in the core. No allowance was made for the effect of the change in cross sectional area on the vertical stress, thus at large strains the vertical stresses are likely to be too high. Rendulic devised a method for comprehensive graphical representation of the state of stress for any stage in a triaxial test. Consider Figure 1a; since in the triaxial test $\sigma_2 = \sigma_3$ and $\sigma_2' = \sigma_3'$, stresses must plot on the shaded plane. To plot points on this plane the radial effective stress (σ_2' or σ_3') must first be multiplied by $\sqrt{2}$. Isotropic consolidation conditions ($\sigma_1' = \sigma_2' = \sigma_3'$) are represented by the space diagonal or line which makes equal angles with the three axes. Figure 1b shows typical consolidated drained and undrained tests plotted on this plane. Compression tests plot above the space diagonal, extension tests below. Plotted points represent different stages in a test, and the line joining these points represents the stress path followed in any one test. In an undrained test on saturated normally loaded clay, the pore pressure rises and the stress path which is also a line of constant water content is some curve as indicated.

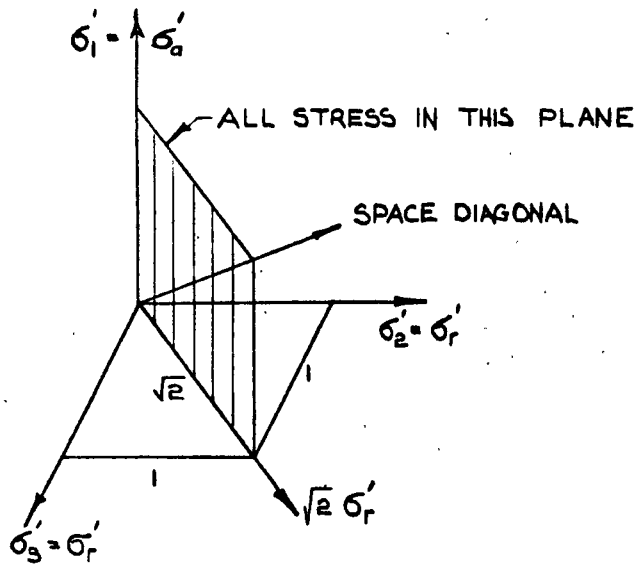


Fig. 1a.

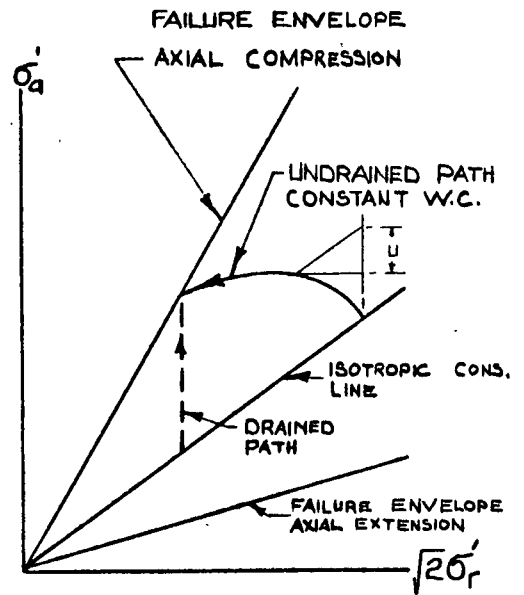


Fig. 1b

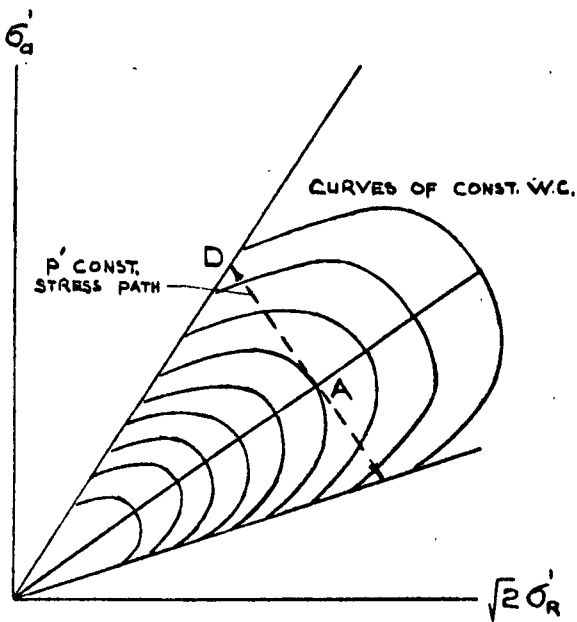


Fig. 1c

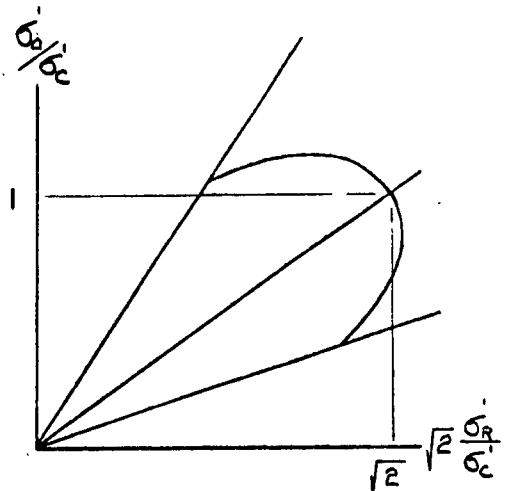


Fig. 1d

Figure 1 - Rendulic Graphical Representation of Stresses in Triaxial Tests

In a drained test the radial effective stress is constant, and thus the stress path is a vertical line. Curves of constant water content can also be obtained from drained tests where volume changes during shearing have been recorded. Contours of water content are shown in Figure 1c. The line A D which makes an angle of 90 degrees with the isotropic consolidation line and all lines parallel to it represent stress paths along which the value of the first effective stress invariant ($J_1' = \sigma_1' + \sigma_2' + \sigma_3'$) is constant. For linearly elastic material and for small strains, J_1' equal to a constant, represents a constant volume condition. It is seen that for normally loaded clay a $J_1' = \text{constant}$ stress path would cause a volume decrease.

Rendulic found fairly good agreement between contours of water content determined from drained and undrained tests, and he concluded that any point in the diagram represents a unique relation between stresses and water content that is independent of the stress path, provided the path does not cause a temporary decrease in water content. If the contours are geometrically similar, they will plot on a single curve on the unified Rendulic diagram, Figure 1d, which is obtained by dividing σ_a' and σ_r' by the effective consolidation pressure σ_c' . Rendulic found that the curves were approximately geometrically similar.

Henkel (1958, 1959, 1960) describes results of a comprehensive series of triaxial tests on saturated remolded Weald and London clays. The series included isotropically consolidated drained and undrained compression and extension tests on both normally loaded and overconsolidated samples. A few tests were performed keeping

the mean effective stress p' ($1/3 J_1'$) constant, and some samples of Weald clay were anisotropically consolidated. Henkel found that there was a unique relationship between effective stresses and water content which was independent of the stress path whether the clay was isotropically or anisotropically consolidated, provided normally loaded and overconsolidated samples were considered separately. Maximum principal stress difference was considered to be failure and he found that the failure envelope was independent of the stress path. Contours of water content from drained and undrained tests for normally consolidated London Clay are shown on the Rendulic diagram in Figure 2. It is seen that the contours are essentially independent of the effective stress path. Thus from undrained tests alone, the water content and deviator stress at failure for a drained test starting from a water content of 29.3 per cent and a consolidation pressure of 90 p.s.i. could be predicted to be 25.9 per cent and 82 p.s.i. respectively. If the average effective stress, p' , were kept constant, then starting from the same water content and pressure as before, the water content and deviator stress at failure would be 27.4 per cent and 62 p.s.i. respectively. It is seen that J_1' constant does not imply a zero volume change condition as it does for linear elastic material and that change in water content is a function of both p' and the deviator stress q .

Henkel (1960) suggests that similar relationships may also apply to undisturbed clays. However, for sensitive soils in which structure is an important factor and for clays in which the secondary compression is large, he felt that the relationship between

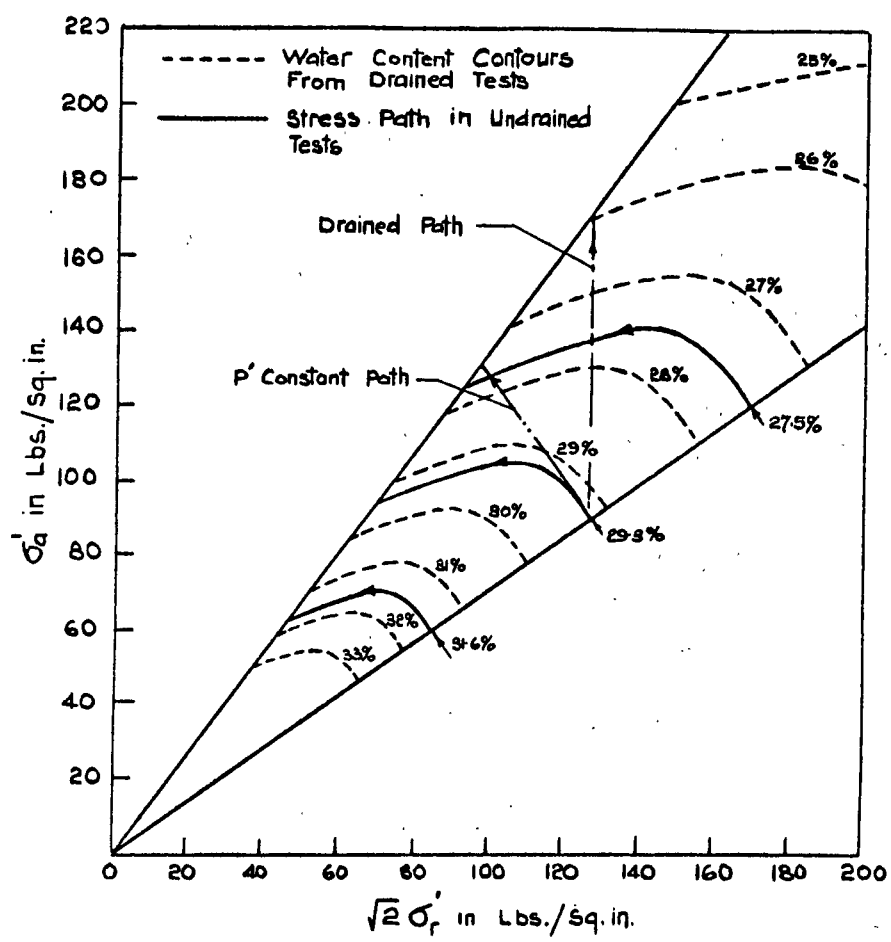


Figure 2 — Contours of Water Content for Normally Consolidated London Clay (After Henkel 1960)

stresses and water content might be more complex than that suggested for remolded soils.

Whitman, Ladd and P. da Cruz (1960) describe a series of tests on saturated remolded samples of backswamp clay from the lower Mississippi River valley. It was found that comparison of samples consolidated isotropically and anisotropically did not produce a unique relationship between stresses and water content as suggested by Henkel. For the same void ratio, the samples which were anisotropically consolidated had the higher strength, $(\sigma_1 - \sigma_3)$. The maximum principal stress ratio appeared to be the same for both.

Henkel and Sowa (1963) working with a new batch of Weald clay obtained results similar to Whitman. It was found that the water content after consolidation, whether the consolidation was isotropic or anisotropic was a function of p' only. This is shown in Figure 3. The stress paths followed for samples of the same void ratio are also shown in Figure 3 in terms of p' and q ($\sigma_a - \sigma_r$). Anisotropically consolidated samples are seen to follow a markedly different stress path and it can be seen that for the same void ratio they have a higher maximum deviator stress but that the strength envelope is the same for both. They state that the results are quite different from the data presented by Henkel (1960) on an earlier batch of weald clay using similar testing techniques.

Roscoe et al. have presented a number of papers since 1958 on the yielding of soils. They consider soil to be an elasto-plastic isotropic continuum material. Roscoe, Schofield and Wroth (1958) were primarily concerned with the establishment of a critical void ratio (C.V.R.) line. It was suggested, however, that for saturated

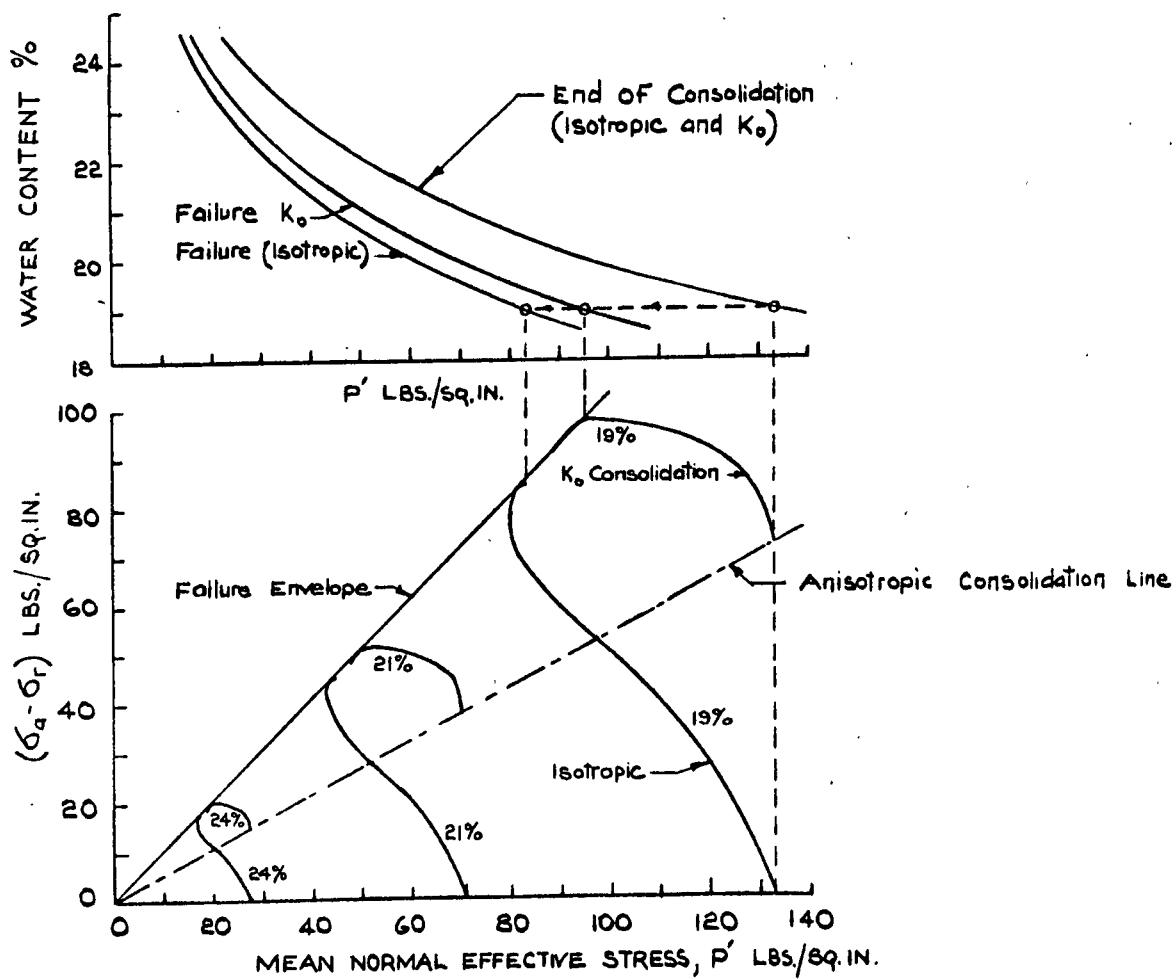


Figure 3 — Stress Water Content Relations for Normally Consolidated Weald Clay
(After Henkel and Sowa, 1963)

remolded clay tested under triaxial conditions, the envelope of all loading paths would form a unique surface in space which could be expressed in the form of an equation:

$$w = f(p', q)$$

where

w = water content

f = function of

$$p' = 1/3 (\sigma_1' + 2\sigma_3')$$

$q = (\sigma_1 - \sigma_3)$ corrected for boundary energy.

This surface is shown in Figure 4. It is seen that the envelope is comprised of two parts. Part A is a surface on which stress paths from all normally loaded samples lie throughout the shearing process whether drained or undrained. Part B applies to over-consolidated samples, and stress paths lie on this surface only at or near failure. Part A of the surface which is the portion of interest, suggests that there is a unique relation between stresses and water content which is independent of the stress path, provided that a correction for boundary energy is applied to the shear stress $(\sigma_1 - \sigma_3)$ in the case of drained tests to allow for the work done in changing volume. The corrected deviator stress was given by the following equation:

$$q = (\sigma_1 - \sigma_3) + \sigma_3' \frac{\delta V}{\delta \epsilon_1} \quad \text{---- (1)}$$

where

δV = increment of volumetric strain

$\delta \epsilon_1$ = increment of major principal strain

Poorooshasb and Roscoe (1961) presented data for normally loaded isotropically consolidated remolded samples of Weald clay

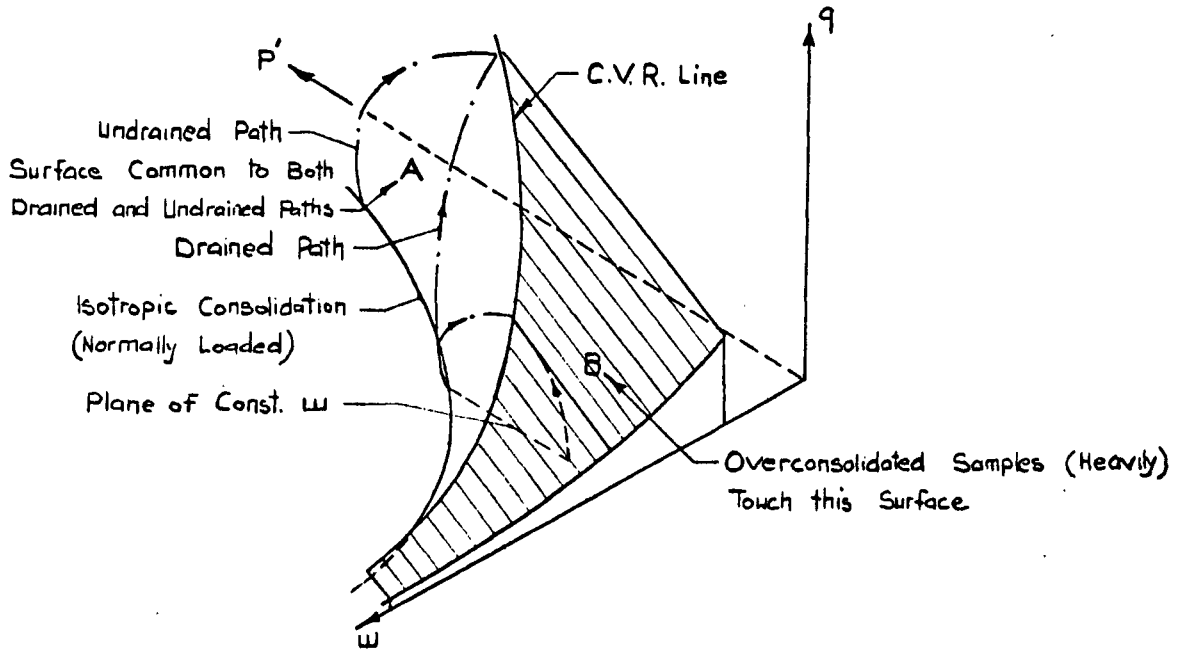


Fig. 4a — Isometric View of Roscoe et al. Yield Surface.

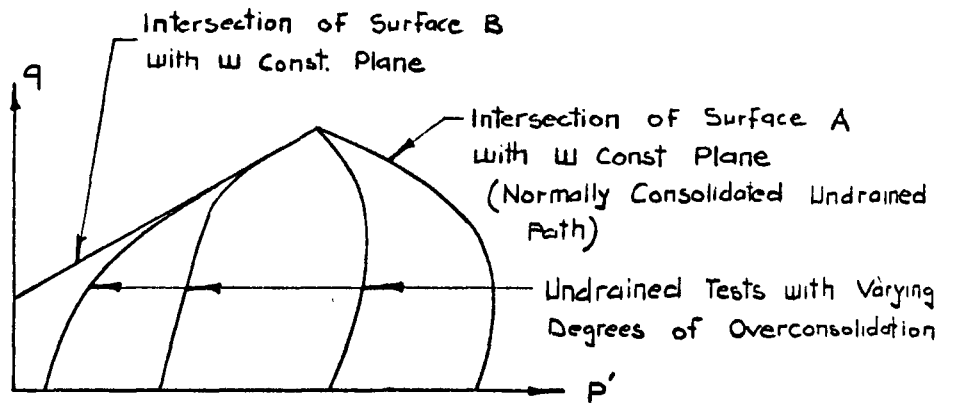


Fig. 4b — Constant w Plane.

Figure 4 — Roscoe et al. Yield Surface.

which indicated that there was a unique relation between stresses and water content provided no boundary energy correction was applied to the shear stresses. A two dimensional plot of the unique surface was devised which allowed easy comparison of drained and undrained tests.

Equation (1) above arises from the assumption that all energy transferred across the boundaries of the sample is dissipated in work done by the shear stresses. This may be reasonably true in the case of a sand. However, it is likely that in a clay, some of this energy will be stored elastically (Hvorslev 1960). Poorooshasb and Roscoe (1961) derived the following equation for the corrected deviator stress:

$$q_R = (\sigma'_1 - \sigma'_3) + (p' - r) \frac{\frac{\delta V}{\delta \epsilon_1}}{1 - \frac{\delta V}{3\delta \epsilon_1}} \quad \text{---- (2)}$$

where r is a parameter expressing a measure of the energy stored.

If $r = p'$, then all the energy is stored and $q = (\sigma'_1 - \sigma'_3)$.

If $r = 0$, then no energy is stored and

$$q = (\sigma'_1 - \sigma'_3) + \frac{p' \frac{\delta V}{\delta \epsilon_1}}{1 - \frac{\delta V}{3\delta \epsilon_1}}$$

which the authors feel should replace equation (1). It is suggested, therefore, that for normally loaded clays all energy transferred across the boundary is stored elastically and hence drained and undrained tests can be compared directly.

Roscoe and Schofield (1963) present a theory for the mechanical behaviour of an ideal continuum referred to as "Wet Clay". The following equation is derived for the state boundary surface:

$$q = \frac{Mp'}{\lambda - K} (\Gamma + \lambda - K - e - \ln p') \quad \text{---- (3)}$$

where M, λ, K, Γ are four soil constants

M = ratio of q and p' at failure

Γ = void ratio at failure for $p' = 1$

λ = slope of e vs $\ln p'$ curve for both isotropic and failure conditions

K = slope of e vs $\ln p$ curve for unloading and reloading.

$\delta \xi$ = increment of shear strain

δV = increment of volumetric strain

Equation 3 expresses the unique relationship between effective stresses and void ratio or water content.

A new energy or work equation is derived which supersedes equation (2):

$$p' \delta V + q \delta \xi = \frac{K \delta p'}{1 + e} + M p' \delta \xi \quad \text{---- (4)}$$

The terms used have already been described. The left hand side of Equation 4 expresses the energy transferred across the boundaries of a unit volume of soil subject to stresses p' and q on application of a probing stress increment $\delta p'$, δq . The terms on the right hand side express to what use this energy is put. The term $\frac{K \delta p'}{1 + e}$ represents the energy stored elastically and the term $M p' \delta \xi$ represents the energy dissipated by the shear stresses. It is assumed that no energy can be stored by the shear stresses.

Equation 4 can be rewritten as follows:

$$q_w = M p' = q + p' \frac{\delta V}{\delta \xi} - \frac{K}{1 + e} \frac{\delta p'}{\delta \xi} \quad \text{---- (5)}$$

This means that if at any stage in a drained or undrained triaxial test the deviator stress q is corrected for both energy due to

volume change and energy stored elastically, the corrected $q = q_w$ will be on the failure envelope $q = Mp'$. Figure 5 shows how these corrections would be applied to both normally loaded drained and undrained tests. In an undrained test $\delta V = 0$ and since $\delta p'$ will be negative because p' is decreasing, the elastic energy correction will add to the measured q . In a drained test the energy due to volume decrease will add to the measured q while the energy absorbed elastically will subtract.

Roscoe suggests therefore that for normally loaded remolded samples there is a unique relationship between stresses and water content provided no energy correction is applied. If an energy correction is applied in the form of equation 5, then the corrected q will lie on the failure envelope for all points of the stress path, i.e. $q_w = Mp'$.

Roscoe has also predicted stress strain relations. Poorooshasb and Roscoe (1963) presented a graphical means of determining stress strain relations for normally loaded remolded clay where the stress paths lie on the state boundary surface, which is the surface expressing the unique relation between stresses and water content (no energy corrections). Undrained tests were performed which show that for remolded spestone kaolin, contours of shear strain are radial lines. Consolidation tests were performed at different ratios of q to p' and relations between the shear strain and the volumetric strain were determined graphically. It is shown that volumetric strain also causes shear strain. The higher the ratio of q/p' the higher the shear strain for a given volumetric strain. It is stated that for any increment of applied stress the change in strain can be considered to be the sum of a change in strain at

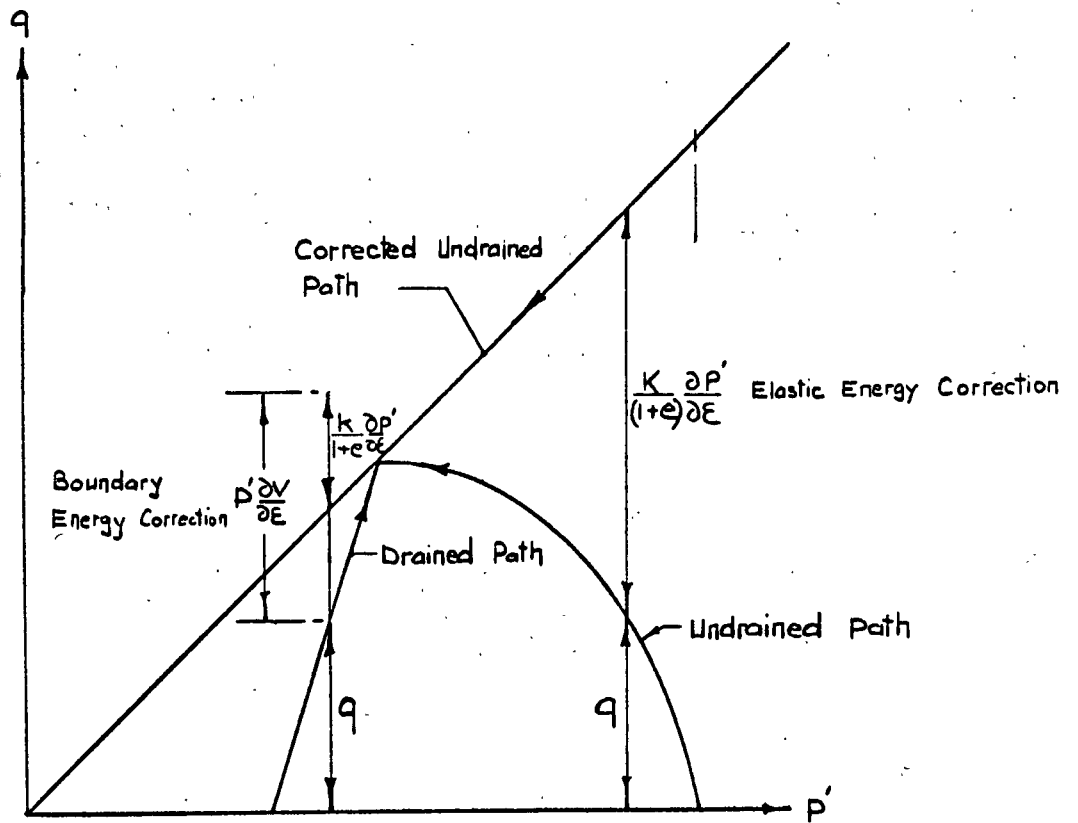


Figure 5 — Roscoe et al. Energy Balance (After Roscoe et al. '63)

constant volume, and a change in strain at constant q/p' . Thus, if the stress path is known, the applied stress can be considered to comprise of a number of stress increments and each increment can be subdivided into an increment at constant volume and an increment at constant q/p' . From the undrained tests the change in shear strain at constant volume is known, and also the change in volumetric strain due to the increment at constant q/p' . The change in shear strain due to the change in volumetric strain is determined from the results of consolidation tests. The total change in shear strain is the sum of changes at constant volume and constant q/p' . This method is shown for a stress increment AC on Figure 6.

Figure 6a shows stress paths from consolidated undrained tests on kaolin. Contours of strain at constant volume are superimposed and are seen to be radial line from the origin. Figure 6b shows the relationship between increments of shear strain and volumetric strain as a function of q/p' derived from consolidation tests. A stress increment AC can be resolved into increments AB and BC. The shear strain increments arising from these are .75 per cent at constant volume and 6.4 per cent at constant q/p' thus the total shear strain increment is 8.2 per cent. In this manner a relation between shear stress and shear strain can be obtained for any stress path.

Landanyi, La Rochelle, and Tanquay (1965) present a graphical method of predicting shear strains in saturated normally loaded and over-consolidated clays. It implies that contours of shear strain are independent of the stress path followed. Relationships between shear strain and principal stress ratio and shear strain

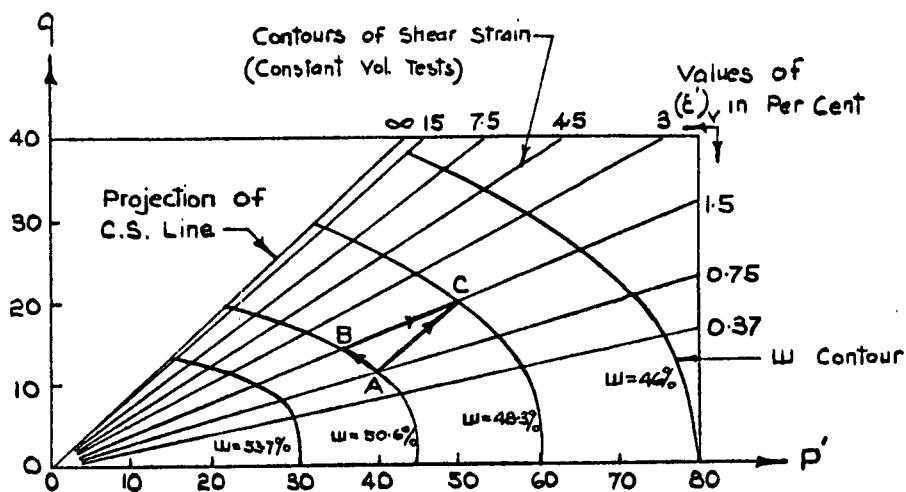


Fig. 6a Stress Paths and Contours of Strain for Constant Volume Tests on Kaolin

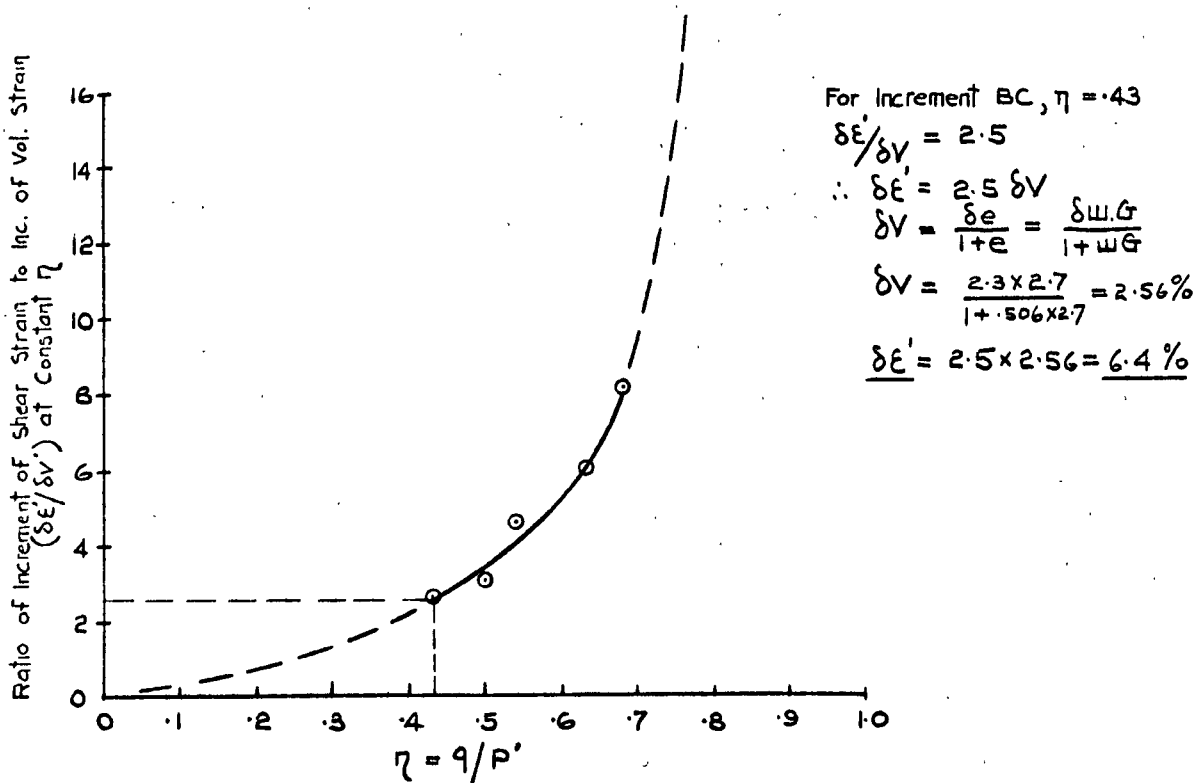


Fig. 6b Relation Between Increments of Shear and Volumetric Strains at Constant η

Figure 6 Method of Determining Stress-Strain Relationships for Kaolin
 (After Poorooshasb and Roscoe 1963)

and water content were determined from drained tests at various confining pressures. Using this information the principal stress ratio versus strain relation was predicted for an undrained test and compared with an actual test. Agreement was quite reasonable. This theory would imply that if there is a unique relation between stresses and water content that contours of shear strain are also unique.

The unique relationship between stresses and water content implies a failure envelope which is independent of stress path. Casagrande and Wilson (1953) found that for both an organic clay and for Boston Blue clay the undrained strength envelope was higher than the drained strength envelope. Maximum principal stress ratio was considered as failure. The difference amounted to 9 degrees for the organic clay and between 2 and 5 degrees for the Boston Blue clay. In an undrained test on normally loaded clay, the pore pressure rises such that the normal effective stress on the failure plane falls as shearing progresses. Thus at failure the soil could be considered to be overconsolidated. This overconsolidation is referred to as prestress effect and was considered responsible for the additional strength of the undrained tests.

The strain rate in the undrained tests was considerably higher than the drained tests and it has been argued by subsequent writers that this could account for the higher strength. However, undrained tests were performed as stress controlled and strain controlled and although the maximum deviator stress was higher for the stress controlled, the principal stress ratio was the same for both. It could therefore be implied that the strain rate affected the stress

path but not the strength envelope in terms of the principal stress ratio. Energy corrections were not considered.

Bjerrum and Simons (1960) present data from drained and undrained tests on normally loaded undisturbed clays. The sensitivity of these clays varied from 3 to 100. It was found that for almost all the Norwegian clays the pore pressure was still rising at maximum deviator stress and the maximum principal stress ratio was reached at higher strain. Kenney (1959) has suggested that this phenomenon is a function of the sensitivity of the clay. The greater the sensitivity the larger the difference in the strength envelope determined by both methods. Bjerrum and Simons found the undrained envelope to be slightly lower (about one degree) than the drained envelope, provided maximum principal stress ratio was taken as the criterion of failure. This, they state, is opposite to the findings of Casagrande and Wilson. However, the writers have corrected their drained tests for boundary energy due to volume change, whereas Casagrande and Wilson did not. They suggest that the prestress effect is of secondary importance and state that it is the overconsolidation ratio before application of the shear stresses that is important.

Barron (1960) states that the volume change occurring in drained tests causes considerably more remolding than in undrained tests. He suggested that the undisturbed drained strength envelope and the remolded undrained envelope are only slightly different and that the undisturbed undrained strength envelope is higher because of structure and prestress effect.

Scott (1963) considers that the prestress induced in the

undrained tests may or may not be important depending on the failure strain. If failure is occurring at large strains then the soil will be fully dispersed at failure and no memory of previous past pressure will remain. On the other hand, if failure occurs at low strains, as is likely with a soil initially flocculated, memory of past pressure will be retained and the soil will exhibit a prestress effect. Thus, Scott suggests that the prestress effect will be most pronounced for undisturbed soils and particularly for sensitive soils, these being highly flocculated. For compacted soils, and particularly for those soils compacted wet of optimum, with low salt concentrations in the pore fluid, the prestress effect will be of minor importance.

2.2 Discussion

It is seen that there is considerable difference of opinion both with regard to the unique failure envelope and the unique relationship between effective stresses and water content. It would appear that for normally loaded remolded material, the strength envelope is essentially independent of the stress path, and that the failure criterion, whether maximum principal stress ratio or maximum deviator stress makes little difference. The volume change at failure in the case of drained tests is generally very small or zero so that a boundary energy correction if applied, will have negligible effect on the strength envelope. For undisturbed normally loaded material and particularly for sensitive material, the maximum principal stress ratio occurs at a higher strain than the maximum deviator stress in undrained tests, leading to two possible failure envelopes. In drained tests,

maximum deviator stress and maximum principal stress ratio must occur at the same time. However, volume decrease at failure leads to a measurable boundary energy correction, and thus gives rise to two possible drained failure envelopes, i.e., one with a boundary correction and one without.

It appears that if maximum principal stress ratio is taken as the failure criterion, then drained and undrained tests have approximately the same failure envelope provided a correction for boundary energy be applied to drained tests. If no correction is applied, then the drained envelope will lie below the undrained.

Evidence for the unique relationship between effective stresses and water content is rather conflicting, but suggests that for normally loaded remolded clays which have been isotropically consolidated, the relationship is approximately true. No data on sufficiently uniform undisturbed clay is available but it has been suggested that a similar relationship might hold for undisturbed clays of low sensitivity. For sensitive clays it was thought that the relationship would be more complex.

The literature suggests that the relationship between effective stresses and water content determined from both drained and undrained tests may not be unique for any one clay for the following reasons:

1. Rate of testing not identical for both drained and undrained tests;
2. Temperature not the same for all tests;
3. Non-uniform distribution of stresses and water content due to end restraint;

4. Residual excess pore water pressure in drained tests;
5. Different structure arising from different stress paths followed in drained and undrained tests.

The effects of 1. and 2. may be eliminated by testing at the same strain rate and at constant temperature. Non-uniform stresses give rise to unequal pore pressures within undrained tests. If tests are run at sufficiently slow strain rates, these will largely become equalized by migration of water within the sample. In drained tests non-uniform stresses will give rise to non-uniform water content. This aspect will be considered in detail in Chapter 5. Residual excess pore pressures in drained tests cannot be completely eliminated, as theoretically it would take an infinite time for one hundred per cent dissipation of excess pore pressure. A method for estimating the excess pore pressure at all stages of a drained test was devised and is presented in Chapter 6. The prestress effect in undrained tests and the additional remolding effect of volume change in drained tests are macroscopic factors reflecting different microscopic structure in the clay. The macroscopic behaviour of a clay is very much dependent on the structure and this will be considered in Chapter 3.

CHAPTER 3

MACROSCOPIC COMPONENTS OF SHEAR STRENGTH

The shear strength of a saturated clay is often considered to comprise of a friction component, a cohesion component and a surface or boundary energy component. The friction component is that portion of the shear resistance which is linearly related to the normal effective stress. Cohesion implies a shear resistance which is independent of the normal effective stress. The surface energy component of shear strength arises when a soil is undergoing volume change. Taylor (1948) demonstrated that the work done by the boundary stresses during shearing could account for the difference in strength between a loose and a dense sand. Bishop (1954) calculated the energy component for triaxial conditions ($\sigma_2 = \sigma_3$) at maximum deviator stress as follows: If an element of material under stresses σ_1' and σ_3' undergoes changes in strain $\delta\varepsilon_1$ and $\delta\varepsilon_3$, then the boundary energy transferred to the sample, δW , will be

$$\delta W = \sigma_1' \delta\varepsilon_1 + 2\sigma_3' \delta\varepsilon_3$$

now $\delta V = \delta\varepsilon_1 + 2\delta\varepsilon_3 =$ volumetric strain increment, decrease

in volume positive

$$\text{therefore } \sigma_1' - \sigma_3' = \frac{\delta W}{\delta\varepsilon_1} - \sigma_3' \frac{\delta V}{\delta\varepsilon_1} \quad \text{---- (6)}$$

$\sigma_3' \frac{\delta V}{\delta\varepsilon_1}$ is the surface energy component of shear strength. It is positive for volume increase, negative for volume decrease and zero for constant volume or undrained conditions. Although Bishop mentions that his equation would apply at maximum deviator stress Roscoe, Schofield and Wroth (1958), Gibson (1953) and others applied the correction at other points on the stress path in addition to

the point of maximum deviator stress. Hvorslev (1960) suggested that part of the energy involved in volume change might be stored or released elastically and hence should not be considered in the term involving energy dissipated. Bishop (1964) considered that the rate of change of elastic energy at maximum deviator stress would be small. Roscoe and Schofield (1963) developed an energy equation discussed in Chapter 2 which considered both boundary energy and elastic energy within the sample. Rowe, Oates and Skermer (1963) extended the stress dilatancy theory to cohesive soils.

The modified coulomb equation

$$\tau_{ff} = c' + \sigma_f' \tan \phi' \quad \text{---- (7)}$$

where τ_{ff} = shear stress on failure plane at failure

c' = apparent cohesion

σ_f' = normal effective stress on failure plane at failure

ϕ' = effective angle of internal friction

is often used to express the shear strength of clays. For saturated normally loaded clays it is generally found that $c' = \text{zero}$. If the clay has been overconsolidated, the strength in the overconsolidated region of interest may generally be expressed by Equation 7. However, the friction angle determined in the overconsolidated region will be less than that of the normally loaded region. Therefore, for the one clay there is more than one possible friction angle. Friction and cohesion in this form are now considered to be merely parameters expressing the slope and intercept which best approximate the strength envelope in the region of interest (Figure 7). Hvorslev, at the suggestion of Terzaghi,

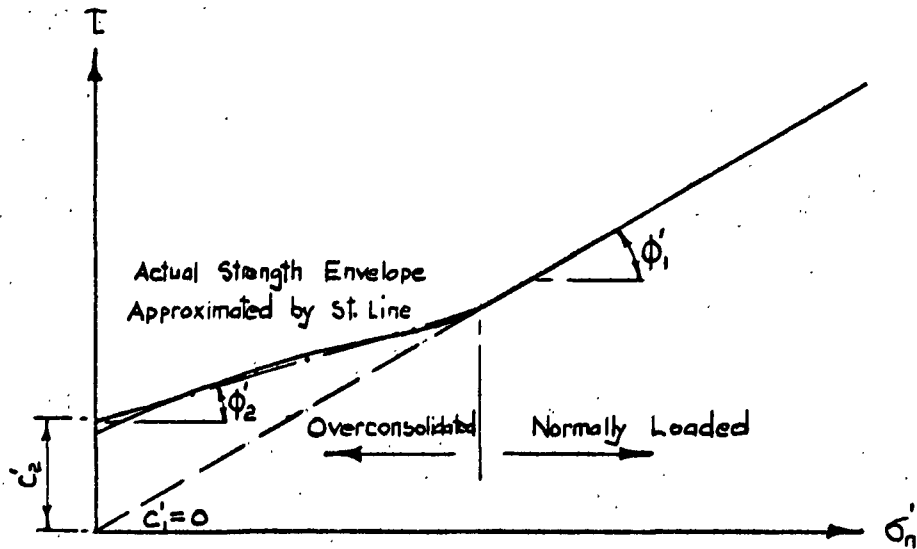


Figure 7a — Modified Coulomb Strength Parameters

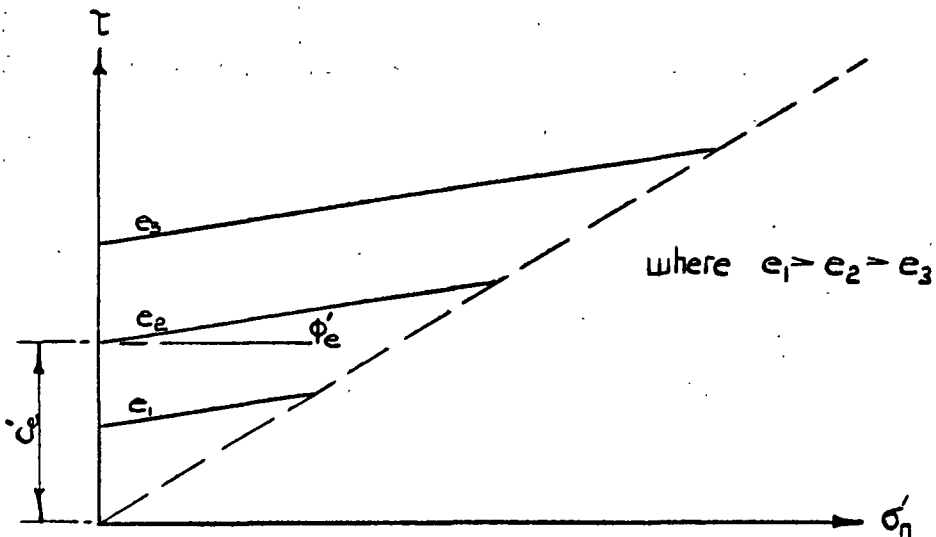


Fig. 7b — Hvorslev Strength Parameters

Figure 7 — Strength Parameters

performed direct shear tests on saturated remolded clay in such a manner that it was possible to compare shear strength at the same void ratio but with different applied normal effective stresses. It was found that for the same void ratio, the shear strength was a linear function of effective normal stress and plotted with an intercept on the shear strength axis as shown in Figure 7. Lower void ratios plotted as parallel lines with higher intercepts on the shear strength axis. The slope and intercept determined in this fashion were given the symbols ϕ'_e and c'_e and were thought to reflect true friction and true cohesion. Hvorslev (1960) preferred to refer to ϕ'_e and c'_e as effective friction and effective cohesion. The terms imply that at any one void ratio the cohesion is constant and independent of the effective stress. Hvorslev (1960) suggested that this would only be so if there were no significant differences in structure. Scott (1963) stated that due to the irreversible nature of the compressibility of clay it would not be possible to have two samples at the same void ratio with differing effective stresses and the same structure. The very fact that the stress is different signifies a different structure.

Gibson (1953), Bjerrum (1954) and many others have determined the effective friction and effective cohesion components for remolded soils. If the components were determined from drained tests, then the surface energy component was generally removed using the Bishop equation. Gibson found that application of the energy equation reduced c'_e and increased ϕ'_e . Simons (1960) determined these parameters for an undisturbed soil. Bjerrum and Simons (1960) found that the effective friction component was

lower for a soil in the remolded than the undisturbed state. It is apparent that the same friction and cohesion components will not be present for the same soil in the undisturbed and remolded states. This is particularly true for sensitive soils. Hvorslev (1960) considered that the components might only apply to remolded soils.

Schmertmann (1963) considered that the components as determined by Hvorslev on remolded clay might be correct. The differing consolidation ratios necessary to produce samples at the same failure void ratio but with differing effective stresses would result in samples which before shearing would have different structures. However, he thought it possible that the differing failure strains could cause structures which were not initially the same to be the same at failure, and hence the Hvorslev parameters could be correct. He suggested that this would not generally be the case and proposed a method of "curve hopping" to produce what he considered to be identical samples at the same strain under different effective stresses from which the friction and cohesion components could be determined at any strain. These he termed the Dependent and Independent components.

Noorany and Seed (1965) proposed a method of obtaining samples at the same void ratio and almost the same structure but with differing effective stresses. The method involved anisotropic consolidation of two samples to the same void ratio, after which time the deviator stress was removed from one, resulting in two samples at the same void ratio but with different effective stresses. The samples were then sheared at constant void ratio and

separation of Mohr circles at failure allowed the effective friction and cohesion components to be determined. The authors suggested that the Mohr circles might plot quite close to each other for insensitive clays making separation of components quite difficult, whereas for sensitive material, considerable separation could be expected. However, this could also mean that the observed separation in Mohr circles is due to structural change caused by release of the anisotropic stress condition, and as would be expected, this is more marked for sensitive material.

The Roscoe concept discussed in Chapter 2 indicates that a soil which is yielding has only one strength parameter, M , which implies a linear relation between p' and the deviator stress corrected for both boundary energy and internal energy. M can be considered as a friction component and the theory suggests that the full value of M is mobilized at all strains. In undrained tests it is generally conceded that considerable strain is necessary to mobilize full friction. However, the Roscoe concept indicates that this conception is due to neglect of the release of internal energy from the sample. The release of internal energy is of course governed by the soil structure.

Although it is of considerable interest from theoretical considerations to try to isolate the components of shear strength, in practice it is generally the measured combined value that is required. In addition, from the above discussion, it appears that the effective friction and cohesion components may have no physical meaning but arise from structural effects. It may be necessary to try to isolate the surface energy component if the laboratory tests do not duplicate the field conditions with regard to volume changes.

CHAPTER 4

TESTING PROCEDURES

4.1 Description of soil tested.

The clay used in this testing program was taken from a deposit located in the Fraser Valley, British Columbia. The deposit is centred around the town of Haney which is about thirty miles from the mouth of the Fraser River, and is known locally as Haney clay. It is presently being used for the manufacture of bricks and it was from the pit at the brick factory at Haney that samples were obtained.

The clay is thought to have been deposited in a marine or brackish environment during or shortly after the last glaciation of south-western British Columbia (Armstrong, 1957). Subsequent uplift of the land relative to the sea has exposed the deposit and percolating rain water has since leached out much of the salt, with the result that the clay now has a sensitive structure. Marine shells were found while sampling and attest to the depositional environment.

Haney clay has a dark blue-gray colour when wet, and has the colour of neat cement when dry. In the partially dry state, light and dark laminations of various thickness are evident. Standard laboratory identification tests were performed and the results are shown on Table I and Figures 8 and 9. A small dry sample of the clay was subjected to X-ray diffraction analysis to determine its mineral composition and the results are shown in Table II. It may be seen that the silt size particles are composed primarily of quartz and feldspar, while the clay size particles are mainly chlorite.

TABLE I
PHYSICAL PROPERTIES OF HANEY CLAY

Specific gravity	2.80
Liquid Limit	44%
Plastic Limit	26%
Plasticity Index	18%
Natural Water content	42% \pm 1%
Per cent finer than 2 microns	46%
Activity	0.4
Undisturbed unconfined compressive strength	1550 lbs./sq.ft.
Remolded unconfined compressive strength	130 lbs./sq.ft.
Sensitivity	12
Maximum past pressure	5500 lbs./sq.ft.

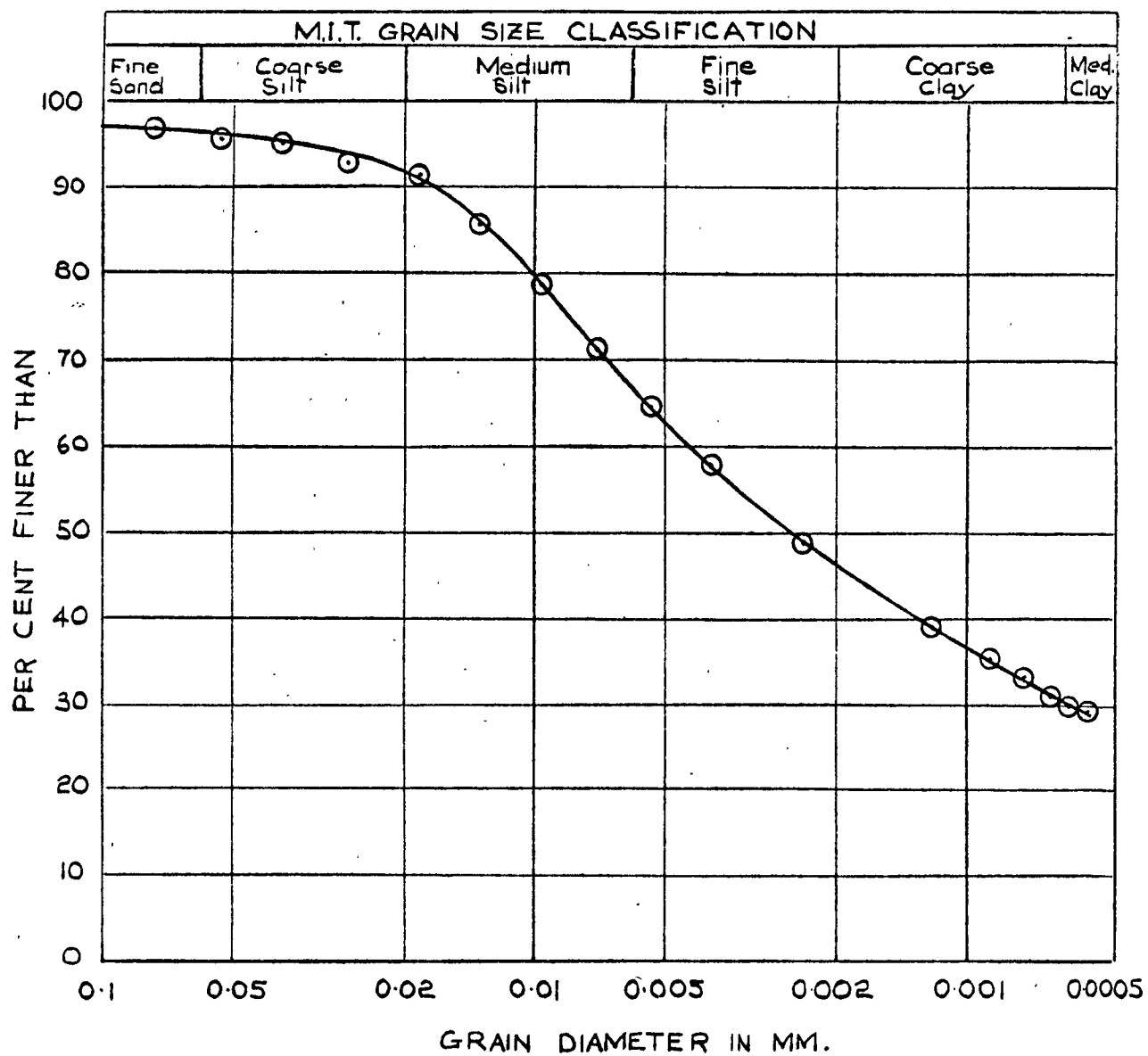


Figure 8 — Grain Size Distribution Curve for Honey Clay

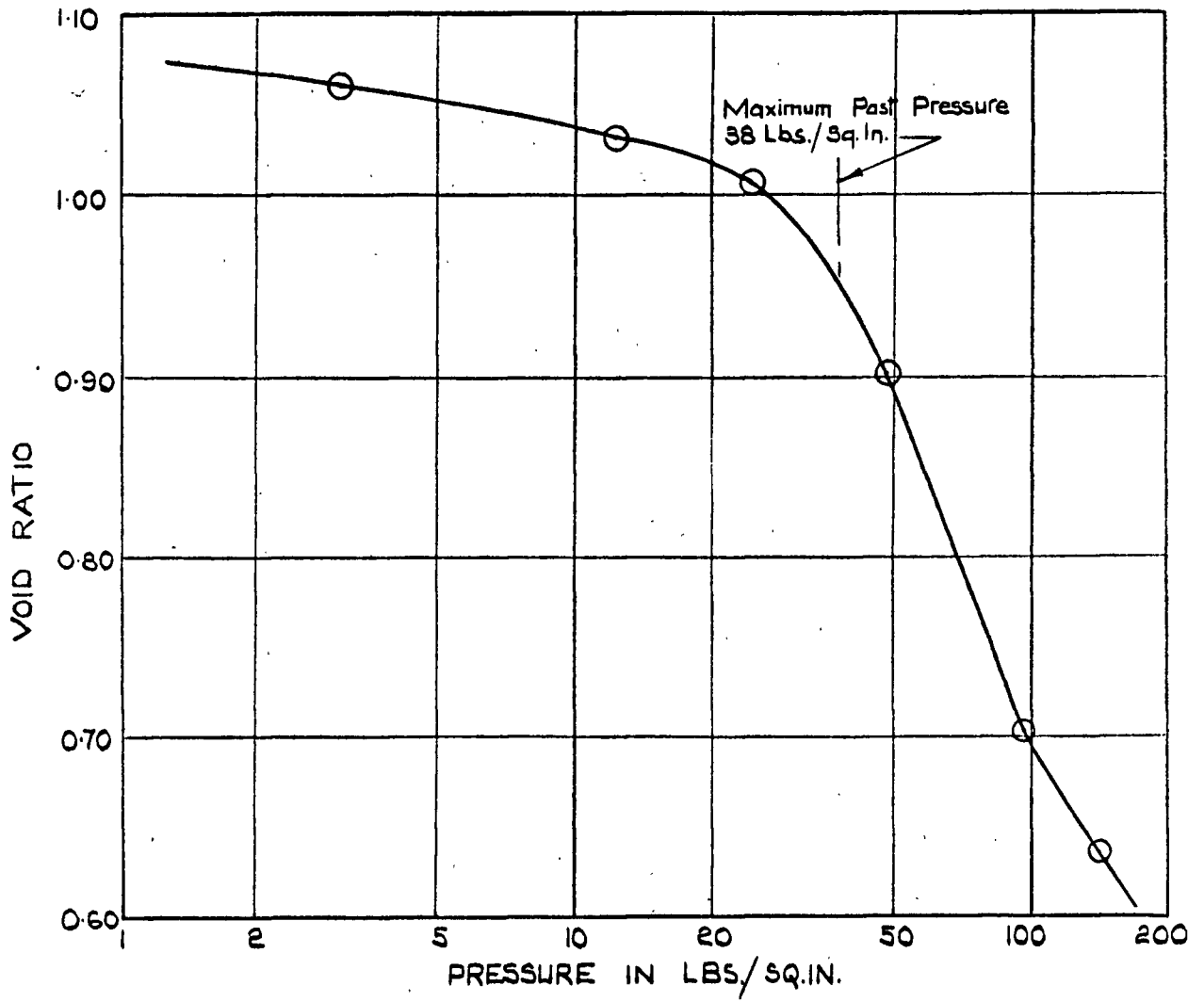


Figure 9—Typical Standard Consolidation Curve for Honey Clay

TABLE II
 CHEMICAL PROPERTIES OF HANEY CLAY

GRAIN SIZE	MINERAL	AMOUNT PRESENT
Silt Fraction (greater than 2 microns)	Quartz	Large
	Feldspar	Large
	Chlorite	Moderate - small
	Mica	Moderate - small
	Amphibole	Small
Clay Fraction (less than 2 microns)	Chlorite	Large
	Feldspar	Moderate - small
	Mica/chlorite	Moderate - small
	Quartz	Small
	Mica	Small
	Amphibole	Small - questionable

4.2 Field Sampling and storing of block samples.

Block samples were obtained by hand excavation from the clay deposit at Haney in an area that had recently been worked by the brick factory. A trench was dug around an area of about 12 square feet to a depth of 3 feet, thus isolating a large block of soil. The top 18 inches or so of disturbed clay was removed and block samples were cut using fine piano wire. These were trimmed to rough cubes of side 9 inches, and were coated with wax at the site as shown in Figure 10. The blocks were carefully transported to the laboratory and the next day were given further coatings of wax and then stored in a moist room until required.

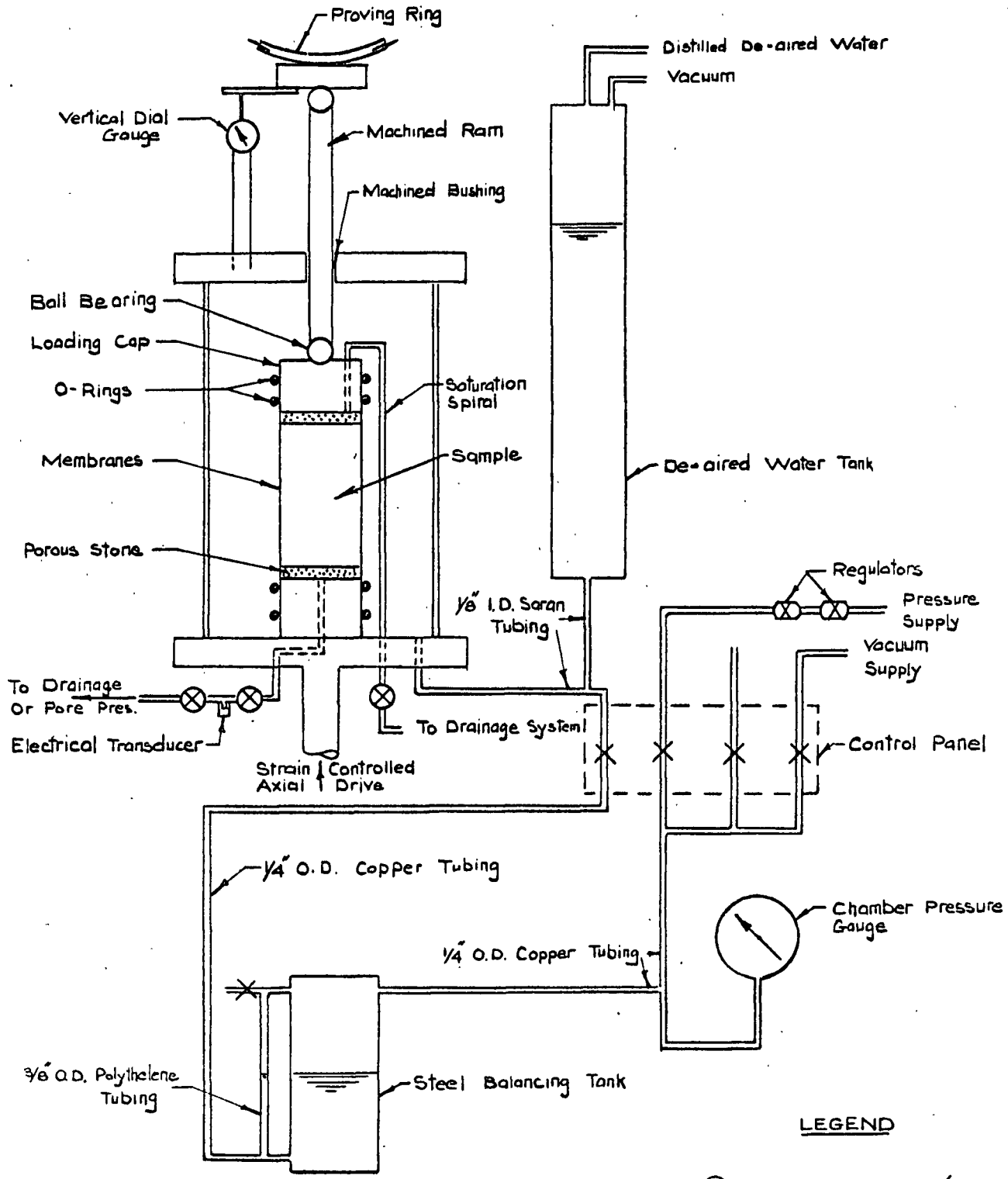
4.3 Description of test equipment.

The testing program was shared with Mr. T. J. Hirst. Drained tests were performed by Hirst and undrained tests and some very slow drained tests were performed by the writer. After completion of the drained series some modifications were made to the equipment, principally the installation of a de-aired water tank and a form of temperature control. At the end of the undrained series a further change was made. A transducer was introduced to measure pore pressure and an undrained test was run for comparison purposes. Two very slow drained tests were then run with pore pressure measurements in order to determine the magnitude of residual pore pressures in drained tests. These modifications will be indicated in the description of the test equipment which follows.

The test equipment used is shown in Figures 11, 12 and 13. The triaxial cell was a clockhouse Engineering T.10 capable of receiving 1.4 inch diameter samples. The ram and bushing were



Figure 10 - Block Samples of Haney Clay at Site



LEGEND

- ⊗ Hoke Ball Valve (Non-Disl.)
- × Hoke Stem Valve (Displ.)

NOT TO SCALE

Figure 11 - Triaxial Cell and Chamber Pressure System.

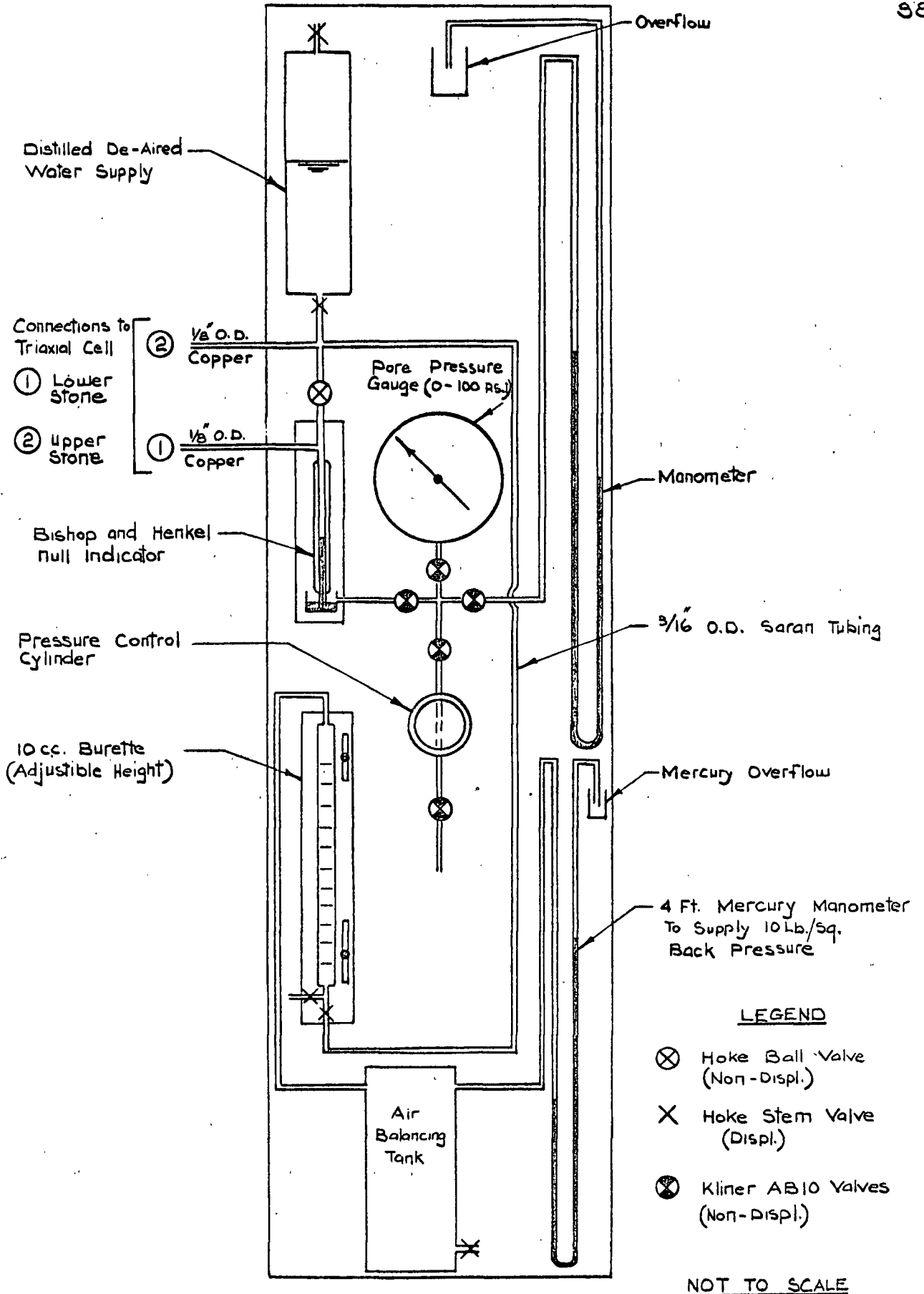


Figure 12- Drainage and Pore Pressure Measuring System

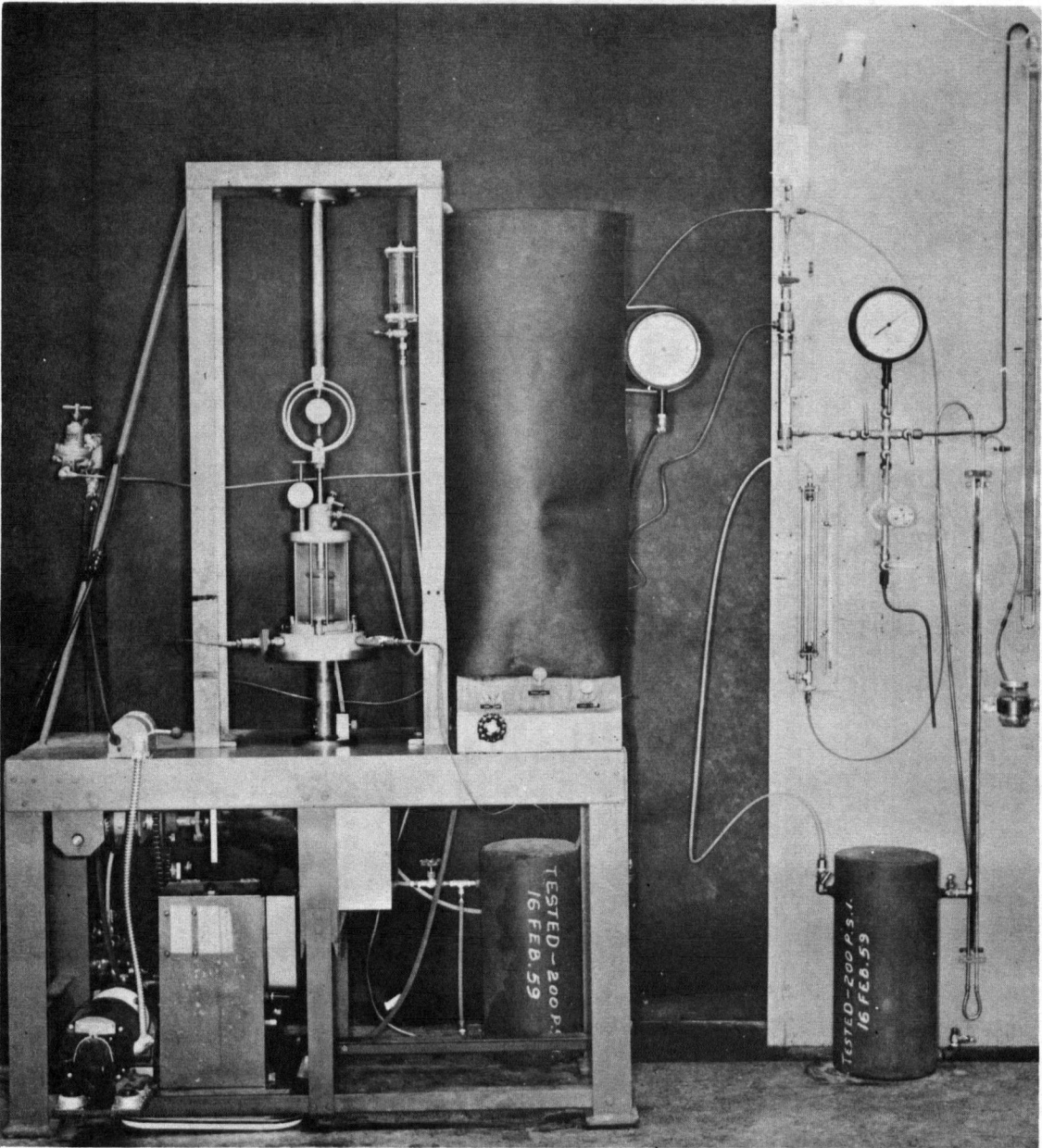


Figure 13 - Test Equipment

of stainless steel machined to a fine tolerance and were greased with "lubriplate" before each test. No significant leakage of water past the ram occurred. A loading cap which was free to rotate was used to minimize the lateral force and moment transferred to the ram and thus reduce friction at the bushing. Distilled de-aired water was used as a chamber fluid to reduce diffusion of air and water through the membranes into the sample. In the drained test series boiled distilled water was introduced into the air-water steel balancing tank under a vacuum and allowed to cool overnight. It was then fed into the chamber under a small air pressure. In the undrained series a distilled de-aired water tank was installed. Distilled water was de-aired by sprinkling it into the tank under a vacuum. The vacuum was removed and water fed into the chamber under gravity.

A constant chamber pressure was obtained by regulating compressed air from a house line and applying it to the air-water steel balancing tank. The water in this tank was subject to a vacuum before each test, but during the test in the presence of air at a high pressure it was expected that air would go into solution and find its way into the cell. In the drained series the air-water tank was connected to the cell by a length of $3/8$ in. O.D. polyethelene tubing. In the undrained series a 6 ft. length of $1/8$ in. I.D. Saran tubing was installed in the line to reduce the amount of air reaching the cell as suggested by Poulos (1964). If leakage of water from the cell occurs then air is carried to the cell by the water instead of diffusing through the water along the length of the tube and the effect of the tubing is

then lost. The chamber pressure was measured by a 0-100 lbs./sq.in. bourdon gauge graduated to 0.5 lbs./sq.in., and fitted with a mirror to reduce parallax. It was possible to estimate the pressure to 0.1 lbs./sq.in. The gauge was calibrated against a dead weight tester before each testing series and was found to creep under load. Variations of up to 0.4 lbs./sq.in. were found to occur in successive calibrations. The balancing tank was fitted with a transparent tube so that the water level in the tank was known and an elevation correction could be applied to determine the chamber pressure at the level of the centre of the sample.

Drainage lines from the top and bottom of the sample led to a 10 cubic centimeter moveable burette, graduated to 0.1 cubic centimeters. Wherever possible 1/8 in. O.D. copper tube was used, but where movements were large relative to the length of tube, such as for the saturation spiral and the connection to the burette, flexible plastic tubing was used. The level of the water in the drainage burette was kept at the level of the mid height of the sample, so that as drainage proceeded it was necessary to adjust the burette from time to time. To insure complete saturation of samples a 10 lbs./sq.in. back pressure was applied to the burette. This was accomplished by means of a mercury column and a 1200 cubic centimeter air balancing tank. The tank was sufficiently large that the change in the volume of air caused by drainage of 10 cubic centimeters of water would alter the back pressure by less than 0.1 lbs./sq.in. Changes in temperature of $\pm 1.0^{\circ}\text{C}$ would alter the pressure by about $\pm .05$ lbs./sq.in. However, changes in atmospheric pressure caused changes in the level of

the mercury which were not realized until the electrical transducer was installed at the end of the testing program. The reason for this is as follows: A constant volume in the back pressure tank is maintained by a constant absolute pressure. If atmospheric pressure falls then there is a tendency for the air in the tank to expand. This is prevented by rise of mercury in the standpipe equal to the change in atmospheric pressure (the small volume increase due to the rise of mercury can be neglected). The chamber pressure gauge reads pressures above atmospheric, the back pressure should therefore also be referenced to atmospheric pressure. Errors in the back pressure may have occurred but it is thought these amounted to no more than about 0.2 lbs./sq.in., as the level of the mercury was corrected occasionally during a test by allowing air into or out of the tank. Later, when the transducer was present, the correct back pressure was attained by moving the drainage burette until the desired transducer reading was obtained.

Pore water pressure was measured at the bottom stone only using the Bishop and Henkel null tube device (1 mm. I.D. tube). A 5 foot length of 1/8 in. outside diameter copper tube connected the null tube to the bottom stone. The compliance of this system produced a movement of 7/40 in. in the null tube over a range of 100 lbs./sq.in. that was fully reversible. Bishop and Henkel (1962) suggest that the movement should not be more than 1/2 in. over a pressure range of 100 lbs./sq.in. and the system was therefore considered satisfactory from the compliance point of view. During a test the position of the null point was varied

with the pressure to account for this compliance. The pressure was measured with a 0-100 lbs./sq.in. bourdon gauge similar to that used for measuring the chamber pressure. The gauge was calibrated using a dead weight tester to apply a chamber pressure which was then read on the pore pressure gauge. In this way no calculation was necessary to account for the height of mercury in the null tube or the change in the height of the mercury due to change in the null point with pressure. After calibration, care was taken to insure that the height of mercury for zero gauge reading was always kept the same.

Towards the end of the testing program an electrical transducer of the bonded type and made by Data Sensors Incorporated was installed. It was placed as close as possible to the cell to minimize the compliance of the system. The transducer had a range of 0 - 150 lbs./sq.in. absolute and a rated compliance of 0.00027 cubic in. for 100 lbs./sq.in. change in pressure. The rated compliance was checked with the null tube and found to be correct (9/40 in. rise in null point for 100 lbs./sq.in.). This could be compensated for during a test by using the null tube device to add or remove water to the transducer system to take the place of the volume change caused by the expansion and contraction of the active face of the transducer. If this were done immediately after a reading was taken, then flow into or out of the sample would allow the slight pressure surge to dissipate before subsequent readings were taken.

The transducer is accompanied by an electrical read-out device and the system was calibrated against the dead weight tester. The calibration was found to be linear with pressure to an accuracy

of ± 0.1 lbs./sq.in., and pressure changes of 0.025 lbs./sq.in. could be detected. The transducer measures pressure on an absolute scale and a barometer was installed so that the pressure could be referred to gauge pressure.

All tests were strain controlled. A constant deformation rate was applied to the loading platform on which the cell was placed by means of a 1/4 horse power electric motor and a system of gears. The gear system allowed thirty deformation rates ranging from about 2 in. per hour to 1 in. per year. A proving ring was used to measure the deviator force in the ram. The force on the ram caused by the chamber pressure and by friction at the bushing was measured by moving the loading platform upward at the intended testing rate without the ram being in contact with the sample. The friction force may change during a test mainly because of induced lateral forces but no attempt was made to measure this. The deformation of the sample was measured by a dial gauge placed such that the deformation of the sample only was measured.

Hoke valves were used wherever leaks could not be tolerated. The stem type displacement valves were used where displacement was not a problem. Four Hoke non-displacement ball valves were used on the drainage and pore pressure lines where it was essential to have no volume change on opening and closing valves. Klinger valves were used on the pore pressure device in locations where small leaks were of no consequence. All Klinger valves tested were found to leak. Four new Klinger valves were separately tested with the null tube device and all were found to leak. Leakage ranged up to 0.003 cubic in. per day under 100 lbs./sq.in., which corresponds to a rise in the null point of about 2 inches. Poulos

(1964) found similar results, and this writer now understands that, where Klinger valves are used by other investigators in positions where leakage cannot be tolerated, either the valve linings have been replaced or the valve has been treated in some way. Hoke non-displacement valves were tested in the same manner as the Klinger valves and no leakage could be detected in a three day period. However, after some usage it was apparent that these valves also leaked. Tightening of the stem seals appeared to stop the leakage and this was done from time to time. Subsequently, for other apparatus in the laboratory, Whitey non-displacement valves were used and were found to behave in a very satisfactory manner. Hoke displacement valves were also tested and none was found to leak.

The equipment was de-aired by drawing large quantities of boiled distilled water at a temperature of about 180°F through the drainage lines. Due to the many problems encountered in getting the equipment operational, de-airing was done a number of times and presented no particular difficulties. However, care is required in de-airing the Hoke non-displacement valves as the sealing surface is not continuous and so an air space exists behind the seal. These valves must be held in the half open position while water is flushed through to remove this air. After de-airing, the system was allowed to cool and the null tube was then used to check the drainage system for compressibility and leakage.

After the drained test series had been completed a form of temperature control was installed. This was accomplished by constructing an insulated compartment around the equipment which was kept below the general room temperature by a cooling unit.

The compartment comprised of a frame 15 feet long, 8 feet wide and 8 feet high constructed of 2 in. by 4 in. timber members and covered inside and outside with a layer of polyethelene to produce a 4 in. insulating air gap. A water cooled air conditioning unit of 9400 B.T.U. capacity was used. It was capable of keeping about a 10°C difference in temperature between the room and the compartment but during the test series the difference was never more than 5°C. A typical cycle was: air conditioner on for 1½ minutes, off for 3 minutes with a temperature variation within the compartment of 0.5°C. The fan setting could be adjusted and it was found that the optimum adjustment gave a fairly uniform temperature over most of the testing area. A thermometer placed in a 100 cubic centimeter flask did not record any noticeable variation in temperature due to the cyclic fluctuations of air temperature, and it could be concluded that the sample which was surrounded by a considerably larger volume of water underwent negligible temperature variation. However, the air temperature variation did have a small effect on the Bishop and Henkel pore pressure measuring device. The effect on a closed system was for the pressure to fall on a rising temperature and rise on a falling temperature. This is opposite to what one usually expects and may be explained as follows: On a rapidly rising air temperature the aluminum case of the pressure cylinder having a high conductivity and low specific heat increases in temperature and expands allowing the water to increase in volume and hence reduce in pressure. The water having a low conductivity and high specific heat does not have time to heat and expand. The copper line to

the cell behaves in a similar way to the pressure cylinder although to a lesser extent. If, on the other hand, the temperature rise is slow then the water has time to heat and expand and water having a higher coefficient of thermal expansion than copper or aluminum tends to expand more, causing a pressure rise. This effect was essentially eliminated by binding the pressure cylinder and copper line by insulating tape. When the transducer was later installed, no variation in pore pressure in a closed system could be detected.

4.4 Testing technique

Cylindrical samples 2.8 in. long and 1.4 in. in diameter were prepared in a moist room using a wire saw, miter box and trimming lathe. A trimmed sample and equipment is shown in Figure 14. Side and end trimmings were used for water content determinations. It was found that due to the laminated nature of the material, the water content calculated from the end trimmings varied considerably from the side trimmings. These were not therefore used in estimating the average initial water content but served to indicate the range of water content within the sample. Four tests were performed by Mr. Hirst with whom the testing program was shared to determine if the side trimmings were a reliable measure of the average initial water content of the sample. The greatest water content difference between a sample and its side trimmings was found to be 0.2 per cent and it was concluded that the trimmings were a reliable measure of the average initial water content of the sample. However, a precaution had to be observed in taking side trimmings. When side trimmings

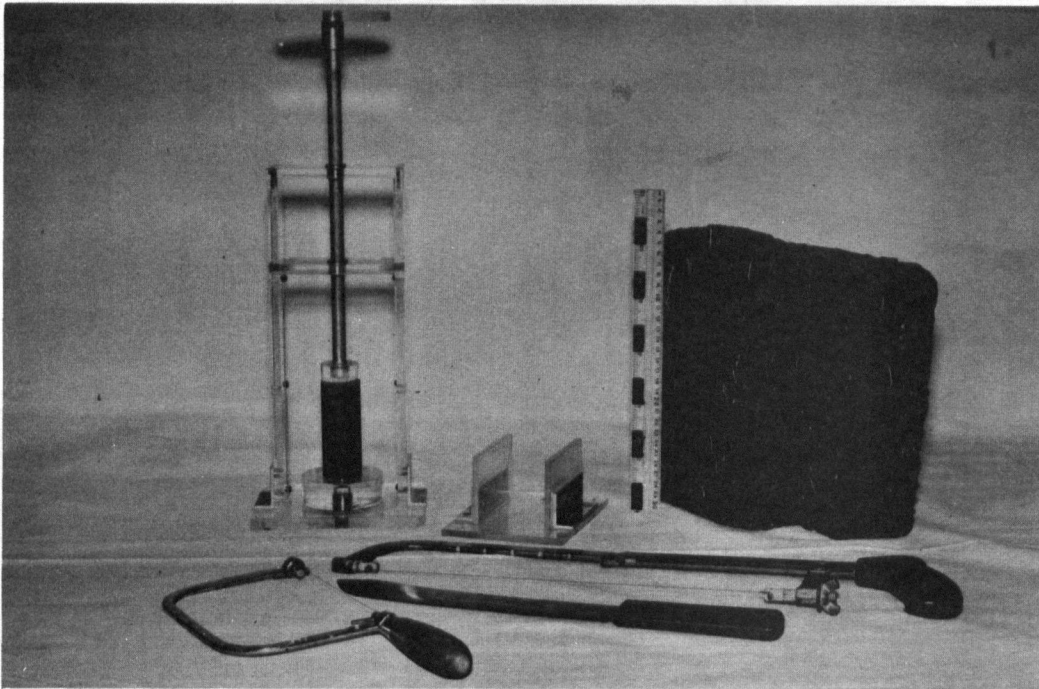


Figure 14 - Sample Trimming Equipment

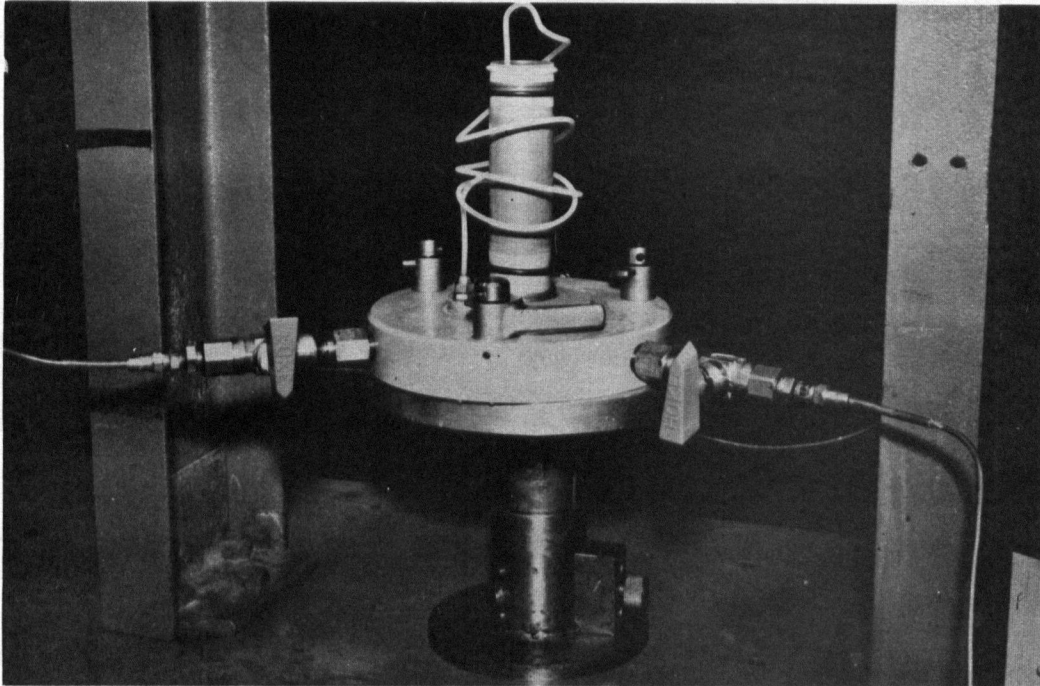


Figure 15 - Sample in Place on Triaxial Base

were taken the sample had not been trimmed top and bottom and therefore the trimmings did not represent the final sample. Further trimming was necessary to allow for this. If this further trimming were not done, and it was not always done by the writer, the check between initial and final water contents based on side trimmings was as poor as 1.5 per cent, whereas for those samples in which it was done the check was always within 0.2 per cent.

The trimmed sample was measured and weighed. Three circumferential measurements (top, centre and bottom) and four length measurements were obtained and averaged to determine the dimensions of the sample. Samples were handled with extreme care and were carried in a $1\frac{1}{2}$ in. wide rubber sling to reduce stresses.

Prior to the preparation of the sample the equipment was made ready. The porous stones were boiled for 10 minutes in distilled water and allowed to cool. Four O-rings on ring expanders were fed over the top loading cap and down the saturation spiral. These were followed by a rolled membrane. A rolled membrane was also placed down over the pedestal. The cylindrical surface of the pedestal was then covered with a film of silicon grease and the membrane rolled to the top. Water was allowed to flow from the bottom drainage line to cover the top of the pedestal and form a convex meniscus. The bottom stone now cooled to room temperature was slid into place. The sample was then slid onto the bottom stone. The top cap was inverted and water allowed to flow out and form a meniscus. The top stone was then placed and the cap and stone righted and slid onto the top of the sample. Silicon grease was now smeared on the top cap and with one hand on the top

cap the lower membrane was rapidly rolled up, any excess water being pushed ahead of the membrane. This membrane was then covered with a film of silicon grease and the second membrane rolled down from the top. Two O-rings were then placed over both membranes at top and bottom. Figure 15 shows a photograph of an installed sample during a preliminary test series when only one membrane and two O-rings were being used.

The top of the cell was then placed in position and the alignment of the ram with the ball bearing on the loading cap was checked. This was done by observing if any lateral movement of the top cap occurred when the ram contacted the ball. The sample was positioned by trial and error until no movement could be detected. The ram was then brought into contact with the sample and the vertical dial set. Water from the distilled de-aired water tank was fed into the chamber under gravity. A 10 lbs./sq.in. chamber pressure was applied and the pore pressure measured. In those later tests where the transducer was used to measure pore pressure, the pore pressure was measured as soon as the first membrane was in place. The effect on the pore pressure of placing the second membrane and aligning the sample could be observed. It was found that the pore pressure fluctuations of not more than 0.5 lbs./sq.in. occurred and were elastic. The chamber pressure was then applied in increments of 10 lbs./sq.in. at four minute intervals until the desired chamber pressure was attained. The pore pressure was recorded before each increment was applied allowing the Skempton B parameter to be calculated. It was found that B was equal to unity for all increments, indicating that the

clay was 100 per cent saturated.

Samples were allowed to consolidate for exactly 24 hours. Drainage from both top and bottom of specimens led to a burette to which a 10 lbs./sq.in. back pressure was applied. Since the time for t_{90} was never more than 200 minutes, it was considered that all pore pressure due to primary consolidation was essentially dissipated at the end of the consolidation period. Burette readings were taken during consolidation so that the coefficient of consolidation c_v and the coefficient of permeability k could be calculated.

In preliminary tests it was found that the sample would generally not consolidate uniformly in the vertical direction, so that at the end of consolidation the ram would no longer be aligned with the ball on the loading cap. To prevent this occurring it was necessary to bring the ram into contact with the ball from time to time during the consolidation period. The vertical stress involved in this contact was generally not more than about 0.4 lbs./sq.in. It was important to have good alignment before shearing otherwise there was a strong possibility of sample buckling taking place. In addition, poor alignment caused an irregular initial stress strain curve.

About an hour before the end of the drainage period the loading platform was moved up at the intending testing rate without the ram being in contact with the ball on the loading cap. In this way the force on the ram due to the chamber pressure and friction at the bushing was determined. This was later subtracted from proving ring readings to determine the deviator force.

Samples were then sheared under either drained or undrained strain controlled conditions. Figure 16 shows a specimen during shearing. The strain rate was about 0.5 per cent per hour and was the same for both drained and undrained tests. Some additional tests were run at other rates but were not used for the main purpose of the thesis. Variation in the strain rate occurred due to deformation of the proving ring. In fact, during the early part of the undrained tests the strain rate was about onehalf the average strain rate. The chamber pressure was kept constant throughout all tests. The air regulation system was found to work extremely well and fluctuations of not more than 0.1 lbs./sq.in. were recorded on the chamber pressure gauge. In undrained tests the variables recorded were, time, sample deformation, proving ring deformation and pore pressure. In drained tests the drainage burette reading replaced the pore pressure reading. Approximately 50 sets of readings were taken throughout the duration of any one test. These were later fed to a digital computer to be analyzed.

Two drained tests were performed at one quarter the general strain rate but drainage to the top stone only was permitted. Pore pressure was measured with the transducer at the bottom stone. The transducer was also used to measure the back pressure applied to the drainage line so that a very accurate measure of the excess pore pressure at the bottom of the sample was obtained. This was thought to give a reasonable accurate measure of the excess pore pressure that would exist at the centre of a sample drained to both top and bottom and sheared at the usual rate. This will be discussed in detail in Chapter 6.

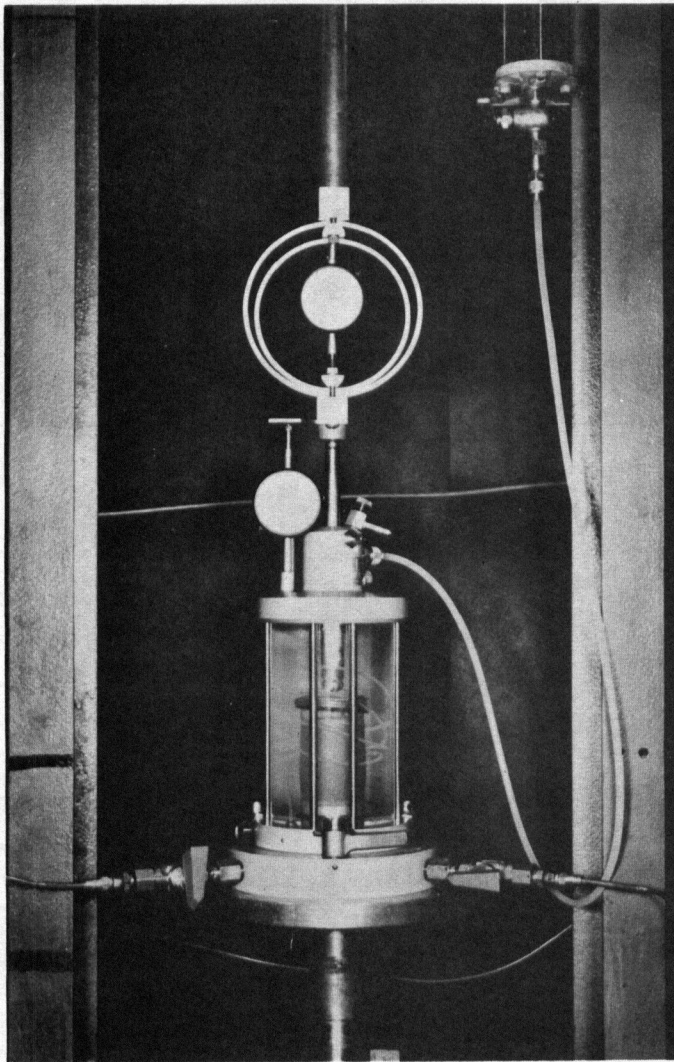


Figure 16 - Sample During Shear

At the end of the shearing process, since a check on the water content was required, water was first allowed to back drain into the sample before removing from the chamber. This procedure was first suggested by Henkel and Sowa (1963) and the reason is as follows: If the effective stresses at the end of the test are high, removal of the chamber pressure under undrained conditions will not change them and hence as the total stresses go to zero, large tensions are set up in the pore pressure. If these are high enough they will cause cavitation in the drainage lines and water will enter the ends of the sample. Even if the tensions are not sufficient to cause cavitation, water may be drawn into the sample from the porous stones during dismantling of the sample. Since it appears impossible to prevent water entering the sample the alternative is to measure the amount that enters. This was done by removing the deviator stress and dropping the chamber pressure to 12 lbs./sq.in. while allowing water to flow from the drainage burette which was maintained at a back pressure of 10 lbs./sq.in. at all times. Back drainage was continued until the rate of flow was very small or in some cases it was continued for 24 hours so that a measure of the coefficients of consolidation and permeability after shearing could be obtained. In this way the effective stress was reduced to 2 lbs./sq.in. After back draining the drainage valves were closed, the chamber pressure reduced to zero and the water removed from the cell. The rubber membranes were cut and removed, the porous stones pulled from the ends and the whole sample was then weighed. It was not thought that much water would enter the sample from the porous stones since the tension in the pore water should not be more than 2 lbs./sq.in.

and the capillary tension of the stones was thought higher than that.

The water content of the whole sample was determined and from the known amounts of water drained and back drained the initial water content could be calculated. This was then checked with both the initial water content calculated using the initial wet weight and final dry weight of the whole sample and the initial water content as determined from side trimmings. It was found that the water content check was always within 0.4 per cent and generally within 0.2 per cent when the whole sample was used for initial water content and was always within 0.2 per cent when side trimmings which were properly representative were used (see discussion earlier in this section). In those tests which were sheared at one quarter the usual rate the shearing process took about 10 days. However, the water content check for those two tests was within 0.1 per cent. It may therefore be concluded that the average water content at the various stages of a test was accurately known and that no significant leakage occurred.

After removal of the sample, the drainage lines were flushed with de-aired distilled water. The cell, bottom pedestal and top loading cap were thoroughly washed with detergent to remove any grease which might later trap air. The equipment was then ready for the next test.

CHAPTER 5

DISCUSSION OF TESTING TECHNIQUE

3.1 Introduction

The main purpose of the testing program was to determine if for Haney clay a unique relationship exists between effective stresses and the water content which is independent of the stress path, drained or undrained. It was important that the drainage condition should be the only variable in the tests and other possible variables, such as temperature and strain rate, were therefore kept constant. However, due to the nature of triaxial equipment errors arise which may not affect drained and undrained tests in the same manner.

In a triaxial test the aim is to subject a sample to homogeneous states of stress and strain. Due to the presence of friction forces at the top and bottom of a sample, the state of stress and consequently the state of strain is seldom uniform. In addition, in undrained tests non-uniform stresses lead to non-uniform pore pressures and or migration of water within the sample. In drained tests residual pore pressures of some generally unknown value are present. Even if the stress system were uniform, errors may arise in measuring the applied pressures and forces, principally the pore pressure and deviator force, and are mainly caused by time lag in the pore pressure measuring device and the presence of ram friction. These errors will be discussed in subsequent sections of this chapter.

5.2 Non-uniform stress and strain

In the standard triaxial test frictional resistance along

porous stones or end platens cause shear stresses to be applied at the top and bottom of a sample. Even during consolidation when no deviator stress is applied, shear stresses are present and prevent diameter decrease at the top and bottom. During shearing, these shear stresses reverse in direction and essentially prevent the end diameters from increasing, resulting in bulging of the sample. When bulging occurs the cross sectional area at the centre of the sample becomes greater than that at the ends and consequently the vertical stress at the centre is less than that at the ends. The shear stress at the ends has the affect of increasing σ'_3 at the ends and the overall result is that both σ'_1 and σ'_3 are higher at the ends than at the centre, but $(\sigma'_1 - \sigma'_3)$ is higher at the centre (Bishop, Blight and Donald 1960). The deviator stress is generally calculated from a cross sectional area which is determined by assuming that the sample deformed as a right cylinder. Roscoe, Schofield and Thuraiajah (1963) indicate that at an axial strain of 20 per cent, the area at the centre may be 1.4 times the area calculated on the usual basis. Casagrande and Wilson (1960) suggest that the relation between the vertical stress at the ends and centre of a triaxial specimen is given by:

$$\sigma_o = \sigma_m (1 + \epsilon_1)^2$$

where σ_o = vertical stress at ends

σ_m = vertical stress at middle

ϵ_1 = axial strain.

So that at 20 per cent strain the vertical stress at the ends would be 50 per cent larger than at the middle.

The axial strain is generally calculated by dividing the deformation of the sample by the consolidated length, and it is assumed that the strain is uniform throughout the sample. Roscoe, Schofield and Thurairajah (1963) showed that for drained compression tests on loose saturated sand, the axial strain varies considerably throughout the depth of the sample. In general, axial strains were found to be larger at the centre than at the ends. This would be in agreement with Bishop's suggestion that the shear stresses are larger at the centre. After about 10 per cent average axial strain, zones of maximum axial strain occurred at about the third points and were thought due to the failure zone moving towards the ends. Failure first occurs around the central zone followed by yielding and bulging and reduced-stresses, and movement of the failure zone towards the ends. In compression tests on normally loaded clay specimens, the strain distribution is unlikely to be the same as for sand. However, a similar trend could be expected, with maximum strains occurring near the centre followed possibly by the development of two zones of high strain between the centre and the ends at large average axial strain.

It is apparent, therefore, that stresses and strains are not uniform throughout a sample. At an average axial strain of 20 per cent, the stresses and strains within the sample may be as much as 50 per cent different from those calculated in the conventional manner. Since the actual stress and strain could not be reliably calculated for any element within the sample, the conventional method was adopted. It was hoped that the errors would be similar in both drained and undrained tests and that calculated average

values would provide reliable comparisons.

5.3 Non-uniform pore pressures in undrained tests

Non-uniform stresses lead to a further problem in the case of undrained tests. If the applied stresses are not uniform, then either the pore pressure is not uniform, or if the rate of testing is such that pore pressure equalization occurs by migration of water within the sample, then the failure zone can hardly be considered to be undrained. Undisturbed clays are not likely to be homogeneous so that non-uniform pore pressures would probably occur to some extent even in the absence of non-uniform stresses.

It is generally agreed that for normally loaded and sensitive materials subject to undrained shear, the pore pressure at the centre of the sample will be higher than at the ends (Whitman 1960, Bishop, Blight and Donald 1960, and Blight 1963). Hence, flow of water will take place from the central zone of higher shear towards the end zones. In overconsolidated soils where shear stresses cause reduction in pore pressure the reverse is true.

If the pore pressure is measured at one end of the sample as is usual, then, if the measured pore pressure is to have any meaning, the rate of testing must be such that the pore pressure throughout the sample is fairly uniform. To speed up equalization of pore pressure, filter paper side drains may be used. These allow drainage to the cylindrical surface of the sample as well as to the top and bottom. They are most effective if the permeability of the clay is very low compared to the permeability of the paper. For clays of relatively high permeability, considerable head loss may occur in the filter paper. The calculated coef-

ficient of consolidation of the soil assuming no head loss in the paper may be very much less than that measured if no filter paper were present. In the past, in order to reduce hoop tension, filter paper strips with alternating gaps were used. This reduces the effectiveness of the drainage surface and causes additional loss in the filter paper due to the reduced cross sectional area of paper. Bishop and Gibson (1963) suggested that continuous filter paper with vertical slits to reduce hoop tension might be used to offset this. Campanella (1965) found that the use of slits rather than slots in the filter paper reduced the time for 100 per cent primary consolidation of bay mud by a factor of about 5.

Bishop and Henkel (1962) and Blight (1963) produced equations and graphs from which the time to any reliable reading can be obtained for drained and undrained tests provided the coefficient of consolidation c_v or the apparent c_v (obtained by assuming no loss in the filter paper) is known. Their results were based on 95% equalization of non-uniform pore pressures in the case of undrained tests, and 95% dissipation of excess pore pressure in the case of drained tests. If it is only required to have a reliable reading at failure, then the time obtained is the time to failure. If, on the other hand, a stress path is required, the time obtained will be that to the first reliable point on the stress path.

Preliminary tests were conducted to determine if the use of filter paper would allow reduced testing times. Isotropic consolidation tests were performed on 1.4 in. by 2.8 in. samples both with and without slotted filter drains (Whatmans No. 54) and the results compared. Without filter paper c_v was found to be about 2×10^{-3} cm.²/ sec., whereas with filter paper and assuming no head loss

in the paper the apparent c_v was about 5×10^{-5} cm.²/sec. Since 2×10^{-3} cm.²/sec. was the correct c_v and would have been measured had no loss occurred in the paper (assuming $k_h = k_v$), the efficiency of the drains, which is the ratio of the apparent c_v to the actual c_v was about $2\frac{1}{2}$ per cent. It has been suggested that the poor performance of the paper may have been due to smear on the lateral surfaces caused by sample trimming, but a similar smear should then have been present at the top and bottom of the sample, and so it seems very unlikely that smear could be responsible for such a poor efficiency. Similar low efficiencies were obtained by Simons (1963) and Crawford (1963) on sensitive clays with c_v 's in the same range and were attributed to head loss in the paper. Based on the c_v values obtained, the times required to reliable readings for undrained tests from Blight's chart are about 4 hours with or without drains. It was therefore decided not to use drains. Unfortunately, at the time of these preliminary tests, the concept of using slits in the filter paper instead of the usual slots was not known to the writer. It is very possible that slit paper would have been considerably more effective.

5.4 Residual pore pressures in drained tests

Since filter paper side drains have a very low efficiency and were not used, it was necessary to have drainage top and bottom in drained tests to reduce the testing time. With a c_v of 2×10^{-3} cm.²/sec. and double-end drainage, a time of 11 hours to the first significant reading was calculated (Bishop and Henkel 1962). Blight (1963) suggests that the theoretical times for 95 per cent dissipation from which the Bishop and Henkel equation is derived

predicts times considerably longer than those actually needed for 95 per cent dissipation. He suggested that the time required for a given degree of pore pressure dissipation in a drained test with double-end drainage would be the same as that required for the same degree of pore pressure equalization in an undrained test without filter paper. The time required for 95 per cent dissipation of excess pore pressure would therefore be 4 hours, the same as it was for undrained tests.

The writer was concerned about the value of residual pore pressures in drained tests because of the highly flocculated nature of sensitive clays. During shearing it was expected that large reductions in permeability would take place due to structural change and decreased void ratio. Hence it was thought possible that residual pore pressures might be larger than usual.

A method was derived for calculating excess pore pressures from the rate of drainage of pore water from the sample. This was checked by running drained tests at $\frac{1}{4}$ the normal speed but allowing drainage from the top only and measuring pore pressure at the bottom. The method and results are discussed in detail in Chapter 6.

5.5 Pore pressure measuring devices

Until quite recently pore pressures in small test samples have been measured by means of the null-indicator. This generally comprises a water-mercury contact surface in a small diameter tube which is maintained at such a level that no flow from the sample to the system occurs. The pressure required to maintain the level is measured and gives the pore pressure at the centre

of the sample when the system is suitably calibrated. More recently electrical transducers have been used to measure pore pressure. Here very small deformations of a diaphragm produce changes in electrical resistance of strain gauges allowing calculation of pore pressure.

If the pore pressure within the sample is changing, and if it is assumed that the change would be uniform throughout the sample in the absence of a pore pressure measuring device then the presence of one may lead to non-uniform pore pressures. In the null tube device, movement of some observable amount must first occur before a pressure change can be applied, and hence a small flow of water into or out of the sample take place creating a gradient within the sample. In the same way deflection of the diaphragm in the transducer causes a small volume change and similar gradients within the sample.

Bishop and Henkel (1962) defined the sensitivity of the null indicator as the time required for a movement Δx to occur in the null point under a small out of balance pressure Δp . A mathematical expression was derived for this time, and for given values of Δx and Δp , it depends on the nature of the soil tested (c_v and m_v) and the ratio of the diameter of the null tube to the diameter of the surface over which the pore pressure is measured raised to a power. For Haney clay with $\Delta p = 0.2$ lbs./sq.in. and $\Delta x = 0.02$ in. and measurement at the bottom stone, the sensitivity was about 30 seconds. Had the area over which the pore pressure was measured been very much smaller, say due to the use of a pore pressure probe, then the sensitivity time would have been very much greater.

A similar time lag occurs with the transducer due to its compliance. When the transducer was installed towards the end of the testing program, it was found that for an ambient pressure increase of 40 lbs./sq.in. under undrained conditions, a time of about 2 minutes elapsed before 98 per cent of this increase was recorded on the transducer. This time is a function of the compliance of the transducer system, the nature of the sample material and the area over which the pore pressure is measured. Had the transducer been connected to a pore pressure probe in place of the bottom stone a very much longer time would have elapsed for 98 per cent equalization.

In general the sensitivity time is very much less than the time required for reasonable equalization of pore pressures due to non-uniform stresses and consequently it is not usually considered. However, if pore pressures are measured with small diameter probes inserted in the sample, sensitivity may well be an important factor.

5.6 Rate of testing

Since the drainage condition was to be the only variable, it was necessary to have the rate of shearing the same for both drained and undrained tests. In addition, stress paths were required rather than just stresses at failure and therefore the rate had to be such as would give reliable values of stresses for a considerable portion of the stress path. The approximate times for 95 per cent dissipation and equalization of pore pressures in drained and undrained tests were 11 and 4 hours respectively. If the more optimistic figure suggested by Blight for drained

tests was taken, then the time for both was about 4 hours. Preliminary tests indicated that for undrained shear the maximum deviator stress occurred at about 3 per cent axial strain while the maximum principal stress ratio occurred at about 15 to 17 per cent axial strain. In drained tests both maximum deviator stress and maximum principal stress ratio occurred at about 30 per cent axial strain. An average shearing rate of 0.5 per cent axial strain per hour was selected. During the early portion of the test, due to the rapid rise in deviator stress, deflection of the proving ring caused the strain rate to be considerably less than the average rate. The time for 30 per cent axial strain was about 60 hours. In drained tests about one half of the stress path occurred in the first 11 hours while one quarter to one third occurred in the first 4 hours. Therefore at best two thirds of the stress path would be reliable and possibly only one half. However, residual pore pressures were calculated and it is thought that the estimated stress path is reliable over almost its complete length.

In undrained tests, since the deviator stress rose very rapidly, with maximum deviator stress occurring after about 8 hours, a considerable portion of the stress path occurred within the first 4 hours. In fact, one third of the readings were taken within the first 4 hours and actually accounted for one half the stress path. Therefore, one half the stress path might be considered unreliable. However, Blight (1963) points out that errors in the measured values of the effective stresses caused by non-uniform pore pressures depend on the overconsolidation ratio of the material tested. For normally loaded material, errors are

likely to be small and consequently readings at a lower per cent equalization may be quite reliable. Simons (1963) suggests that 90 per cent equalization in undrained tests is quite adequate, the time for which would be 2 hours. About one third of the stress path occurs in the first 2 hours. Some preliminary tests were also run at 0.25 per cent per hour average axial strain or one half the rate actually used in the testing program. It was found that the stress path in the early portion was very little different to that obtained at the faster rate. Thus about five sixths of the stress path is known to be reliable.

Many investigators believe that considerably faster strain rates than those suggested by Bishop and Blight can be used and reliable pore pressure measurements still obtained at the base of the sample. Crawford (1963a) describes undrained tests on normally loaded sensitive Leda clay in which pore pressure probes in addition to base measurements were used to determine pore pressures. Specimens were 1.4 in. diameter by 2.8 in. in length and the coefficient of consolidation was about 2×10^{-3} cm²/sec., or about the same as for Haney clay. The strain rate was 0.5 per cent per hour (same as used in this testing program) and maximum deviator stress occurred at about 2 per cent axial strain or after about 4 hours. The theoretical time for 95 per cent equalization would be about 4 hours, thus, according to Bishop and Henkel (1962) a reliable base measurement of pore pressure would only be obtained at failure. Crawford found that a pore pressure probe (0.12 cm outside diameter) placed at the lower quarter level recorded essentially the same pore pressure as that measured at the base of

the sample and that a similar probe placed at mid height recorded a lower pore pressure. He concluded that pore pressure measurements at the base give an accurate estimate of the pore pressure in the failure zone which he felt is near the base due to the restraining effect of the porous stone.

Higher pore pressures at the ends rather than at the centre for normally loaded and sensitive material is not in agreement with the general body of thought and evidence on this matter (Whitman 1960, Bishop, Blight and Donald 1960, and Blight 1963). The sensitivity time for a small diameter probe such as used by Crawford would be high. Crawford (1963b) mentions that the response of the pore pressure probes under ambient pressure changes could not be checked due to "plugging" of the needles. Taylor (1955) considered ambient pressure changes the best method of checking the response time of probes and considered a probe to be unsatisfactory if the delay in reaching 95 per cent of the applied ambient increment was more than about two minutes.

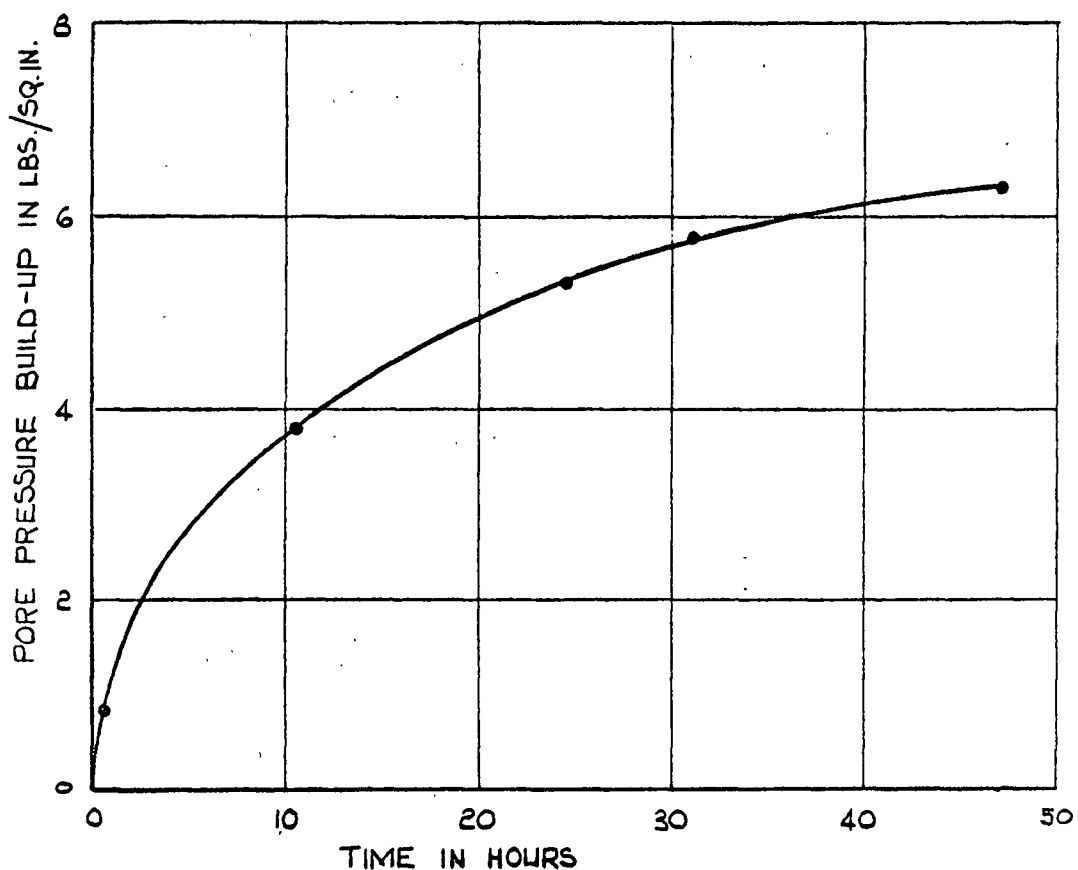
The evidence for the reliability of base pore pressure readings at times which are less than that required for 95 per cent equalization may not always be trustworthy. Bishop, Blight and Donald (1960) have stated that the onus should be on the research worker to prove that his tests satisfy reasonable criteria for accurate determination of pore pressure. It is felt that the preliminary tests performed at the slower rate indicate that the pore pressures are only in doubt for the first one quarter to one fifth of the stress path.

5.7 Pore pressures resulting from secondary effects

Samples were consolidating for a period of 24 hours after which time shearing was commenced immediately and in undrained tests it was assumed that all increase in pore pressure was caused by applied stresses. However, a later test series conducted by Mr. Lou using the same test equipment and the same clay indicated that after consolidation, pore pressure rise will take place in the absence of any applied deviator stress. Figure 17 shows the buildup in pore pressure with time for a sample which was consolidated to 75 lbs./sq.in. for a period of 24 hours. Since the time for t_{90} was less than 200 minutes it is felt that primary consolidation was essentially complete after 24 hours and could not be responsible for the observed rise. It was thought, at first, that part of the build up might have been caused by membrane leakage, or leakage past the O-rings. However, the rate of pore pressure increase decreased with time and after two days had dropped to 0.3 lbs./sq.in. per day. Therefore, leakage could account for only a small portion of the build-up.

The pore pressure rise is thought to be due to structural re-arrangement after drainage. It is closely associated with secondary compression and in fact could be described as the "converse" of secondary compression. If further drainage is allowed secondary compression takes place due to structural re-arrangement, while if drainage is prevented pore pressure rise takes place.

Therefore, some of the pore pressure measured during shearing is not due to applied deviator stresses and this influences the stress paths followed in undrained tests. However, drained tests were treated in the same manner as undrained so that the pre-shear



NOTE:

1. Sample Allowed to Consolidate For 24 Hours at which Time Drainage Valves Closed and Pore Pressure Observed.
2. Time Measured From Close of Drainage Valves.

Figure 17 — Build-Up in Pore Pressure After Consolidation — Honey Clay
(After K. Lou)

conditions were the same for both. The stress path is not affected in the drained test but additional drainage takes place which alters the water content. Since the object of the testing program was to compare contours of water content obtained from drained and undrained tests, it may be that since the same procedures were observed in both, that the water content contours are equally changed in both types of tests.

5.8 Membrane Leakage

The original testing procedure involved the use of glycerene as a chamber fluid as suggested by Lambe (1958). It was thought that the use of glycerene would prevent migration of water from the chamber into the sample and allow the use of a single thin (.003 in. wall thickness) membrane. It was found, however, that the water content determined after shearing was always 1 to 2 per cent below that calculated from initial conditions. The pressure in the glycerene was always 20 lbs./sq.in. higher than the pore pressure and it was at first felt that pore water would not escape from the sample into the chamber against the pressure differential. After a series of check tests had been run, it became apparent that high osmotic pressure differences between glycerene and water were responsible for the loss in water from the sample. Subsequently it was discovered that previous investigators (Poulos, 1964) had found similar losses using glycerene and recommended that de-aired water be used as the chamber fluid. With de-aired distilled water as the chamber fluid and two membranes separated with a film of silicone grease and bound with two O-rings top and bottom, no further leakage problems were observed.

5.9 Ram friction

In most triaxial equipment the applied deviator force is measured outside the cell so that the friction force developed at the bushing where the ram passes out of the cell is also included in the measured force. To minimize this friction force, ball bushings, rotating rams or rotating bushings and closely machined rams and bushings have been used. The ball bushing type would appear to be the most desirable of these because lateral forces on the ram would not produce any additional friction force. A seal to prevent water escaping from the chamber is necessary and will give rise to some friction force which can be measured.

A cell with a closely machined ram and bushing was used in this test series. The ram was greased with "lubriplate" before each test and very little leakage occurred past the ram so that no additional seal was necessary. Ram friction and the force on the ram due to the chamber pressure was measured by moving up the loading platform at the intended testing rate with the ram not in contact with the sample. To determine if the ram was properly machined and or if the duration of the test affected the grease, a check test was run where the loading platform was moved up for the duration of a test (70 hours) with no sample in place. No significant change in friction force occurred. It was thought that significant friction forces might develop during shearing when the axial force would be high and lateral forces might be present. Bishop and Henkel (1962) suggest that additional friction forces only arise because of lateral forces. At Imperial College it was found that with cells similar to those used in

this testing program that the friction force was generally between 1 to 3 per cent of the axial load. Lateral forces were thought to be small in this test series because a loading cap which was free to rotate was used. If large horizontal forces were present rotation of the cap would occur followed by buckling. Bishop and Henkel suggest a fixed type loading cap for undisturbed material to prevent buckling. However, large lateral forces and moments may be transferred to the ram in this case causing higher friction forces and may be responsible for the upper range of friction forces quoted by Bishop and Henkel.

Available evidence indicates that errors in the deviator stress due to ram friction are not likely to be more than from 1 to 3 per cent and it is quite possible that due to the use of a rotating top cap, the errors may be even less than 1 per cent.

CHAPTER 6

RESIDUAL PORE PRESSURES IN DRAINED TESTS

6.1 Introduction

Residual pore pressures of some magnitude are always present in drained shear tests. Flow of water to or from the drainage boundaries is caused by pore pressure gradients within the sample and the resulting pore pressures are referred to as residual pore pressures.

The duration of drained tests is generally chosen such that the average degree of pore pressure dissipation is at least 95 per cent at failure, or if a stress path is required, at the time the first reliable reading is desired. The time required for any given degree of dissipation is usually calculated from the formula:

$$t_f = \frac{h^2}{\eta c_v (1-U)} \quad \text{---- (9)}$$

where t_f = time to failure or a reliable reading

h = one half the height of sample

η = factor depending on boundary drainage conditions

c_v = coefficient of consolidation

U = average degree of dissipation required

The above formula was derived from theoretical considerations by Gibson and Henkel (1954). However, it does not allow the calculation of average pore pressures. An expression for pore pressure was derived by Gibson and Henkel based on the assumption that the rate of pore pressure increase in the undrained condition is constant. This was then used to determine the upper bound for the average degree of dissipation. Since the rate of pore pres-

sure rise in the undrained condition is known not to be constant, their expression for excess pore pressure would not be suitable for estimating residual pore pressures and was not intended to be so.

Alternative methods for estimating pore pressures were therefore considered. Since test data was to be analyzed on the computer, numerical methods of relatively complex form could be tolerated. Two methods were developed and will be referred to as Method 1 and Method 2. The following common assumptions were made:

1. Homogeneous soil.
2. Complete saturation.
3. Soil grains and water are not compressible.
4. One dimensional flow.
5. Validity of Darcy's law.
6. k and c_v constant throughout the sample at any one time, but vary with time.
7. Sample deforms as a right cylinder.

It is assumed for both methods that drainage top and bottom occurs. However, drainage from one end only is obtained by simply replacing h by $2h$. The average pore pressure rather than the maximum pore pressure has been calculated. The reason for this is that a relationship between stresses and water content was being examined and since the water content was the average water content, it was thought the stresses should be the average stresses. It will be shown that when the degree of dissipation is high, as it should be in a drained test, the maximum pore pressure is $1\frac{1}{2}$ times the

average. So that the maximum pore pressure is readily obtained from the average and vice versa.

6.2 Method 1

This method is based on the superposition of pore pressures (Terzaghi, 1943, p. 286). The deviator stress is assumed to be applied in increments, causing pore pressures which can be estimated from the Skempton equation for change in pore pressure under undrained conditions, namely:

$$\Delta u = B (\Delta\sigma_3 + A (\Delta\sigma_1 - \Delta\sigma_3)) \quad \text{---- (10)}$$

Incremental pore pressures are assumed to dissipate independently and in accordance with the one dimensional consolidation equation. The pore pressure at any time is then the sum of the partially dissipated incremental pore pressures at that time. This method is discussed in detail in Appendix 1.

Method 1 was found to predict zero residual pore pressure at maximum deviator stress for samples consolidated to 40 lbs./sq.in. However, drainage from the sample was still taking place at failure, therefore excess pore pressures must be present. It was felt that the quantity of water draining from samples could somehow be used to estimate excess pore pressure. An examination of the work of Gibson and Henkel (1954) indicated that the basic equation of continuity could be used to yield a much simpler expression for excess pore pressure if one assumption were made. This alternative approach is discussed in the next section and is considered to have more merit than Method 1.

6.3 Method 2

The equation of continuity for one dimensional flow leads to the following partial differential equation (Bishop and Gibson 1963):

$$\frac{k}{\gamma_w} \frac{\partial^2 u}{\partial z^2} = - \frac{\partial q}{\partial t} \quad \text{---- (11)}$$

where k = permeability of the soil

γ_w = unit weight of water

u = excess pore pressure

z = distance or length measured from centre of sample

$\frac{\partial q}{\partial t}$ = rate of loss of water per unit volume from any element of soil.

If it is assumed that the rate of loss of water from every element of a sample is the same at any time t_j ; then q will be a function of time only. Since the volume of water leaving a drained test sample was recorded during the shearing process, the rate of loss per unit volume could be calculated. u_j , the pore pressure at time t_j is a function of z only, hence for any one time the partial differential equation (11) can be reduced to the ordinary differential equation:

$$\frac{k}{\gamma_w} \frac{d^2 u}{dz^2} = - \frac{dq}{dt} = - \frac{R}{V} = \text{constant} \quad \text{---- (12)}$$

where R = rate of loss of water from the sample

V = volume of sample

This can be integrated using the boundary conditions $u = 0$ at $z = h$ and $\frac{du}{dz} = 0$ at $z = 0$ to yield the following expression for

the pore pressure at any time t_j :

$$u_j = \frac{1}{2} \frac{\gamma_w R}{kV} (h^2 - z^2) \quad \text{---- (13)}$$

And the average and maximum pore pressures are given by:

$$u_j \text{ (average)} = \frac{1}{3} \frac{\gamma_w R_j h_j^2}{k_j V_j} \quad \text{---- (14)}$$

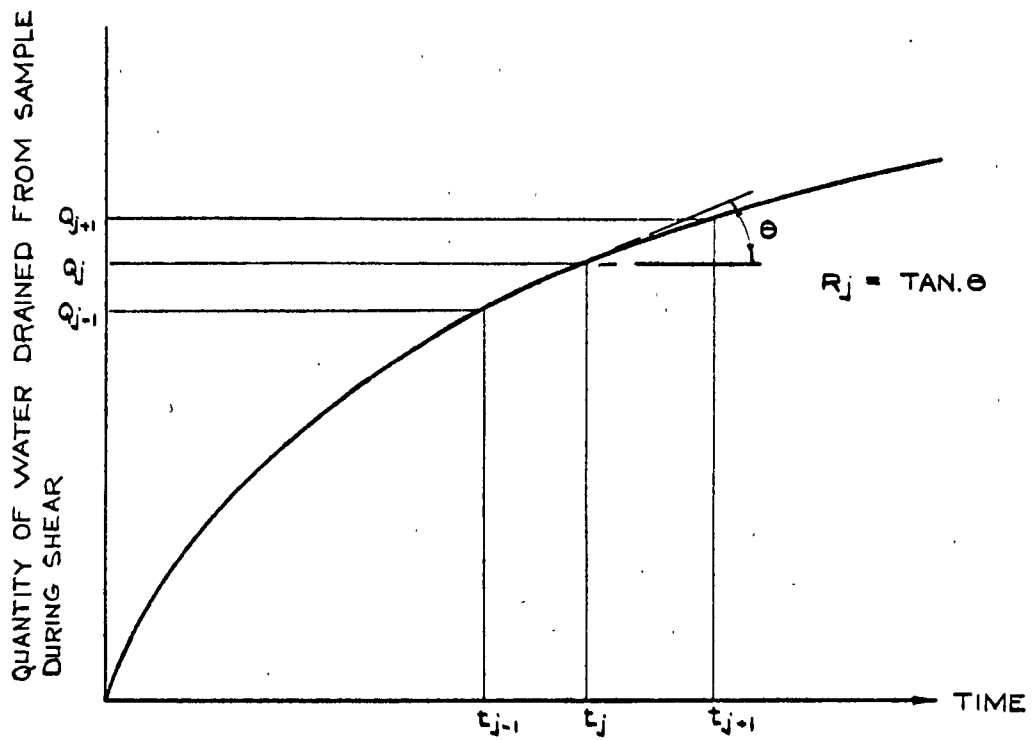
$$u_j \text{ (maximum)} = \frac{1}{2} \frac{\gamma_w R_j h_j^2}{k_j V_j} \quad \text{---- (15)}$$

It is seen from expression (13) that the theory predicts a parabolic distribution of excess pore pressure, and consequently the average pore pressure is two thirds the maximum pore pressure.

Expression (14) is very readily programmed for the computer. It is much simpler than the expression involved in Method 1 since it involves no summation, and in fact, could easily be calculated without a computer. Only one unknown, the permeability of soil appears in the expression instead of the two occurring in Method 1. However, an assumption was made that the rate of loss of water from all parts of the sample was constant at any one time. This implies that the change in void ratio should be uniform throughout a sample between time intervals, which would probably be strictly true only if the rate of testing were infinitely slow so that no excess pore pressures developed and stresses were uniform throughout the sample. For slow testing rates, where the per cent pore pressure dissipation is high, this expression is considered to give a good approximation of average residual pore pressures.

The variables in equations 14 and 15 are; the half height of sample, h ; the volume of the sample, V ; the rate of drainage, R ;

and the permeability, k . The height and volume of the sample are readily calculated. The rate of drainage at time t_j is the slope of the volume drained versus time curve at time t_j and since readings are not likely to be taken at equal time intervals this was approximated as shown in Figure 18. Since the permeabilities calculated from isotropic consolidation prior to shearing and from swelling after shearing were not considered reliable, a method based on measuring the pore pressure and assuming expression (15) to be correct was used. Two slow drained tests were performed at one quarter the normal speed, where drainage to the top only was allowed and pore pressures were measured at the bottom using the transducer. Since the transducer was also used to measure the back pressure, a very accurate measure of the maximum residual pore pressure was obtained. Test samples were consolidated to 40 and 70 lbs./sq.in. respectively which was the range of consolidation pressures used in the drained test program. The calculated permeabilities are shown in Figure 19. It is seen that the relation between void ratio and permeability for both tests can be approximated by a straight line on the semi-log plot except for the initial portion of the test consolidated to 40 lbs./sq.in. It will be shown later that samples consolidated to 40 lbs./sq.in. are not truly normally loaded and this initial portion is due to an overconsolidation effect reflected in the permeability. The permeabilities calculated from initial consolidation and from swelling after shearing are also shown and it appears that although the permeabilities calculated from initial consolidation are reliable, those obtained from swelling appear too low.



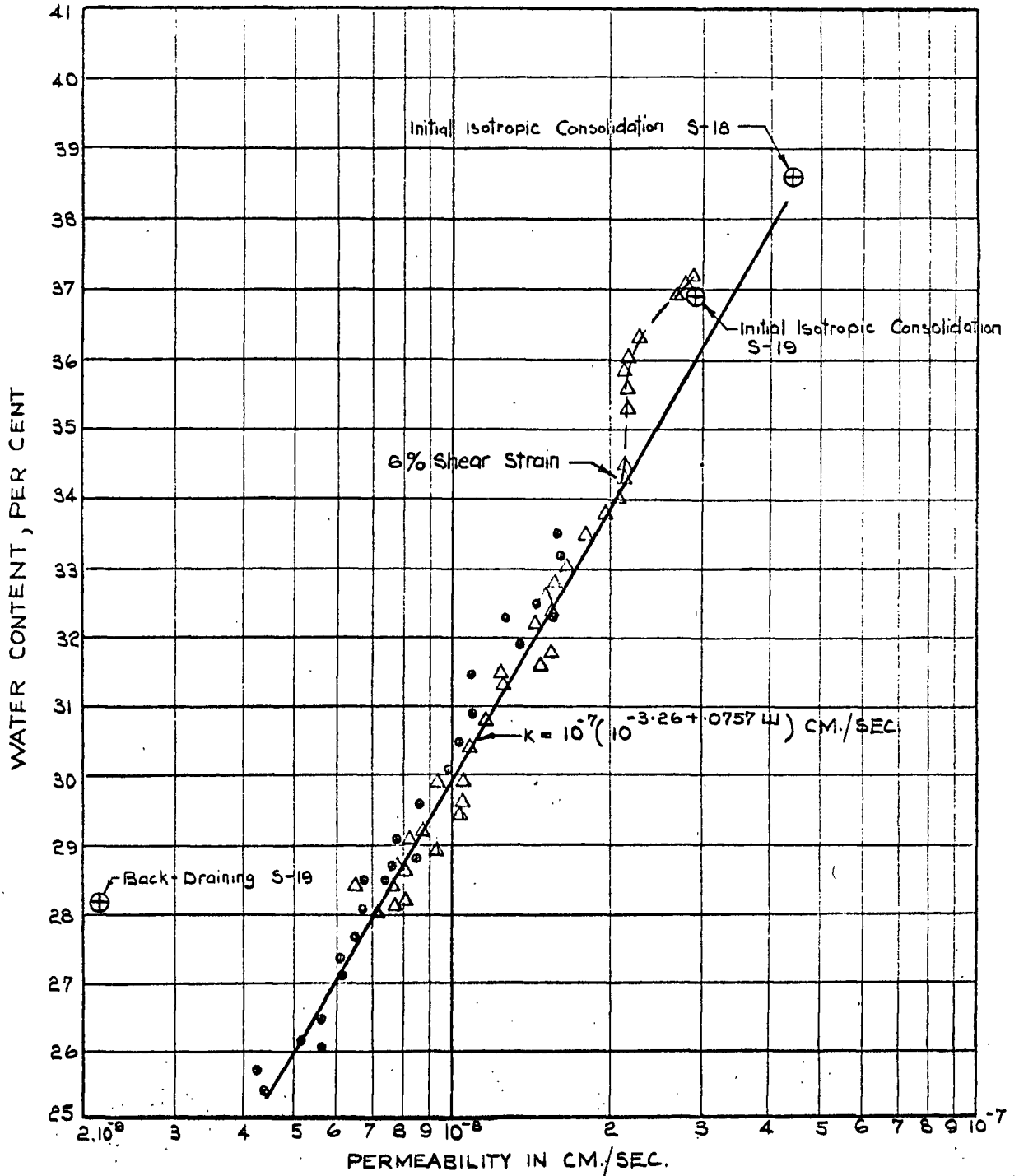
R_j Approximated by the Following Formula:

$$R_j \approx \frac{1}{t_{j+1} - t_{j-1}} \left\{ \frac{Q_{j+1} - Q_j}{t_{j+1} - t_j} (t_j - t_{j-1}) + \frac{Q_j - Q_{j-1}}{t_j - t_{j-1}} (t_{j+1} - t_j) \right\}$$

Figure 18 — Illustration of Method for Determining Drainage During Shearing

LEGEND

- △ Drained Test S-18, $\sigma'_c = 40$ Lbs./Sq. In.
- Drained Test S-19, $\sigma'_c = 70$ Lb./Sq. In



NOTE:

S-18 & 19 sheared at 1/4 the Normal Rate but with Drainage from Top Only. Excess Pore Pres. from which Permeability Calculated Measured at Bottom Stone.

Figure 19 — Relationship Between Void Ratio and Permeability During Drained Shearing of Honey Clay.

Since the tests to determine the permeability were run at one quarter the normal rate but with drainage from one end only, then theoretically, if secondary effects are not considered, the pore pressures measured at the bottom end of the slow tests should be identical to those occurring at the centre of tests run at the normal speed. The average pore pressure, equal to two thirds the maximum measured pore pressure is shown plotted versus shear strain in Figure 20 for both slow tests. Residual pore pressures calculated by Methods 1 and 2 are compared to the measured values in Figure 21. Pore pressures calculated by Method 1 are seen to be quite different from the measured values. For a consolidation pressure of 70 lbs./sq.in. the calculated pore pressures are generally high by a factor of about two, while for a consolidation pressure of 40 lbs./sq.in. they are low, apart from an initial peak at 1 to 2 per cent strain. Pore pressures calculated by Method 2 are seen to be quite similar to the measured values. They are slightly below the measured values at strains up to about 10 per cent. Since samples sheared at the slower rate actually drained more than those sheared at the normal rate, due to additional time for secondary consolidation, it could be expected that residual pore pressures would be slightly higher for the slower rate.

If it is felt that Method 2 gives a reliable measure of excess pore pressure during a drained test. However, since the slow drained tests were run at one quarter the normal speed, the measured pore pressures give reliable values of the excess pore pressures generated at the centre of samples tested at the normal

NOTE:
Average Residual Pore Pres. Assumed = 2/3 Max.
Measured Pore Pres.

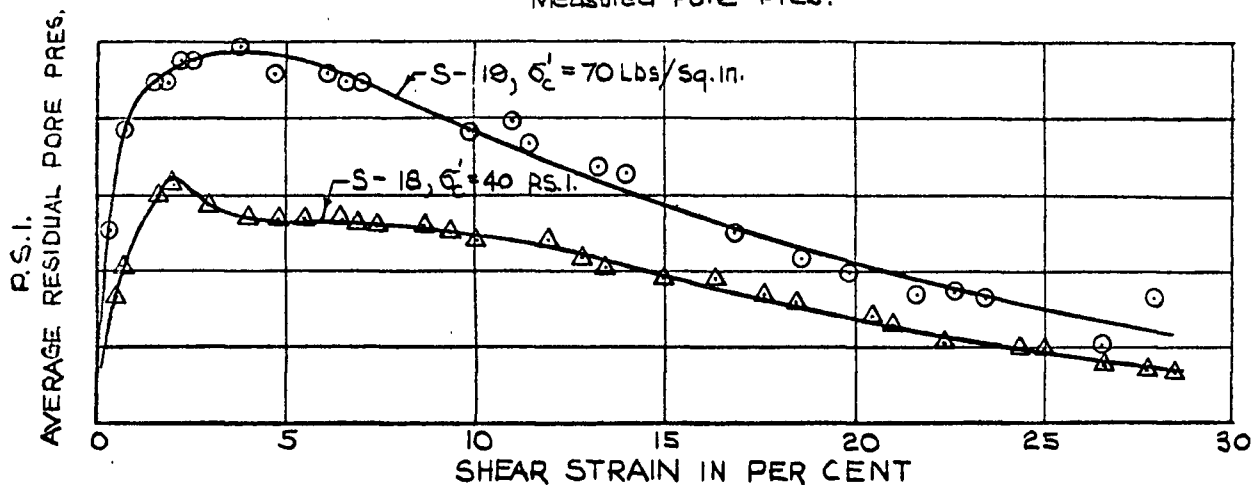
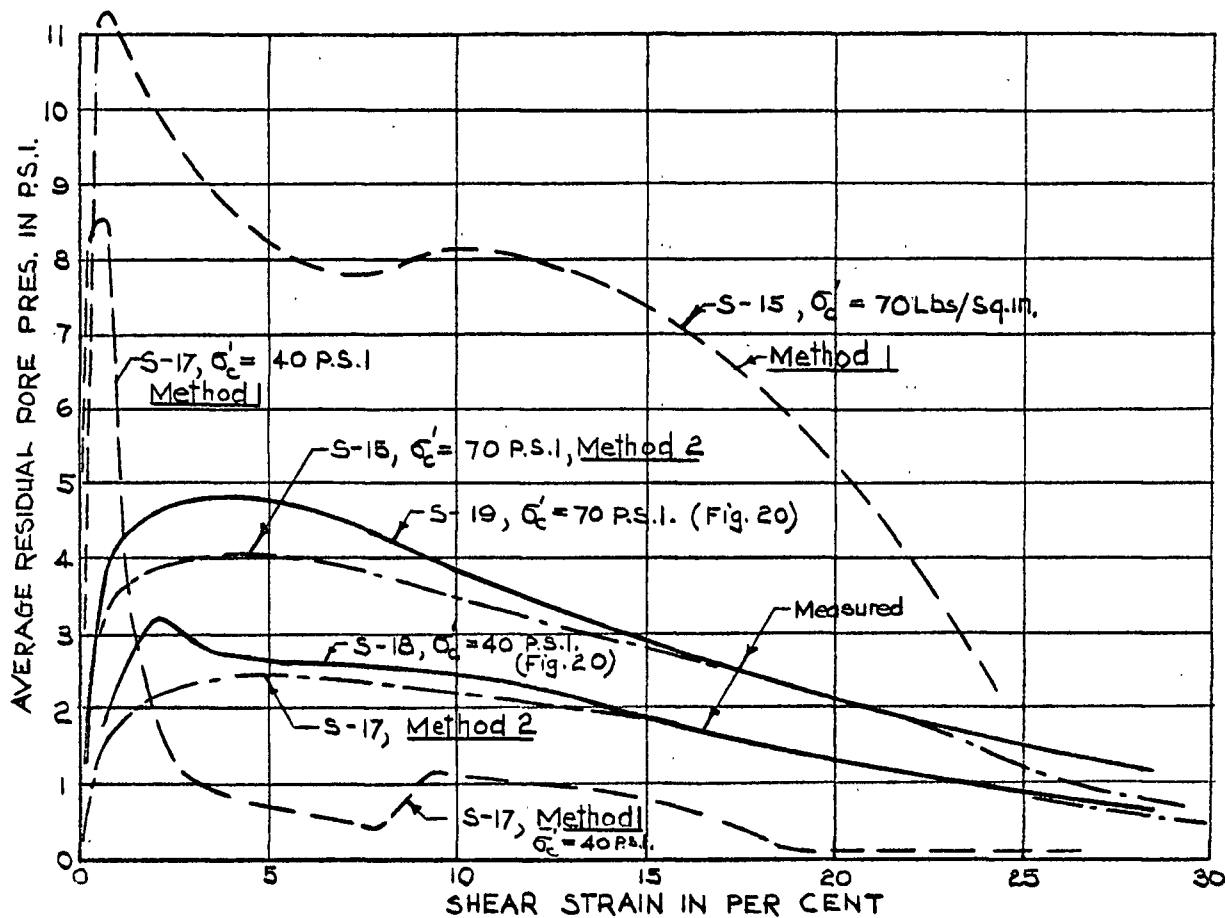


Fig. 20 - Relationship Between Measured Residual Pore Pressure and Shear Strain in Drained Tests



NOTE: S-18 & 19 sheared at 1/4 the Normal Rate but with Drainage from Top Stone only. Pore Pres. Measured at bottom Stone

Fig. 21- Comparison of Measured and Calculated Residual Pore Pressures in Drained Tests.

speed, so that these measured pore pressures could have been used to adjust the effective stresses without any calculations. However, it may not be necessary to run check tests at such a slow rate. In fact the same permeability relation would most likely have been determined had the normal rate been used but with drainage from one end only. For a drained test series in the normally loaded range, it is probable that a few drained tests with pore pressure measurement would be sufficient to determine a relationship between void ratio and permeability from which residual pore pressures in all other drained tests could be calculated.

Method 2 also has the interesting alternative of predicting permeabilities under varying stress conditions when pore pressures are measured in drained tests. If the permeability of a soil is determined by the falling head method, leaching of the soil may take place which in itself may alter the permeability, particularly in undisturbed soils. In Method 2 no such leaching takes place. For any one soil at a given void ratio the permeability is a measure of soil structure, so that a measure of the structural change caused by remolding could be obtained by comparing permeability versus void ratio relationships for the same clay in the undisturbed and remolded states.

Measurement of residual pore pressures and subsequent calculation of permeabilities in drained tests would allow a very simple check on the concept of Hvorslev's strength parameters ϕ'_e and c'_e . If samples at the same void ratio are to have the same structure, then their permeabilities should be the same. If the void ratio versus permeability for normally loaded soil is a

straight line on the semi-log plot as it appears to be for Haney clay, then any overconsolidated sample if it is to have the same structure at failure as a normally loaded sample, must have its permeability on this normally loaded line at failure. Samples of Haney clay consolidated to 40 lbs./sq.in. are in the overconsolidated range, but it was seen from Figure 19 that after about 6 per cent shear strain the permeability lay on the straight line and the sample thereafter behaved as normally loaded. The structure at failure, which occurred at about 25 per cent shear strain could then be said to be the same as if the sample had been normally loaded.

CHAPTER 7

TEST RESULTS

7.1 Introduction

The main purpose of the testing program was to determine if, for Haney clay, a unique relationship exists between effective stresses and water content which is independent of effective stress path.

The main body of the testing consisted of 7 consolidated undrained (C-U) tests and 6 consolidated drained (S) tests on undisturbed samples of Haney clay all of which were sheared at the same strain rate (0.5 per cent per hour). In addition, 2 consolidated drained tests were performed at one quarter the normal strain rate but with drainage from the top only. Undrained test specimens were consolidated to pressures of 60, 75 and 88.5 lbs./sq.in., while drained test specimens were consolidated to pressures of 40, 55 and 70 lbs./sq.in. At least two tests were performed at each consolidation pressure so that the consistency of results could be checked. Test data was analyzed on the I.B.M. 7040 at the University of British Columbia. Results from all tests are shown graphically in the diagrams that follow. Typical test readings, computer programs and computer outputs are shown in Appendix II for C-U-2 and S-17.

Stress-strain characteristics of Haney clay are presented in Section 7.2. It is felt that these curves are useful in interpreting the results discussed in subsequent sections. Contours of water content from drained and undrained tests are compared in Section 7.3. Energy corrections, the possibility of predicting

stress -strain relations and the effect of strain rate on stress-strain relations in drained tests are discussed in Sections 7.4, 5 and 6.

7.2 Characteristics of Haney clay

The most difficult problem in attempting to determine relationships between effective stresses and water content for an undisturbed clay is to find a clay of sufficiently uniform composition that consolidated samples can be obtained which lie on a single void ratio or water content versus logarithm of pressure line. The water content versus logarithm of isotropic consolidation pressure relation is shown on Figure 22. It is seen that consolidated water contents from all drained tests lie on a common straight line, whereas consolidated water contents from undrained tests show some scatter and appear to lie on a straight line of about the same slope although with a water content about $1\frac{1}{2}$ per cent higher for the same consolidation pressure. Block samples of Haney clay were of such a size that 8 triaxial specimens could be obtained from any one block, but in fact the drained test specimens were taken from 3 different blocks. It is unfortunate, therefore, that the undrained test specimens taken from a fourth block do not lie on the same straight line. Haney clay is laminated and if care was not taken to insure specimens were taken from the same level within blocks, different water contents resulted.

When comparing contours of water content from drained and undrained tests, it is necessary to have samples which lie on a common isotropic consolidation line. The scatter, in consolidated water contents for undrained tests (Figure 22) appears to have little

LEGEND

- C-U-1 Consolidated Undrained Test No. 1.
S-12 Consolidated Drained Test No. 12.

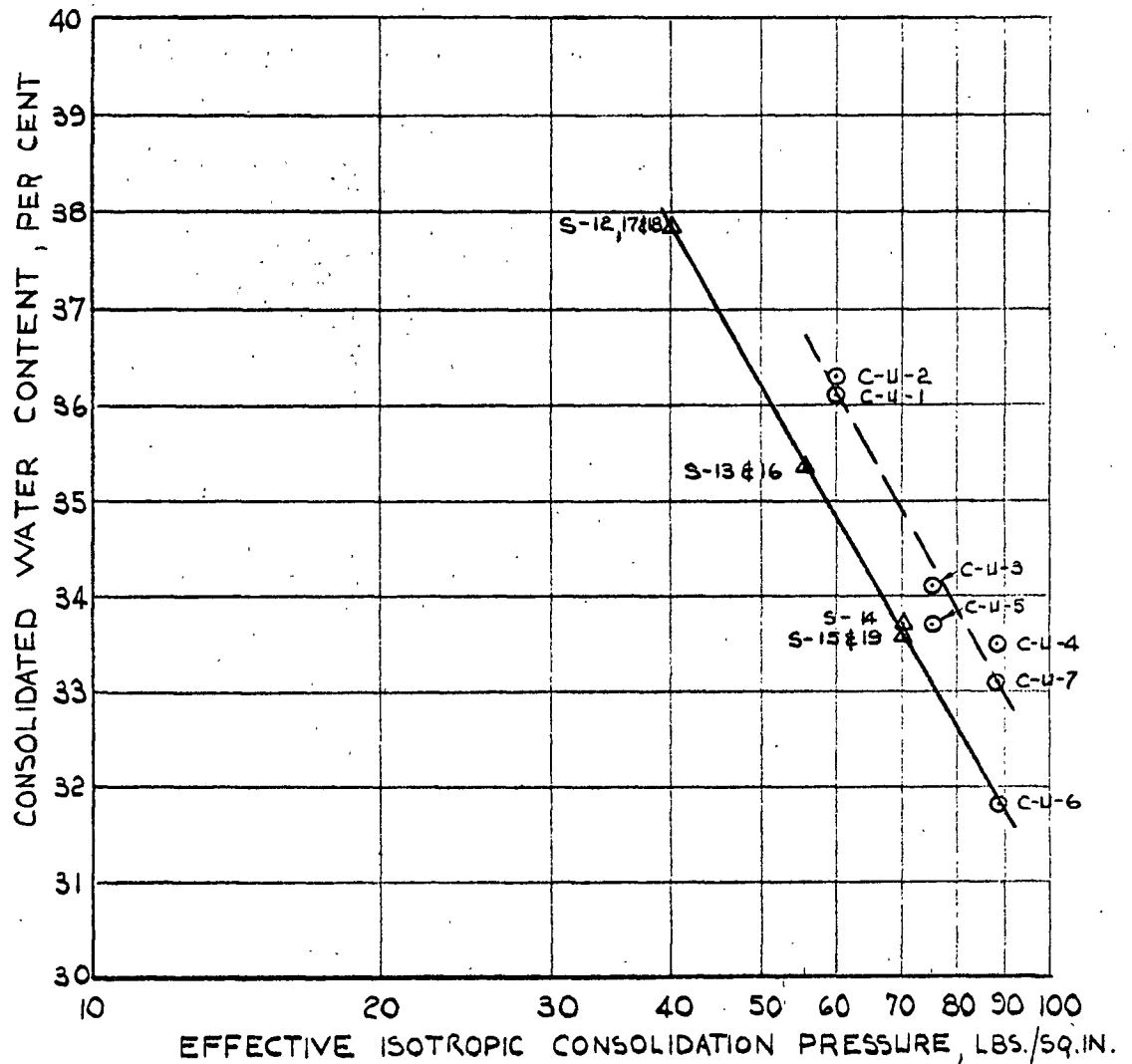


Figure 22 — Relationship Between Void Ratio and Logarithm of isotropic Consolidation Pressure, Haney Clay.

effect on the stress paths followed in undrained tests, as may be seen in Figure 33, Section 7.3. The scatter is such that C-U-6 has a consolidated water content that actually lies on the isotropic consolidation line common to drained tests. Yet the effective stress path followed by C-U-6 is very similar to that followed by C-U-7. It appears that for the samples of Haney clay tested, the consolidation pressure determines the effective stress paths followed in undrained shear. It was concluded from this evidence that for the purpose of comparing contours of water content, it would be reasonable to assume that undrained samples had consolidated water contents which lay on the isotropic consolidation line obtained for drained samples.

Stresses and principal stress ratios are plotted versus shear strain rather than axial strain. The shear strain or more correctly the principal shear strain, ξ , is given by

$$\xi = \epsilon_1 - 1/3 \Delta V = 2/3 (\epsilon_1 - \epsilon_3)$$

where ξ = principal shear strain

ϵ_1 = axial strain

ΔV = volumetric strain

In undrained tests $\Delta V = 0$ and the shear strain equals the axial strain. In drained tests $\Delta V \neq 0$ and the shear strain is therefore not equal to the axial strain. Since the effects of distortion are being examined, it appears more reasonable to compare shear strains from drained and undrained tests rather than axial strains.

The maximum deviator stress versus consolidation pressure relationship for undrained tests is shown in Figure 23. It is

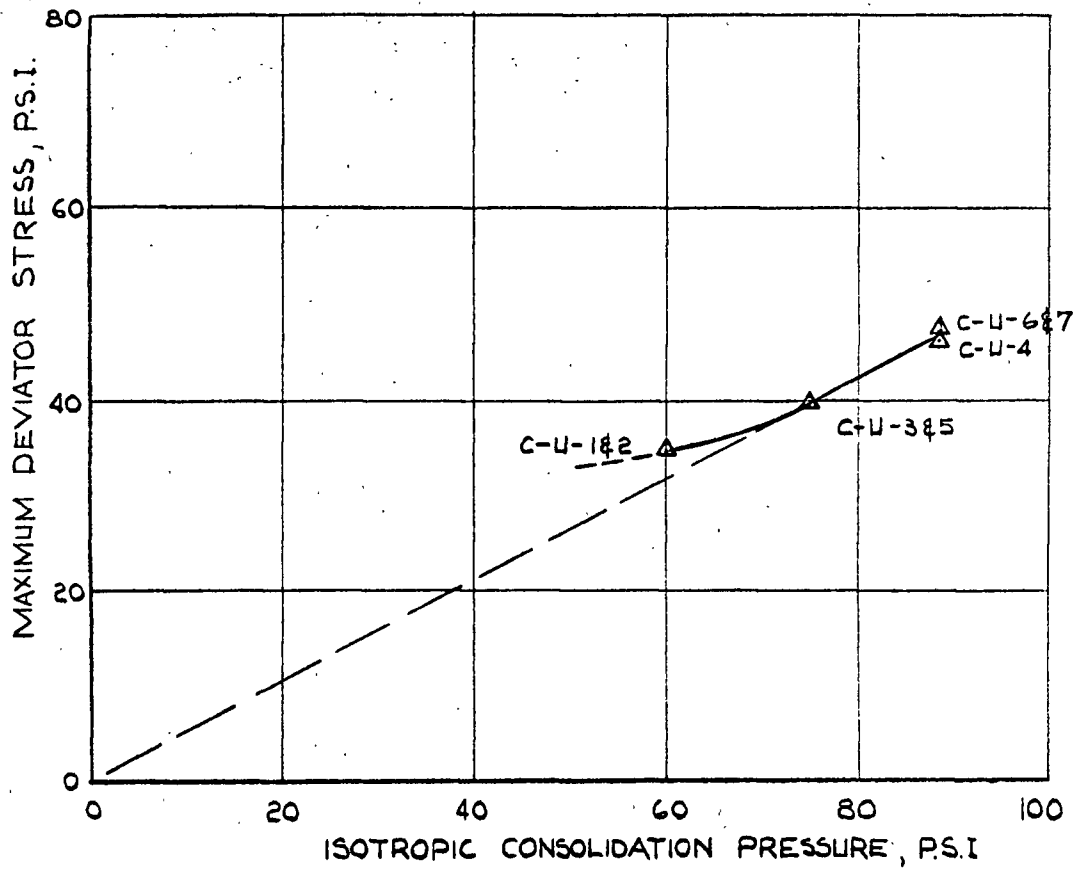


Figure 23 — Relationship Between Undrained Strength and Isotropic Consolidation Pressure, Haney Clay.

seen that while samples consolidated to 75 and 88.5 lbs./sq.in. lie on a straight line passing through the origin as would be expected for normally consolidated material, samples consolidated to 60 lbs./sq.in. show maximum deviator stress above this line, indicating overconsolidation. This is surprising as the water content versus logarithm of consolidation pressure relation appears to be a straight line for pressures greater than 40 lbs./sq. in. It will later be shown that other criteria also indicate that samples consolidated to less than 70 lbs./sq.in. do not behave as normally loaded samples.

Deviator stress, principal stress ratio, pore pressure and the pore pressure parameter A all plotted versus shear strain are shown in Figures 24 to 27 for all undrained tests. Each test is shown by a different symbol so that the reproducibility of results can be examined. It is seen that the maximum deviator stress occurs at about 3 per cent strain, while the maximum principal stress ratio occurs at about 15 per cent strain (Figure 24). Principal stress ratio versus shear strain curves are very similar for all tests and are represented by a single line (Figure 25). Pore pressures (Figure 26) continue to rise with strain, although the rise is very slight from 15 to 30 per cent strain. The A value (Figure 27) increases throughout tests. At maximum deviator stress it is about 1.1, while at maximum principal stress ratio it is about 1.7. At 30 per cent strain it is about 2.3.

Maximum deviator stress occurs at about 3 per cent shear strain in undrained tests, at which time the principal stress ratio is only 2.45. The phenomenon of maximum deviator stress

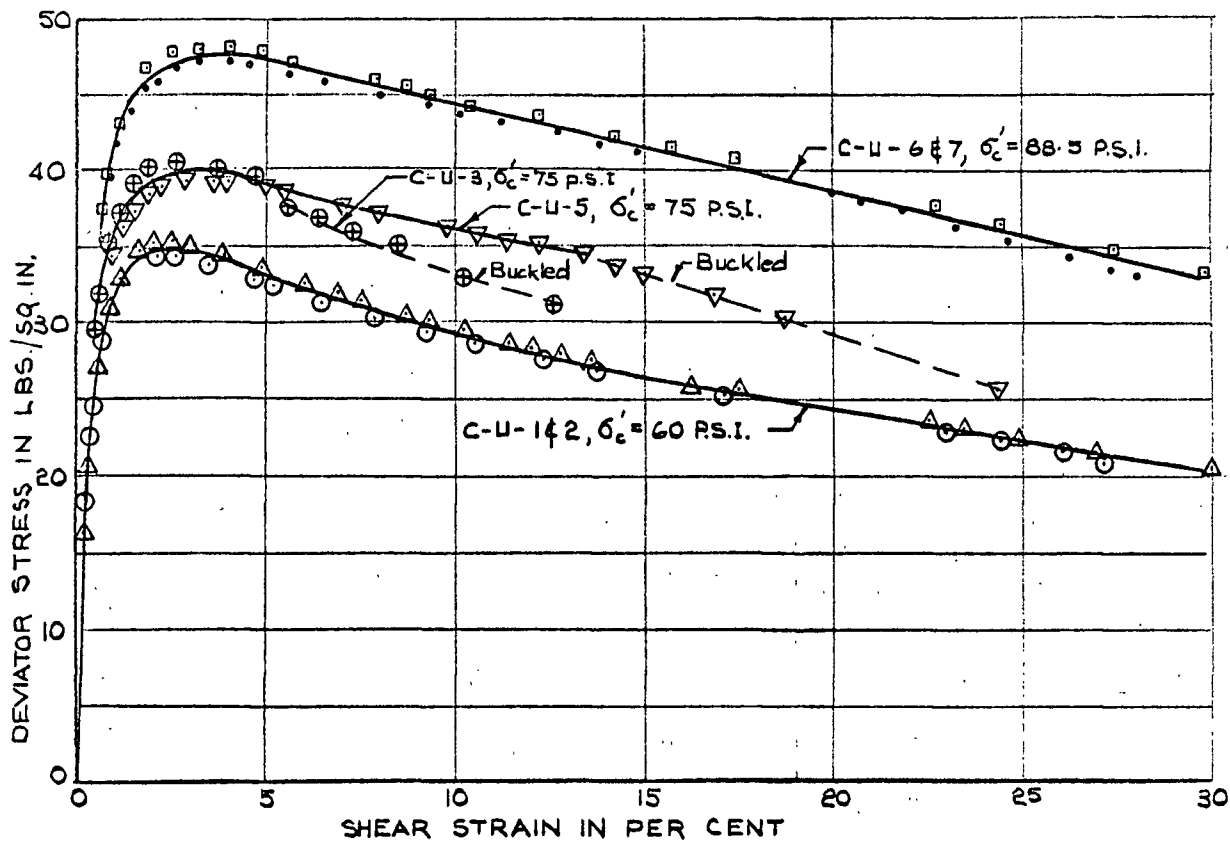


Figure 24 Stress-Strain Relationships for Undrained Tests on Haney Clay

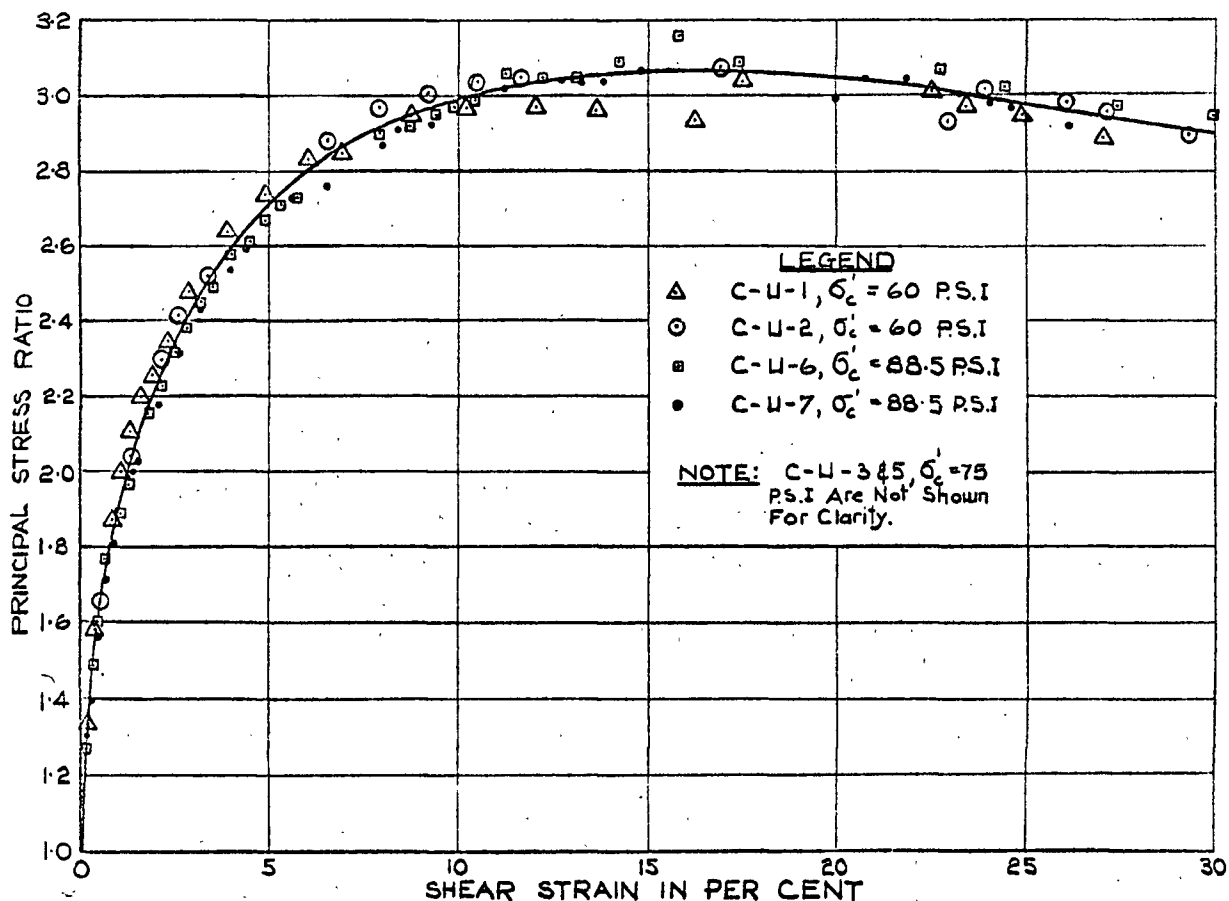


Fig. 25 - Principal Stress Ratio Versus Strain for Undrained Tests on Haney Clay

LEGEND

- △ C-U-1, $\sigma'_c = 60.0$ P.S.I.
- C-U-2, $\sigma'_c = 60.0$ P.S.I.
- ⊕ C-U-3, $\sigma'_c = 75.0$ P.S.I.
- ▽ C-U-5, $\sigma'_c = 75.0$ P.S.I.
- C-U-6, $\sigma'_c = 88.5$ P.S.I.
- C-U-7, $\sigma'_c = 88.5$ P.S.I.

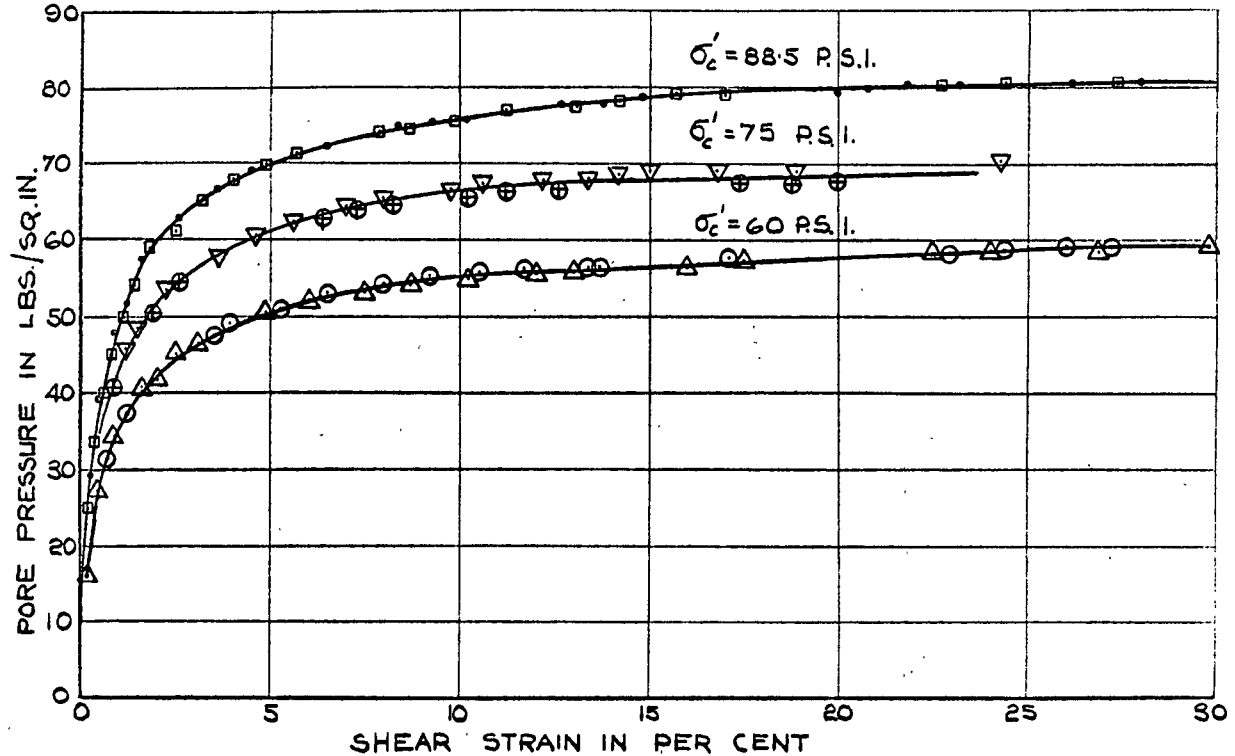


Figure 26—Relationship Between Pore Pressure and Strain For Undrained Tests on Honey Clay

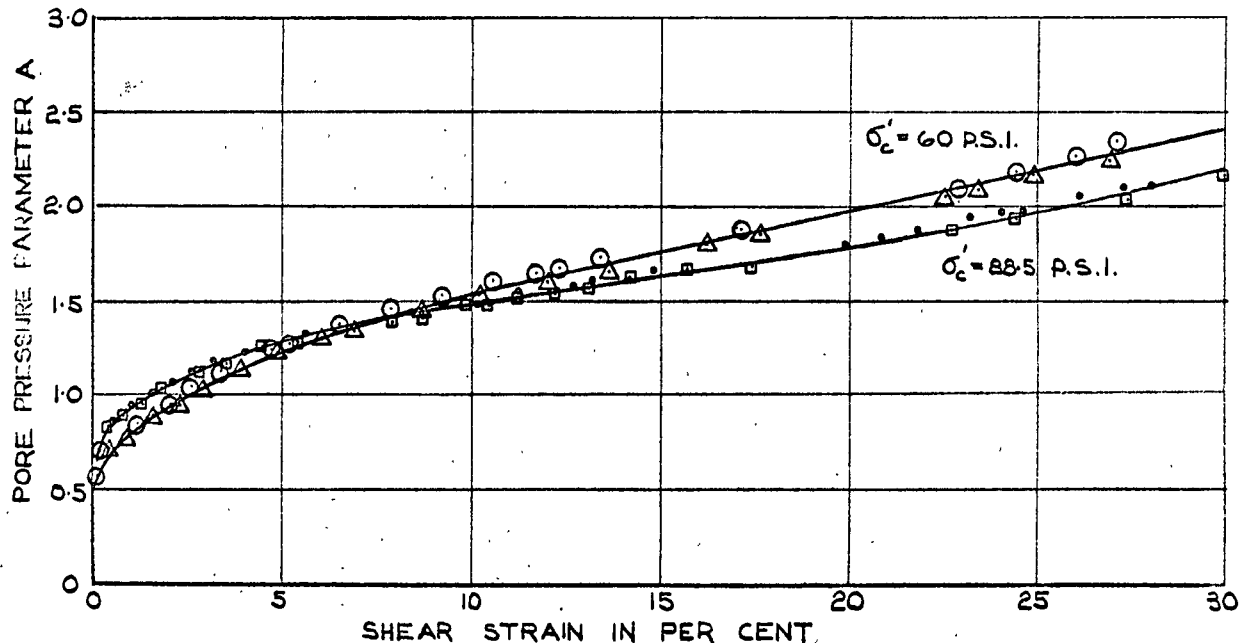


Figure 27—Pore Pressure Parameter A Versus Strain for Honey Clay

occurring before maximum principal stress ratio appears to be a characteristic of sensitive clays and is caused by the pore pressure continuing to rise after maximum deviator stress has been reached. Bjerrum and Simons (1960) found similar results from undrained tests on undisturbed sensitive Norwegian clays. They felt that the lower principal stress ratio or friction angle at maximum deviator stress was due to the fact that not all the available shearing resistance was being mobilized at the low strain. It will be shown in Section 4 of this chapter that increasing pore pressures cause release of internal energy in undrained tests which when corrected for by the Roscoe energy equation suggests that the full "friction angle" is being mobilized at all strains.

Deviator stress versus shear strain relations for all drained tests are shown in Figure 28. It may be seen that a marked kink occurs in the deviator stress at about $1\frac{1}{2}$ per cent strain for samples consolidated to 40 lbs./sq.in., a smaller kink occurs for those consolidated to 55 lbs./sq.in. This is further evidence of overconsolidation at the lower consolidation pressures, but the effect appears to be lost at about 6 per cent strain. Maximum deviator stress occurs at about 26 per cent strain. Residual pore pressures calculated by Method 2 and discussed in Chapter 6 are shown in Figure 29. Maximum average excess pore pressures occur at about 5 per cent strain and vary from 2.5 lbs./sq.in. for samples consolidated to 40 lbs./sq.in. to 4.1 lbs./sq.in. for samples consolidated to 70 lbs./sq.in. At maximum deviator stress excess pore pressures were about 0.9 lbs./sq.in. and 1.2 lbs./sq.in. respectively for samples consolidated to 40 and 70 lbs./sq.in.

LEGEND

- △ S-12, $\sigma'_c = 40$ Lbs./Sq.In.
- ▽ S-13, $\sigma'_c = 55$ Lbs./Sq.In.
- S-14, $\sigma'_c = 70$ Lbs./Sq.In.
- S-15, $\sigma'_c = 70$ Lbs./Sq.In.
- ⊕ S-16, $\sigma'_c = 55$ Lbs./Sq.In.
- S-17, $\sigma'_c = 40$ Lbs./Sq.In.

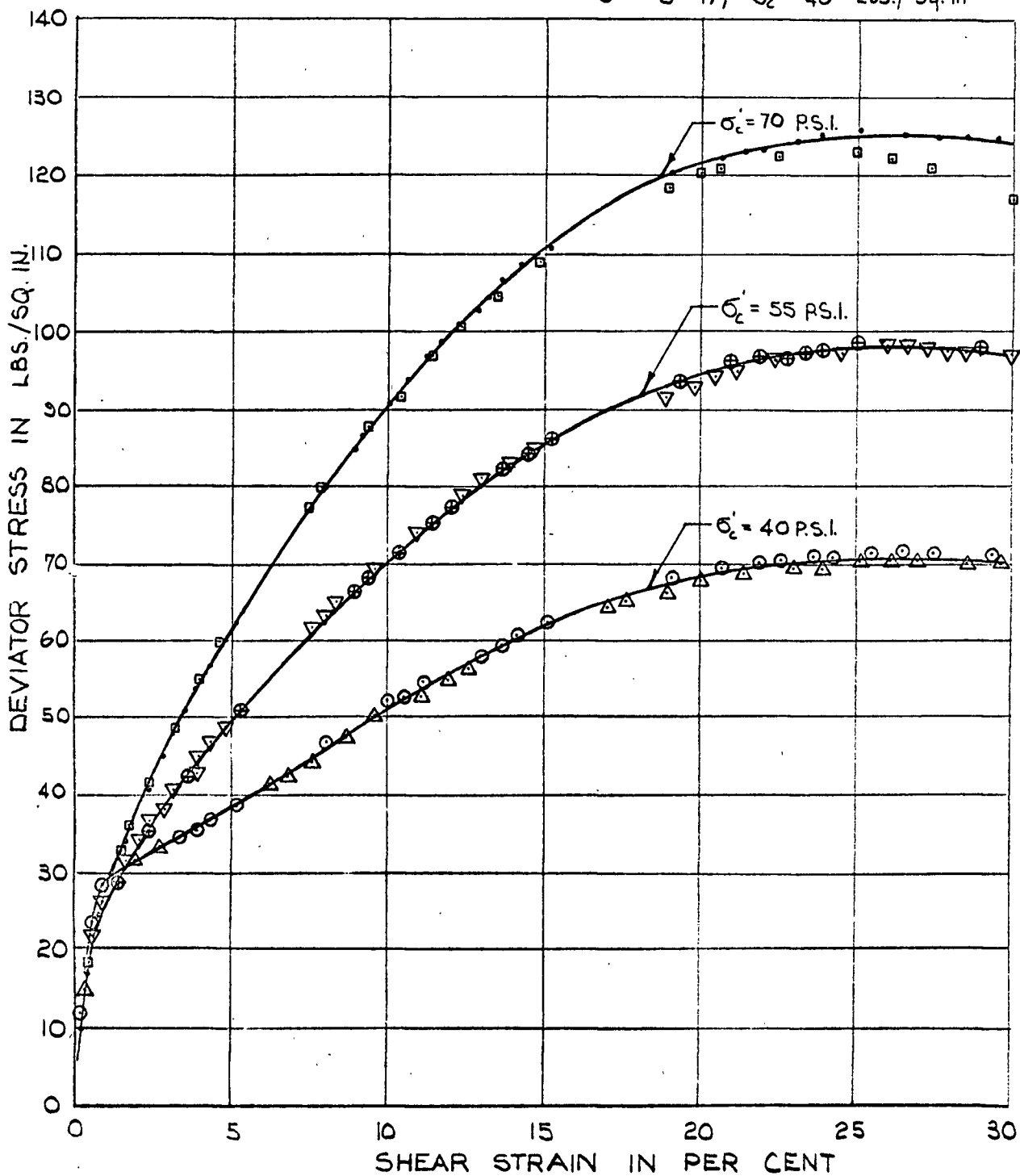


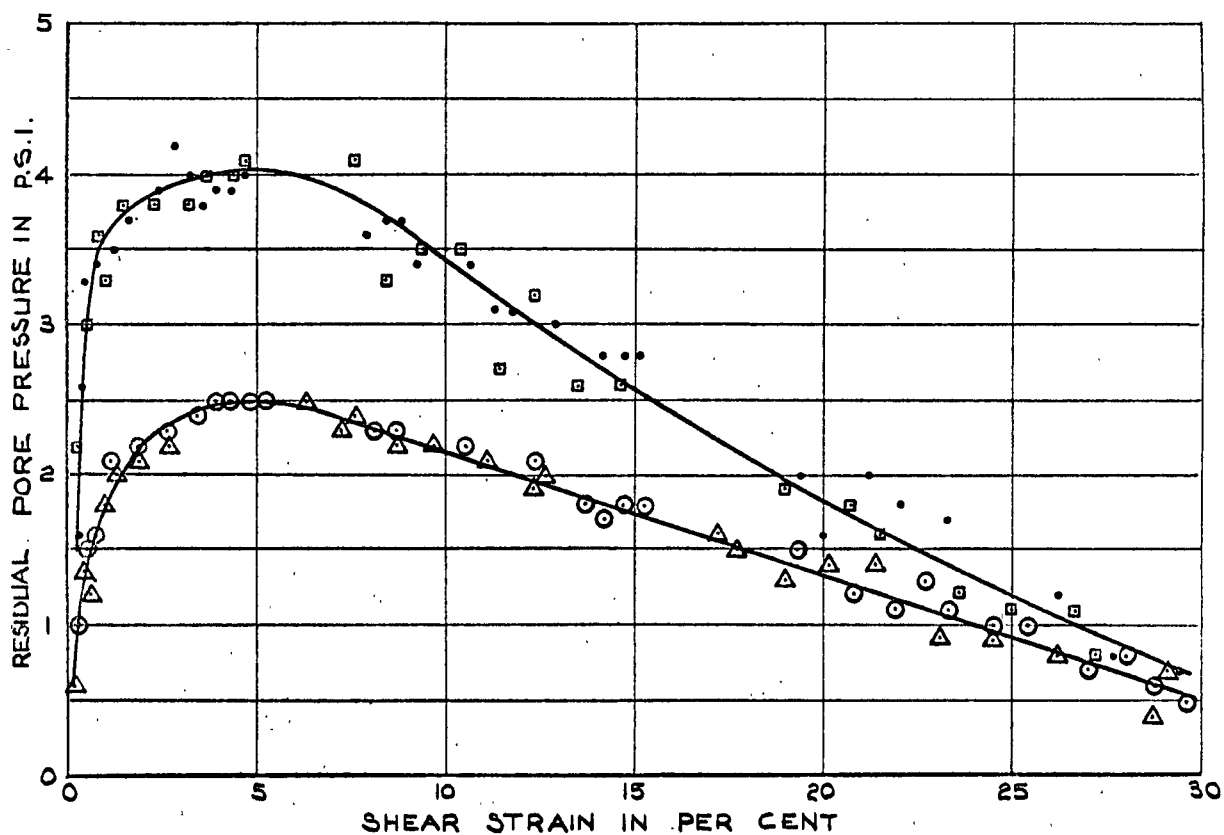
Figure 28— Stress-Strain Relationships for Drained Tests on Hanev Clay

LEGEND

- Δ S-12, $\sigma_c' = 40$ Lbs./sq. In.
 \square S-14, $\sigma_c' = 70$ Lbs./sq. In.
 \bullet S-15, $\sigma_c' = 70$ Lbs./sq. In.
 \circ S-17, $\sigma_c' = 40$ Lbs./sq. In.

S-12 ~ Consolidated Drained
Test No. 12

σ_c' ~ Effective Isotropic Consolidation
Pressure

NOTE

1. Excess Pore Pressures Calculated By Method 2
2. Tests at $\sigma_c' = 55$ p.s.i. Not shown for the sake of clarity

Figure 29 - Calculated Residual Pore Pressure Vs. Strain for Consolidated Drained Tests on Honey Clay

The effect of residual pore pressures on the principal stress ratio in drained tests is seen to be small (Figure 30). The principal stress ratio versus shear strain relations for all drained tests are shown in Figure 31. These have been corrected for residual pore pressures. It is seen that the curves are identical except at strains below about 7 per cent. It is thought that the separation of curves at low strain is due to an overconsolidation effect present at the lower confining pressures. Maximum principal stress ratio for drained tests occurs at about 25 per cent shear strain.

A comparison of principal stress ratio versus shear strain relationships from both drained and undrained tests is shown in Figure 32. It may be seen that the undrained material is much stiffer than the drained. Maximum principal stress ratio equal to 3.05 occurs at about 15 per cent strain in undrained tests while the maximum principal stress ratio in drained tests is 2.82 and occurs at about 25 per cent strain.

7.3 Comparison of contours of water content from drained and undrained tests

Contours of water content determined from drained and undrained tests on Haney clay are shown plotted in principal effective stress space in Figure 33. It may be seen that the contours of water content from drained and undrained tests have quite different shapes. Thus, for Haney clay, there does not appear to be a unique relationship between effective stresses and water content.

The data shown in Figure 33 was prepared from the effective stress paths shown in Figures 34 and 35. Stress paths from un-

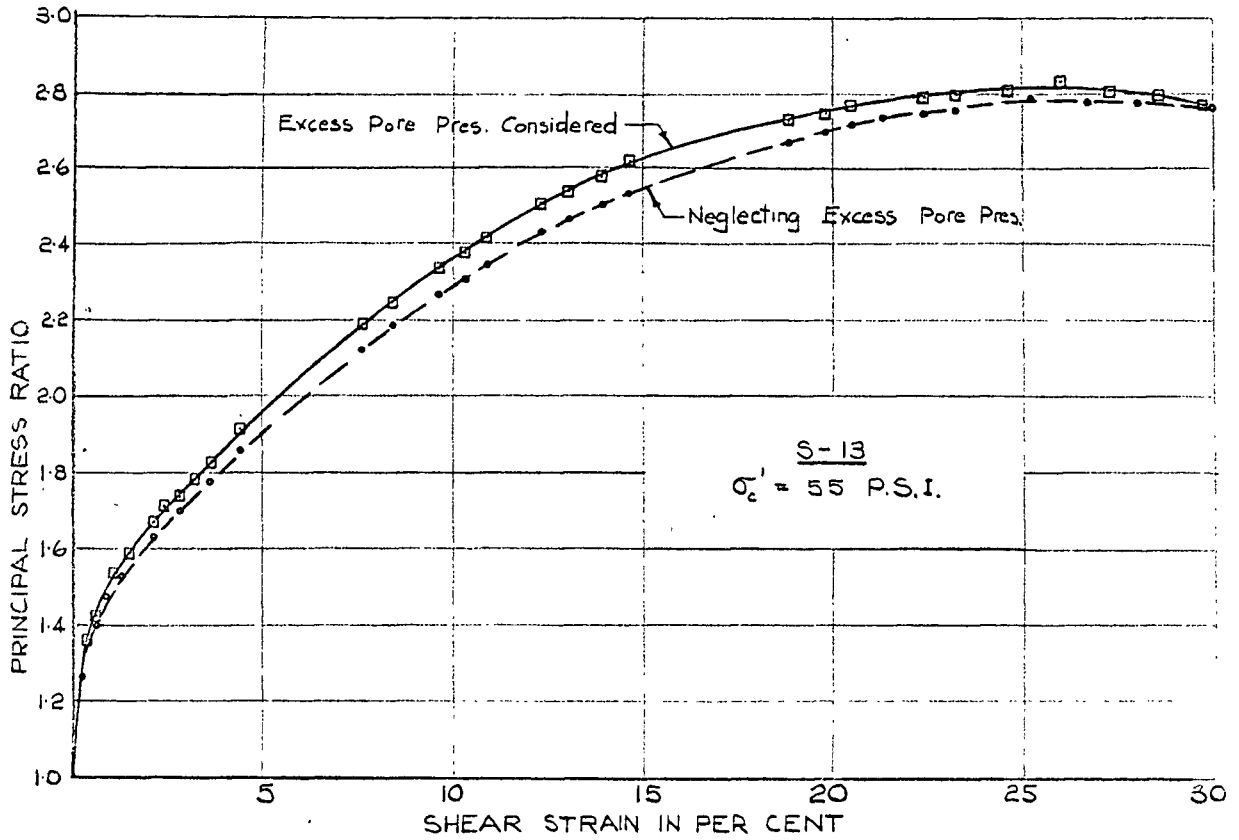


Figure 30 — Effect of Residual Excess Pore Pressure on the Principal Stress Ratio Vs. Shear Strain Relation in Test S-13

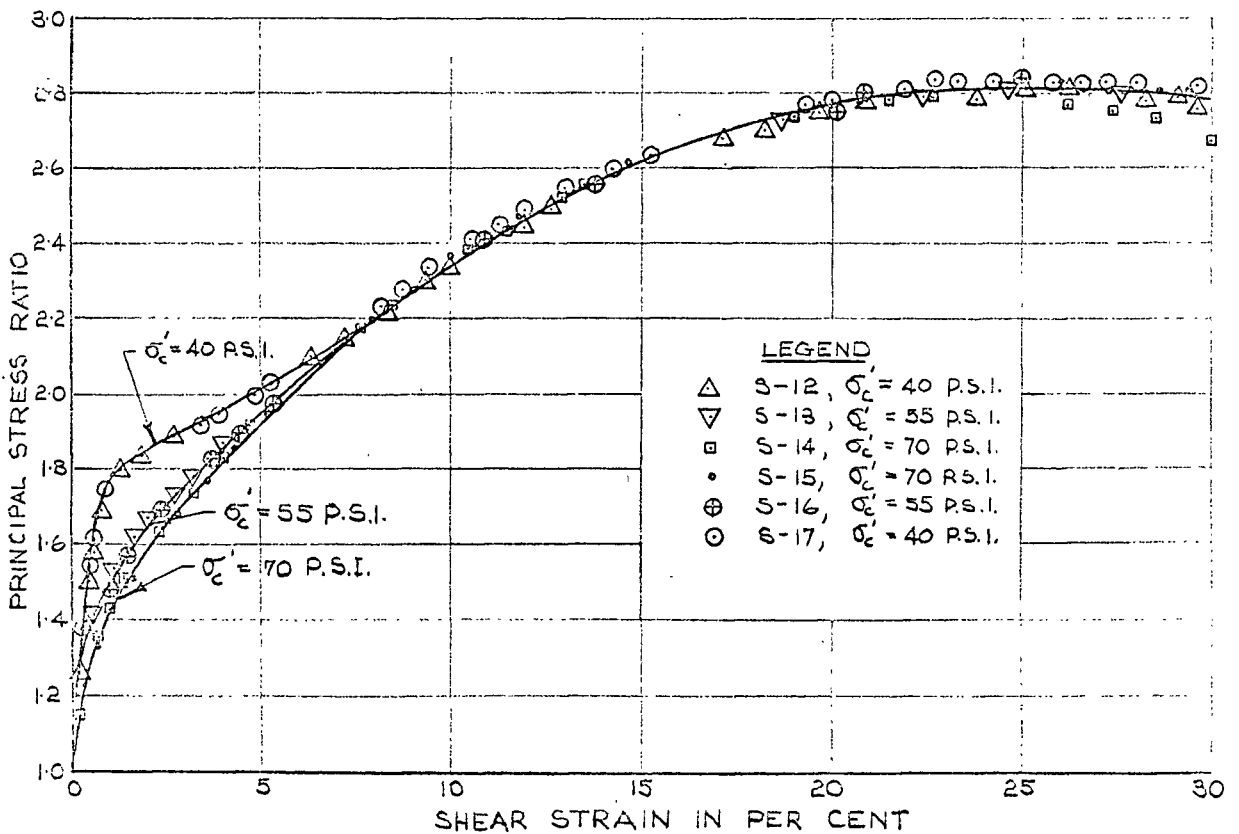


Figure 31 — Relationships Between Principal Stress Ratio and Strain from Drained Tests on Honey Clay

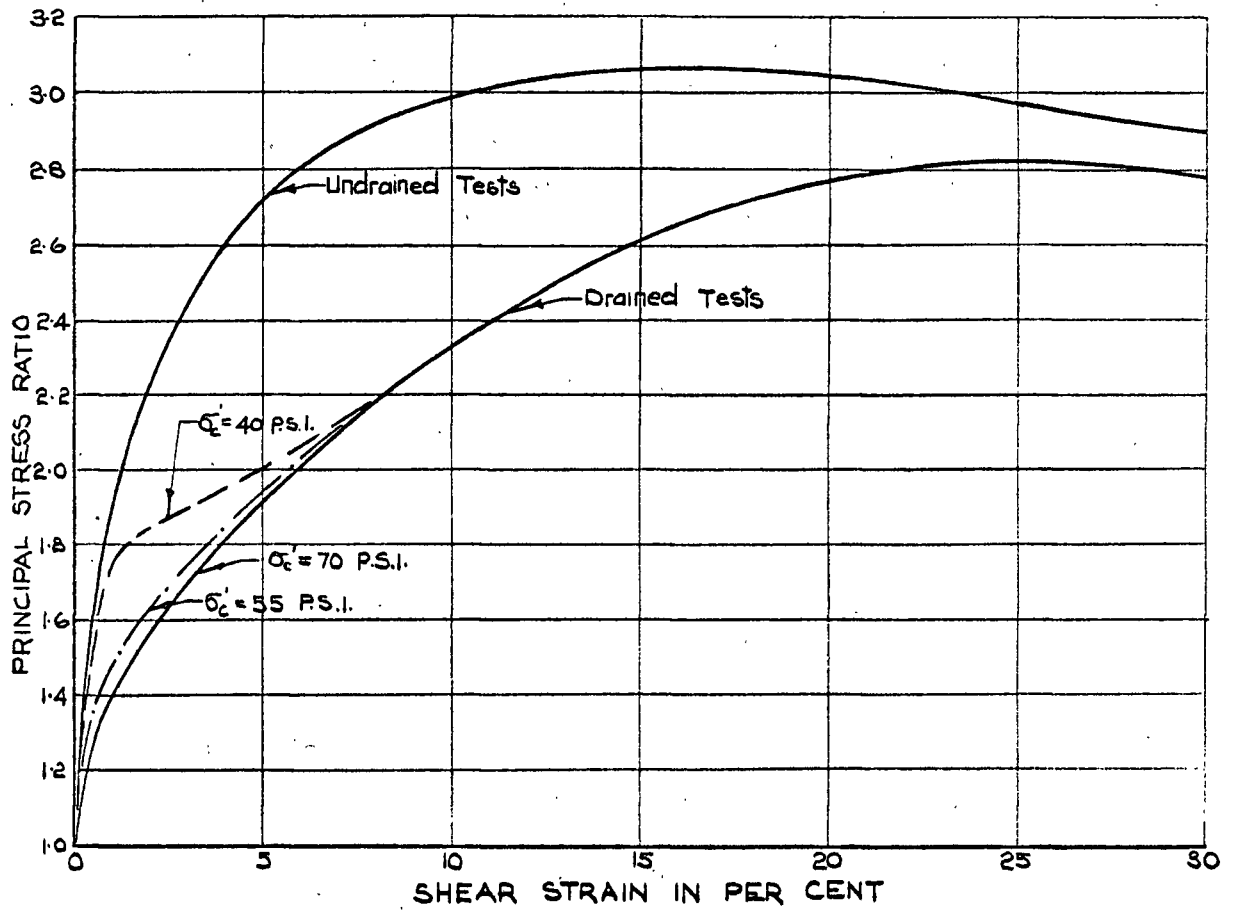


Figure 32—Comparison of Principal Stress Ratio Vs. Strain Relationships From Drained and Undrained Tests on Honey Clay

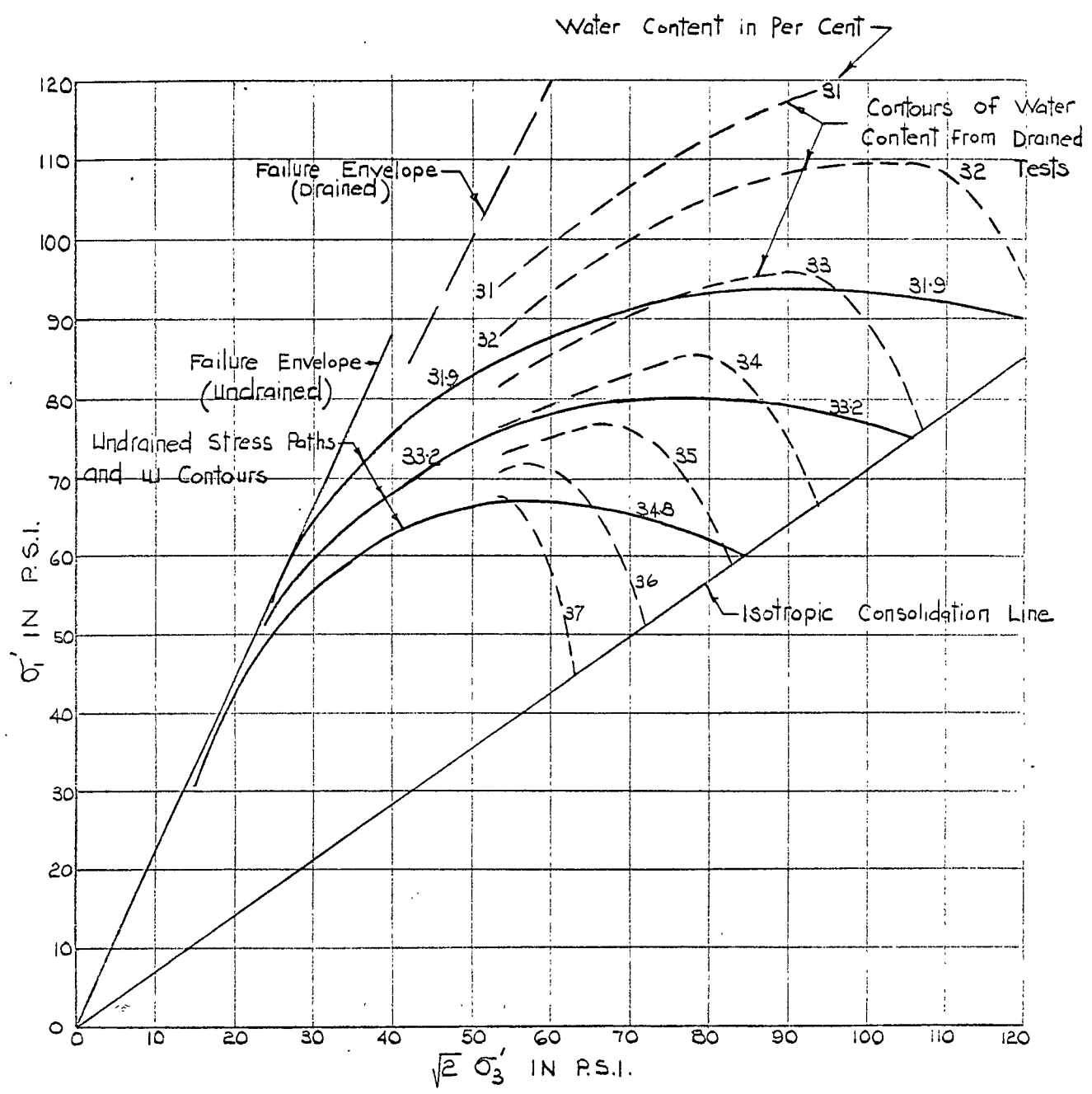


Figure 33—Comparison of Contours of Water Content from Drained and Undrained Tests on Haney Clay

LEGEND

- △ C-U-1, $\sigma'_c = 60$ P.S.I.
- ⊙ C-U-2, $\sigma'_c = 60$ P.S.I.
- C-U-3, $\sigma'_c = 75$ P.S.I.
- ▽ C-U-5, $\sigma'_c = 75$ P.S.I.
- C-U-6, $\sigma'_c = 88.5$ P.S.I.
- C-U-7, $\sigma'_c = 88.5$ P.S.I.

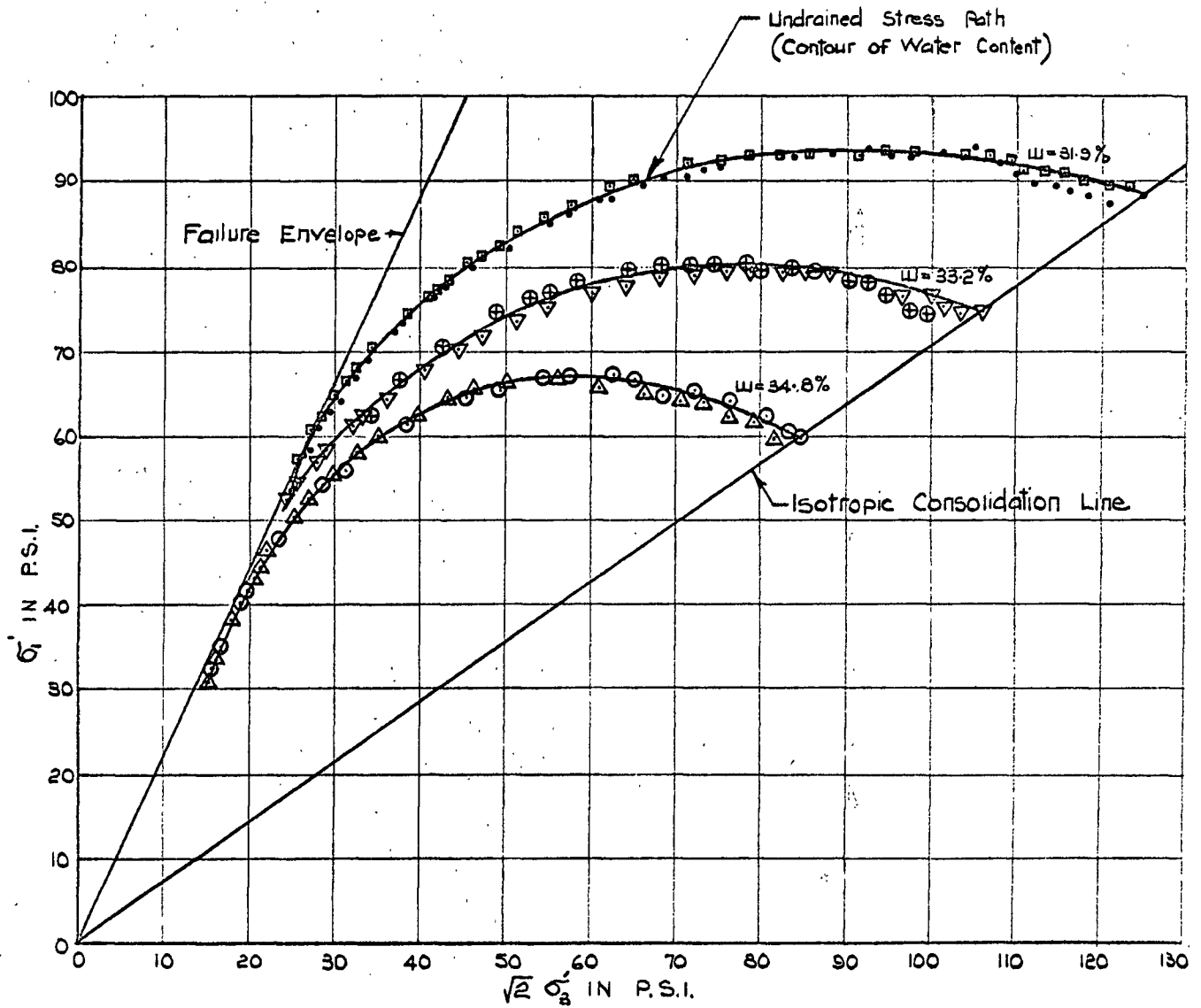


Figure 34 — Effective Stress Paths From Consolidated Undrained Tests on Hanev Clay

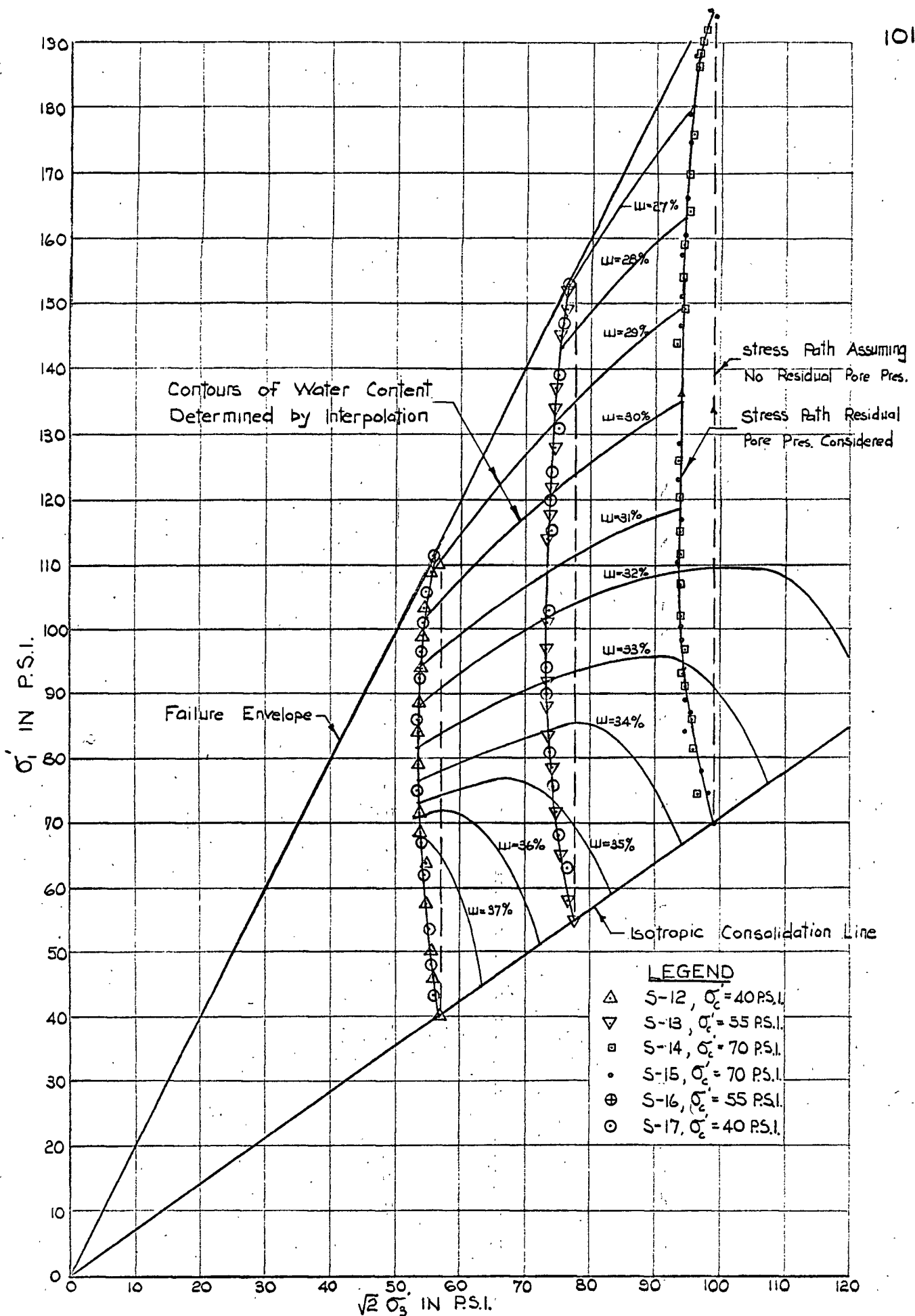


Figure 35 — Effective Stress Paths And Contours of Water Content From Drained Tests

drained tests are shown in Figure 34 and these are also contours of water content. Stress paths from drained tests are shown in Figure 35. Generally drained stress paths plot as vertical lines in the Rendulic diagram, but due to the presence of residual pore pressure, the stress paths plot as curves. Water contents were known at all stages of drained tests allowing contours of water content to be drawn and these are also shown in Figure 35.

It was stated in Section 7.2 that drained and undrained test specimens did not lie on a common isotropic consolidation line. It was assumed for the purpose of comparing contours of water content that drained and undrained samples had consolidated water contents which lay on the isotropic consolidation line for drained samples. However, Figure 33 indicates that the shapes of water content contours determined from drained and undrained tests are quite different. So that, even if values of water content were not assigned to the contours of water content from undrained tests, it could be concluded from the shape alone that contours of water content are not unique for Haney clay.

Due to the small number of tests performed, the Rendulic diagram is not a very satisfactory method of checking the hypothesis. The unique relationship between effective stresses and water content is identical to the Roscoe concept of a state boundary surface discussed in Chapter 2. Poorooshasb (1961) developed a method by which the three dimensional surface could be shown as a line in two dimensions. Burland (1965) suggested an even simpler method of showing this surface in two dimensions. His method is basically identical to that proposed by Rendulic in developing the unified Rendulic diagram to compare the geometry

of constant water content curves. The stresses p' and q at any stage of drained or undrained tests are divided by p'_e , which is the pressure on the isotropic consolidation line corresponding to the particular void ratio of the sample at the time p' and q are measured. For undrained tests p'_e is constant and equal to the initial consolidation pressure. In drained tests p'_e increases from the initial consolidation pressure to the pressure on the isotropic consolidation line corresponding to the final void ratio.

The surfaces for all undrained tests are shown in Figure 36. It is seen that tests consolidated to 75 and 88.5 lbs./sq.in. lie on the same line or surface, while tests consolidated to 60 lbs./sq.in. are clearly on a separate line. It was mentioned earlier that samples consolidated to 60 lbs./sq.in. behave in an overconsolidated manner, and it is this overconsolidation effect that is thought responsible for the separation of curves shown. The state boundary surfaces for drained tests are shown in Figure 37. It is seen that drained tests from each consolidation pressure lie on a different surface. This was to be expected since samples below a consolidation pressure of about 70 lbs./sq.in. behave in an overconsolidated manner and hence would not lie on the normally loaded surface. It may be seen that tests consolidated to 55 and 70 lbs./sq.in. are reasonably similar, while tests consolidated to 40 lbs./sq.in. are quite different. Since the overconsolidation effect is reducing with increased consolidation pressure this result could be expected.

In Figure 38 yield surfaces from drained and undrained tests are compared. Only drained tests at a consolidation pressure of 70 lbs./sq.in. are shown since these alone of the drained

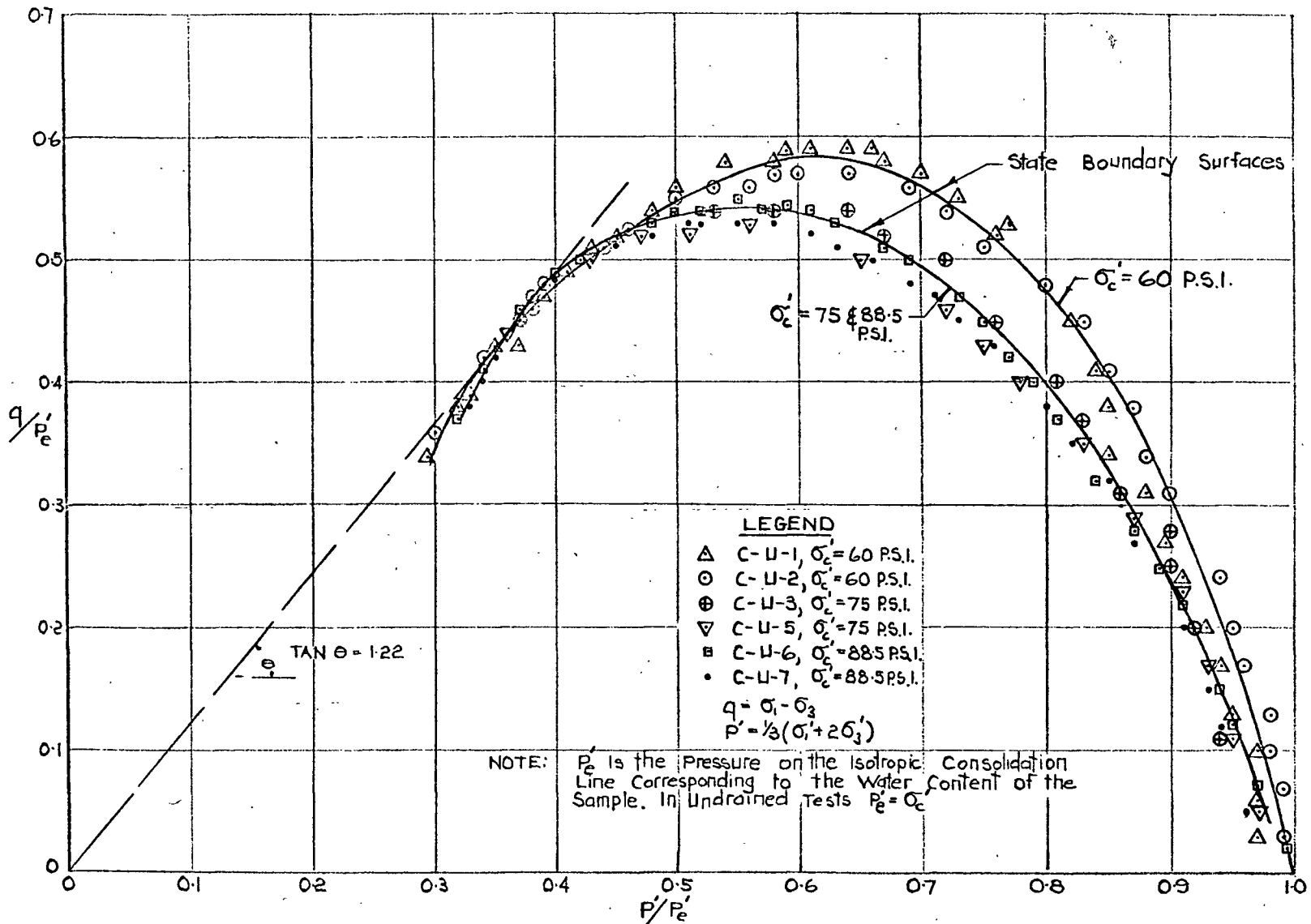


Figure 36 - State Boundary Surfaces from Undrained Tests on Haney Clay (Burland Plot)

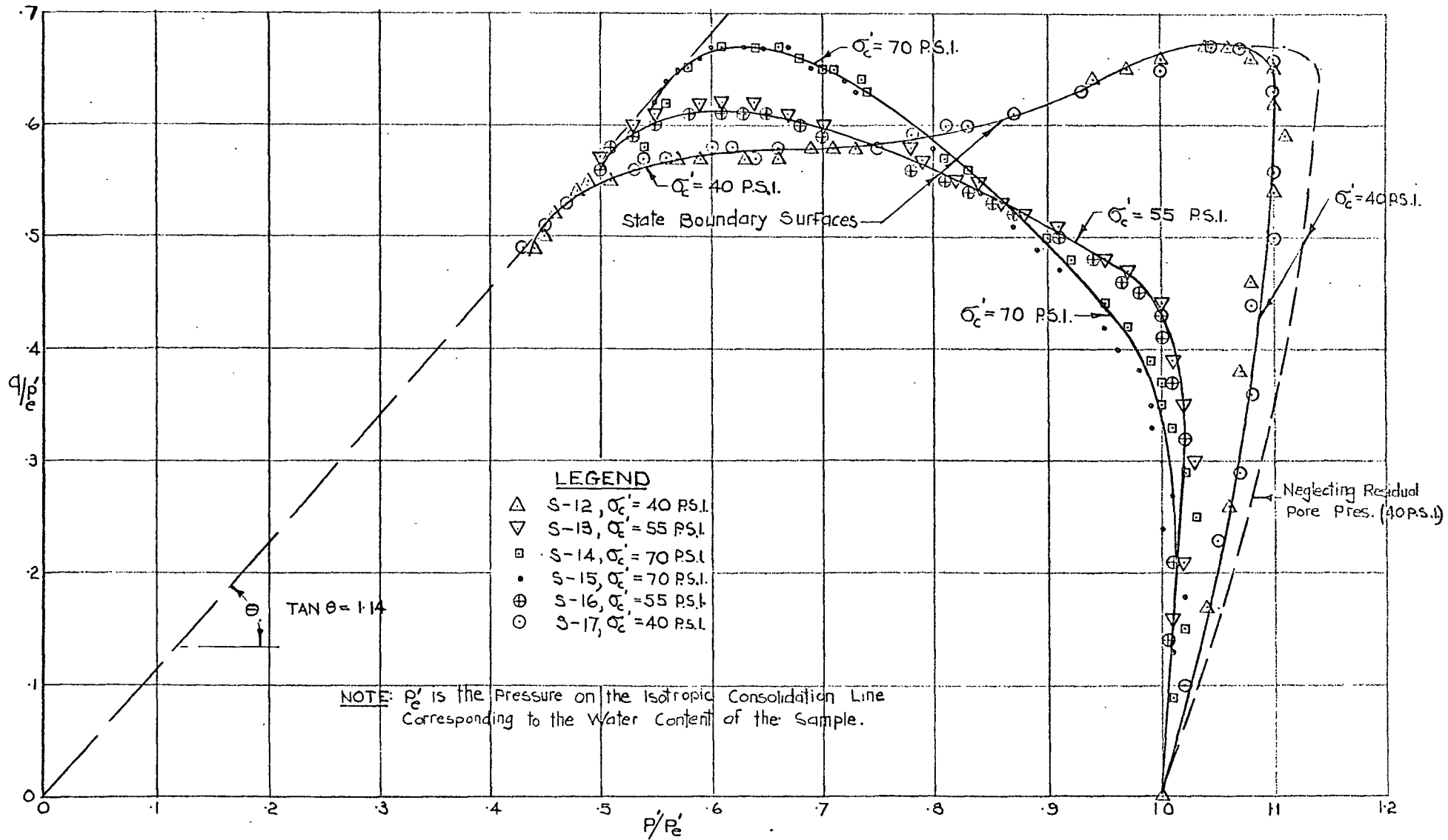


Figure 37—State Boundary Surfaces from Drained Tests on Honey Clay (Burland Plot)

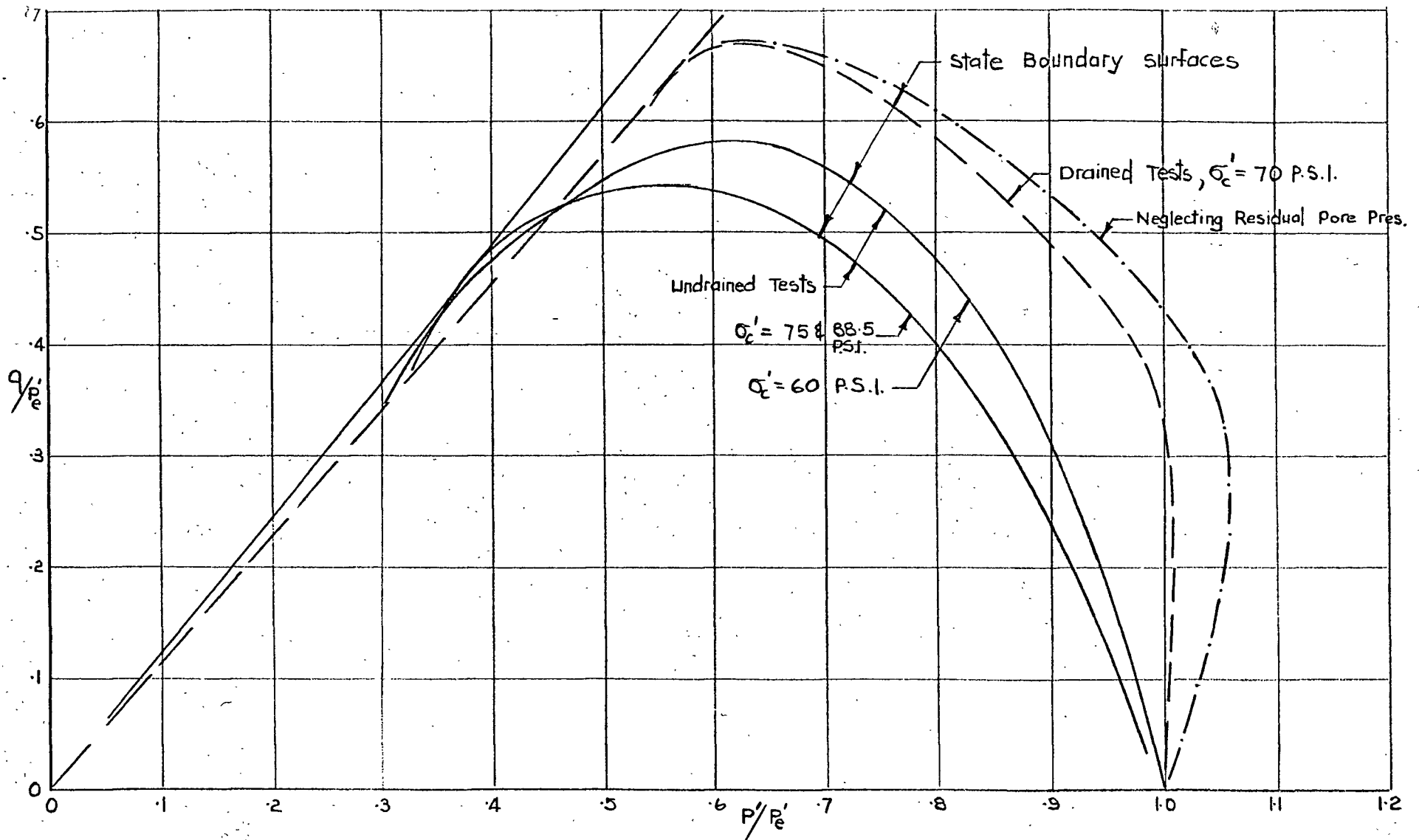


Figure 38 - Comparison of State Boundary Surfaces from Drained and Undrained Tests on Honey Clay.

tests behave in a truly normally loaded manner. Residual pore pressures were allowed for in calculating drained yield surfaces (residual pore pressures are always allowed for unless otherwise stated) but the effect of neglecting them is also shown. It is seen that drained and undrained tests do not lie on the same surface and that neglecting the residual pore pressures in drained tests results in even poorer agreement. Since the drained tests at a consolidation pressure of 70 lbs./sq.in. also lie outside the undrained tests at 60 lbs./sq.in. the effect of overconsolidation cannot be responsible for the lack of agreement. This substantiates the findings from the Rendulic diagram of Figure 33 and indicates that there is not a unique relationship between effective stresses and water content for Haney clay or that the state boundary surfaces are not the same for drained and undrained stress paths.

It may be of interest to note that had drained tests been corrected for energy due to volume change as suggested by Roscoe, Schofield and Wroth (1958), the drained surface would be even further removed from the undrained. The concept of applying an energy correction to determine the state boundary surface is no longer considered valid. Roscoe and Schofield (1963) indicate that no energy correction should be applied to test data when determining the state boundary surface.

7.4 Energy corrections

Energy components of shear strength were discussed in Chapters 2 and 3 and it appears that the Roscoe and Schofield (1963) energy equation which considers both boundary and internal elastic energy changes is the most logical. This energy equation has been applied

to the Haney clay test data and the results are in reasonable agreement with the predictions of the equation.

The equation is as follows:

$$p' \delta V + q \delta \xi = \frac{K \delta p'}{1 + e} + M p' \delta \xi \quad \text{---- (16)}$$

where δV = incremental volumetric strain

$\delta \xi$ = incremental distortional strain

K = slope of e Vs. $\ln p'$ on rebound or reload

and M = ratio of q to p' at failure.

The terms on the left hand side of the equation refer to the energy transferred across the boundaries per unit volume and the terms on the right hand side determine to what use this energy is put. $\frac{K \delta p'}{1 + e}$ represents energy stored or released elastically, while $M p' \delta \xi$ represents energy dissipated by shearing stresses. $M p' = q_w$ can be considered as the internal shear stress and by definition lies on the failure envelope $q = M p'$. Equation (16) can therefore be written in the following form:

$$q_w = M p' = q + p' \frac{\delta V}{\delta \xi} - \frac{K \delta p'}{(1+e) \delta \xi} \quad \text{---- (17)}$$

This equation implies that whenever yielding or slip at grain contacts is occurring the relation between the corrected q (q_w) and p' is always constant and therefore drained and undrained tests corrected for both boundary and internal energy should have stress paths which lie on the straight line $q = M p'$. This was shown diagrammatically in Figure 5, Chapter 2.

The isotropic consolidation and rebound lines for Haney clay are shown in Figure 39. The coefficient of expansion, C_e , was

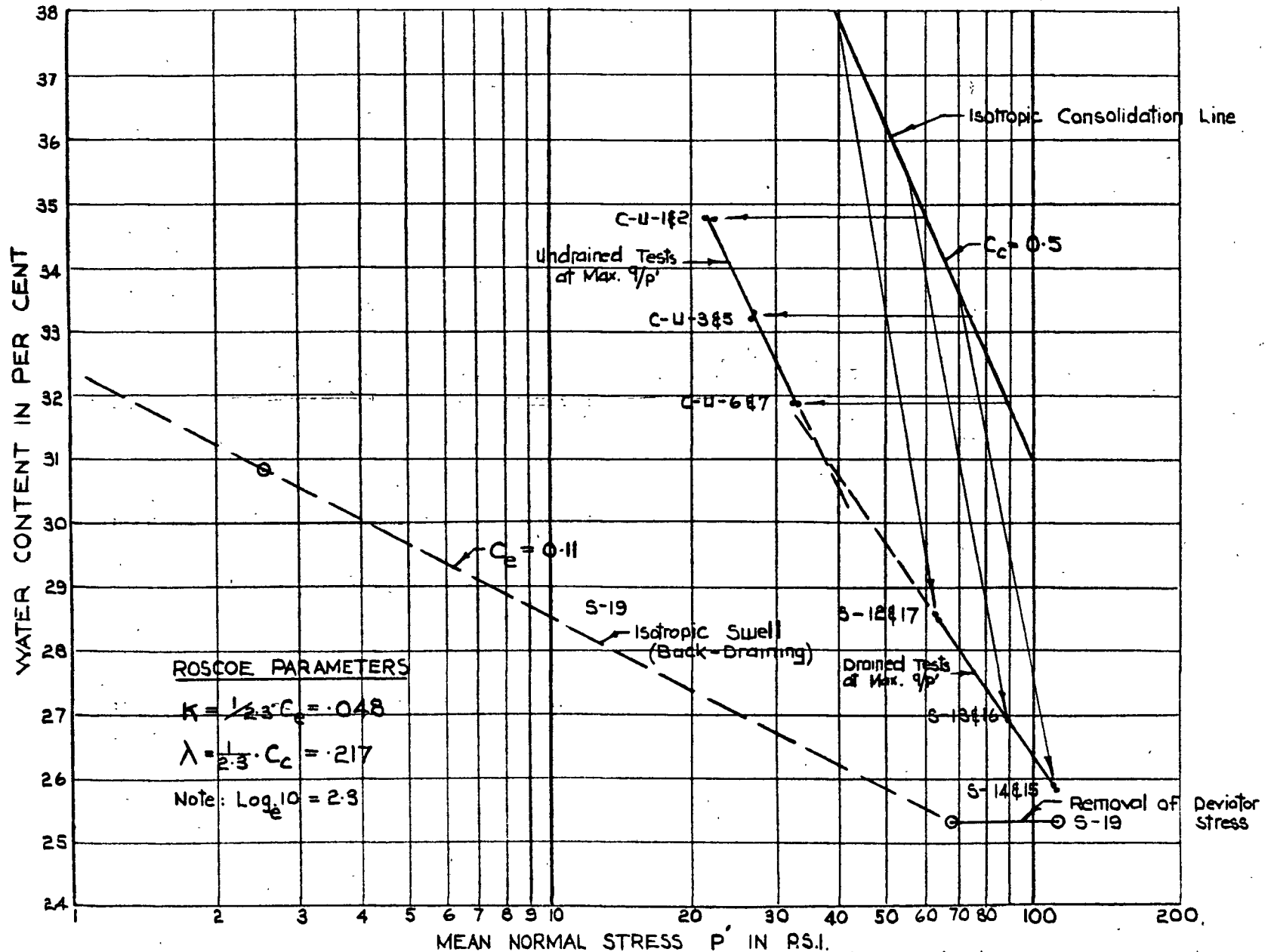


Figure 39—Relationships Between Mean Normal Stress and Water Content for Honey Clay

calculated to be 0.11, and K , which is the slope of void ratio versus natural logarithm of pressure plot is therefore 0.048. Since the computer was used to analyze test results q_w was readily obtained for all readings. Hand calculations of incremental distortional and volumetric strains would have been very time consuming since the incremental strains at the times of readings cannot be directly calculated but must be estimated by averaging the adjacent increments. In addition, the length and volume of sample to be used when calculating strain increments are not the initial ones but rather those existing at the time in question.

The corrected stress paths for all undrained tests are shown in Figure 40. It is seen that the corrected deviator stresses lie close to a straight line for all tests and for all strains greater than about 0.5 per cent. Most of the point scatter shown occurs at strains of less than 0.5 per cent. Figure 41 shows corrected stress paths for all drained tests. Here the points fall within a band rather than on a line. It appears that the M value is decreasing with strain. A plot of M versus strain for a drained and an undrained test is shown in Figure 42. M is seen to decrease with strain, slightly in the case of undrained tests and somewhat more in the case of drained tests. Considering that Haney clay is an extra-sensitive material and that the Roscoe energy equation was developed for an idealized continuum material, the results, especially those for undrained tests appear to be in reasonable agreement with the theory. Scatter in M values at low strain may be due to errors in readings at low strain at which time stresses are changing very rapidly and readings are closely spaced. Alter-

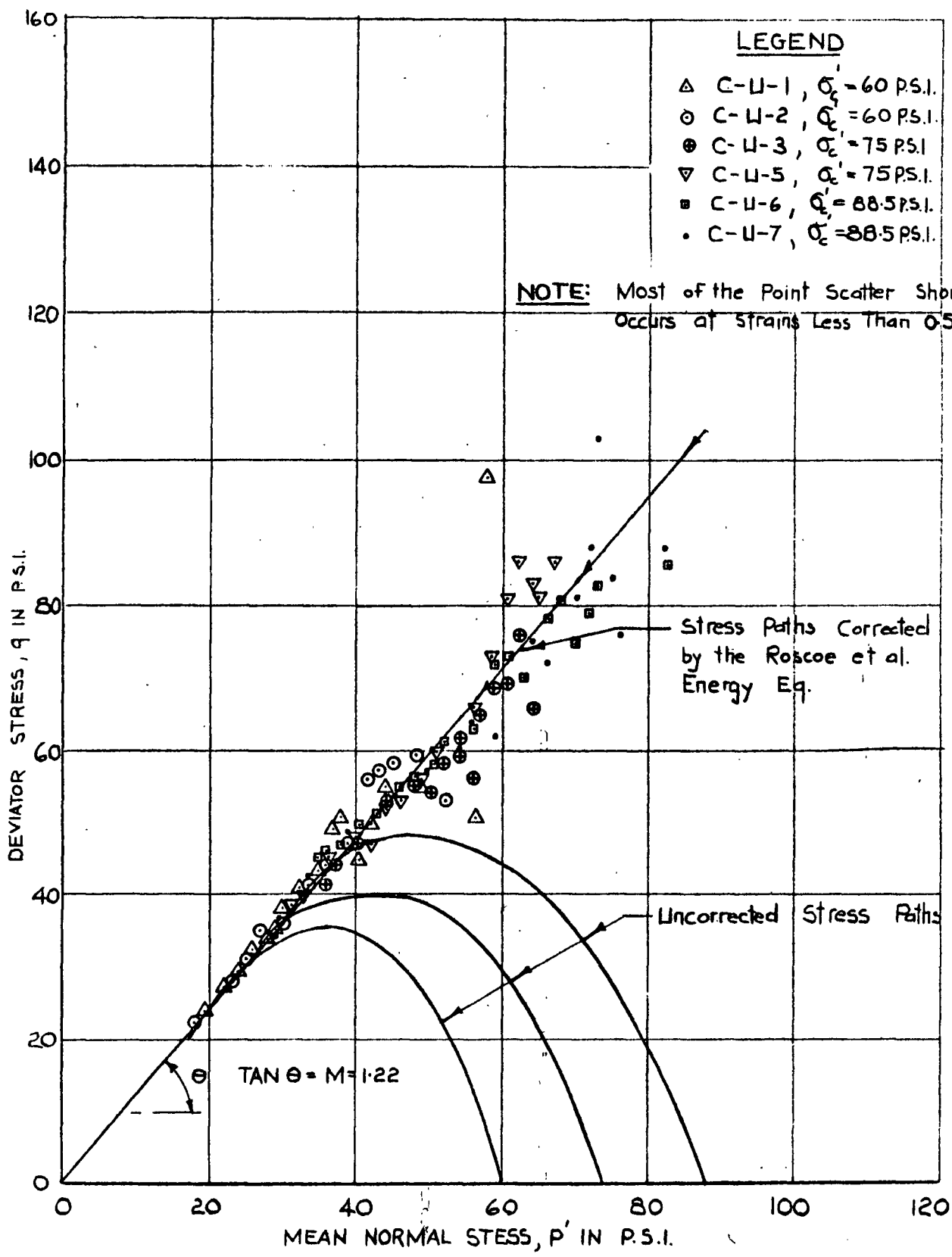


Figure 40—Corrected and Uncorrected Stress Paths From Undrained Tests On Haney Clay (Roscoe et al. Energy Eq.)

LEGEND

- △ S-12, $\sigma'_c = 40$ P.S.I.
- ▽ S-13, $\sigma'_c = 55$ P.S.I.
- S-14, $\sigma'_c = 70$ P.S.I.
- ◻ S-15, $\sigma'_c = 70$ P.S.I.
- S-16, $\sigma'_c = 55$ P.S.I.
- ⊕ S-17, $\sigma'_c = 40$ P.S.I.

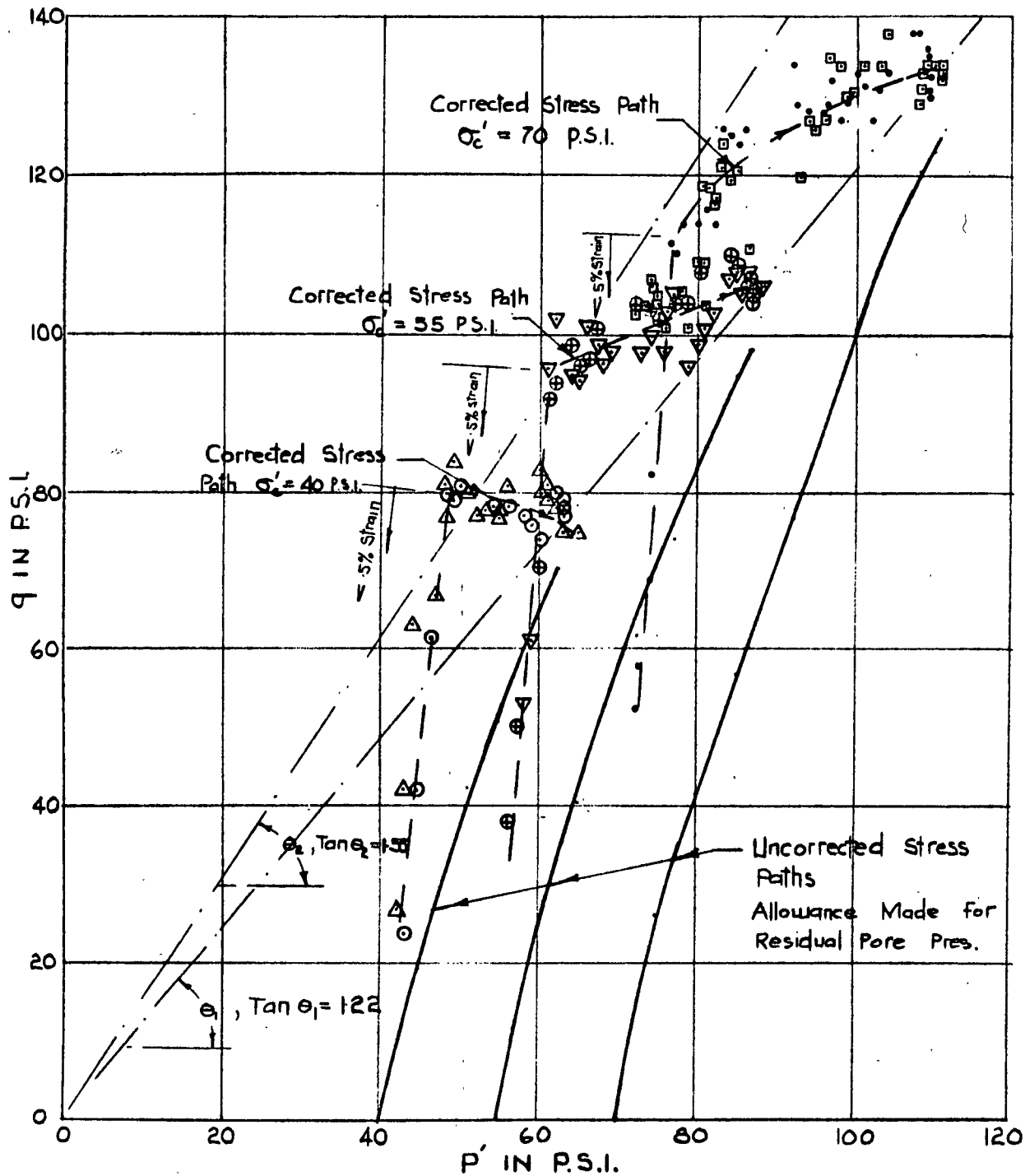


Figure 41 - Corrected and Uncorrected Stress Paths from Drained Tests On Haney Clay (Roscoe et. al. Energy Eq.)

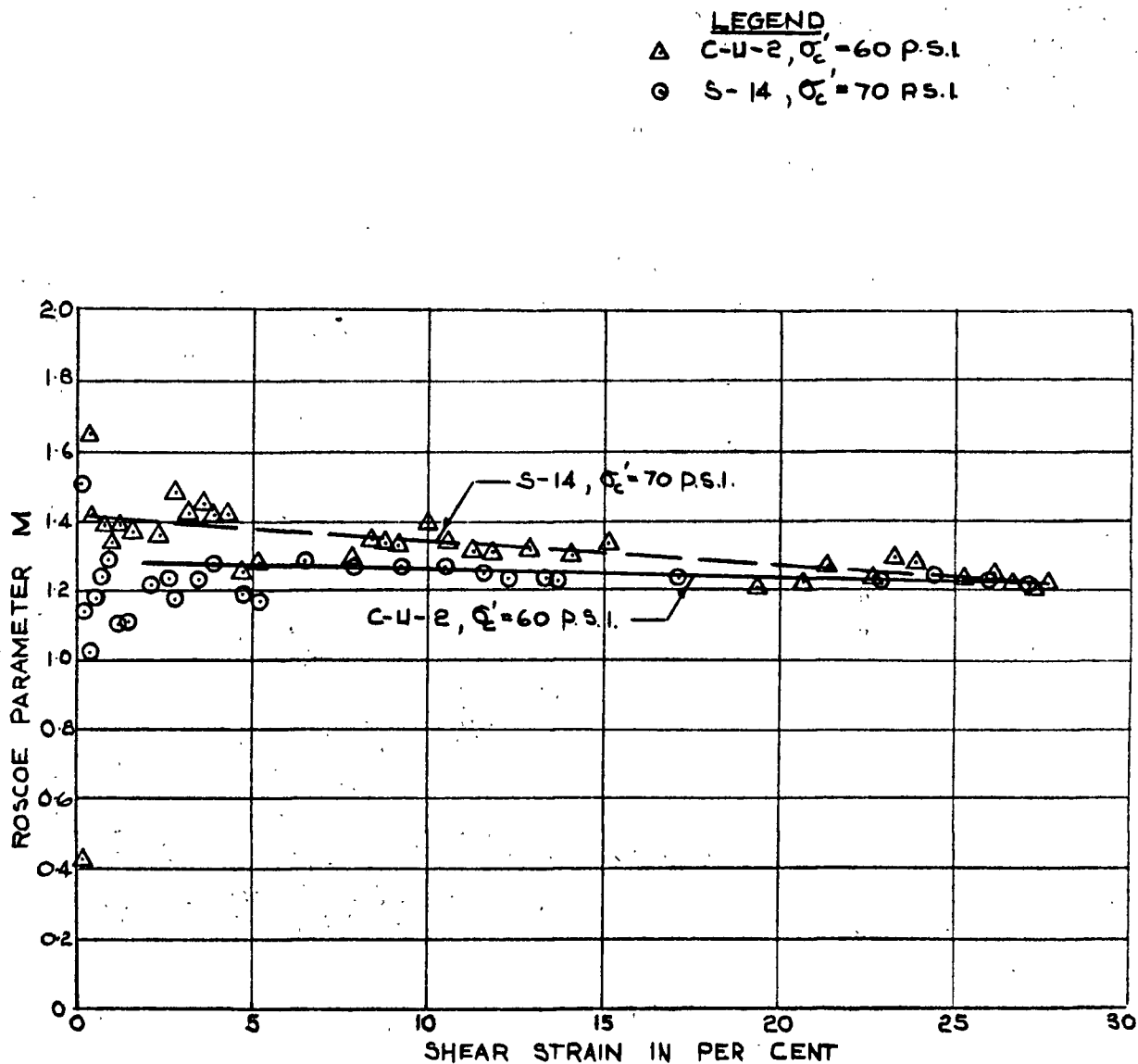


Figure 42 — Roscoe M Parameter Versus Strain, Haney Clay

nately the scatter may be due to neglect of distortional elastic energy which is an assumption of the Roscoe equation.

The Roscoe concept appears to answer many questions regarding the behavior of soil. If the Mohr-Coulomb failure criterion is considered rather than the extended Von Mises criterion as implied by Roscoe, then for triaxial compression tests

$$\sigma_1'/\sigma_3' = \frac{1 + 2/3M}{1 - 1/3M} \quad \text{---- (18)}$$

If $M = 1.27$ is considered an average value of M , then Equation 18 yields $\sigma_1'/\sigma_3' = 3.2$ or a strength envelope of $\phi = 31.6$ degrees. Principal stress ratio curves of Figure 32 indicated that strains of 15 and 25 per cent were needed to mobilize maximum principal stress ratio or maximum friction for undrained and drained tests respectively. Figure 42 indicates that full friction is mobilized at very low strains and remains reasonably constant with strain. It is only when the energy corrections are zero that the internal or corrected shear stress equals the applied shear stress and the soil is then said to be in the critical state. Haney clay never did reach this state. The Roscoe concept does not question the validity of the curves of Figure 35 but helps to explain their shape.

Application of the Roscoe energy equation to the results of undrained creep tests on normally loaded samples of Haney clay presently being conducted by Mr. D. E. Snead at the University of British Columbia shows that the deviator stress, when corrected for release of internal energy due to pore pressure rise, lies on the $q = Mp'$ line for all stages of tests, apart from readings in the first one per cent strain. Here again full friction is

being mobilized at a very early strain.

If the Roscoe concept is correct, then the "Dependent" and "Independent" components of shear resistance as defined by Schmertmann (1963) and mentioned in Chapter 3 have no physical meaning and arise from internal energy changes. The Energy equation applies where plastic deformation or slip at grain contacts is occurring. Overconsolidated material is assumed to remain rigid plastic under distortional stresses until the state boundary surface is reached. If maximum q/p ratio is reached before yielding occurs the energy equation does not apply. It is not clear, therefore, if the same M value applies to normally loaded and highly overconsolidated samples of the same clay.

7.5 Examination of methods for predicting stress-strain relations

Methods of predicting stress-strain relationships are examined in this section. Poorooshasb and Roscoe (1963), Roscoe and Schofield (1963) and Landanyi, La Rochelle and Tanguay (1965) have presented methods for predicting stress-strain relationships. These methods have been discussed in detail in Chapter 2. An attempt has been made to apply these methods to Haney clay but none yields results that are in satisfactory agreement with the measured relations.

Poorooshasb and Roscoe (1963) presented a graphical method for normally loaded remolded clays by which stress-strain relations in drained tests could be predicted from the results of undrained tests and consolidation tests conducted such that the ratio of q/p' remained constant. The method presupposes a unique relationship between effective stresses and water content. Since for Haney

clay the relationship could hardly be considered to be unique (Section 7.3) the method is not strictly applicable. However, if it is assumed that the water content contours from undrained tests are unique, the shear strain for a drained path can be predicted by the Poorooshasb and Roscoe method. In Figure 36 it was shown that contours of water content from undrained tests consolidated to 75 lbs./sq.in. or higher are geometrically similar. Contours were therefore extrapolated for lower water contents and are shown on Figure 43. Shear strains were also extrapolated and contours of undrained shear strain appear as straight lines radiating from the origin. A drained stress path for a test consolidated to 70 lbs./sq.in. (allowance made for residual pore pressure) has a stress path as shown. The method for determining strains was discussed in detail in Chapter 2. The stress path is idealized into increments of stress at constant volume and constant q/p' as shown in Figure 43 for a typical increment CE. The increment of strain from constant volume is determined from the contours of strain and equals about 0.5 per cent for the increment shown. Since no tests were performed to determine the relation between shear strain and volumetric strain at constant q/p' , the following relation (Roscoe and Schofield 1963) was used:

$$\delta V = \left(\frac{M - \eta}{1 - K/\lambda} \right) \quad \text{---- (19)}$$

where δV = volumetric strain increment

M = ratio of q to p' at critical state

η = q/p'

K = slope of e Vs. $\ln. p'$ rebound curve

λ = slope of e Vs. $\ln. p'$ for virgin consolidation

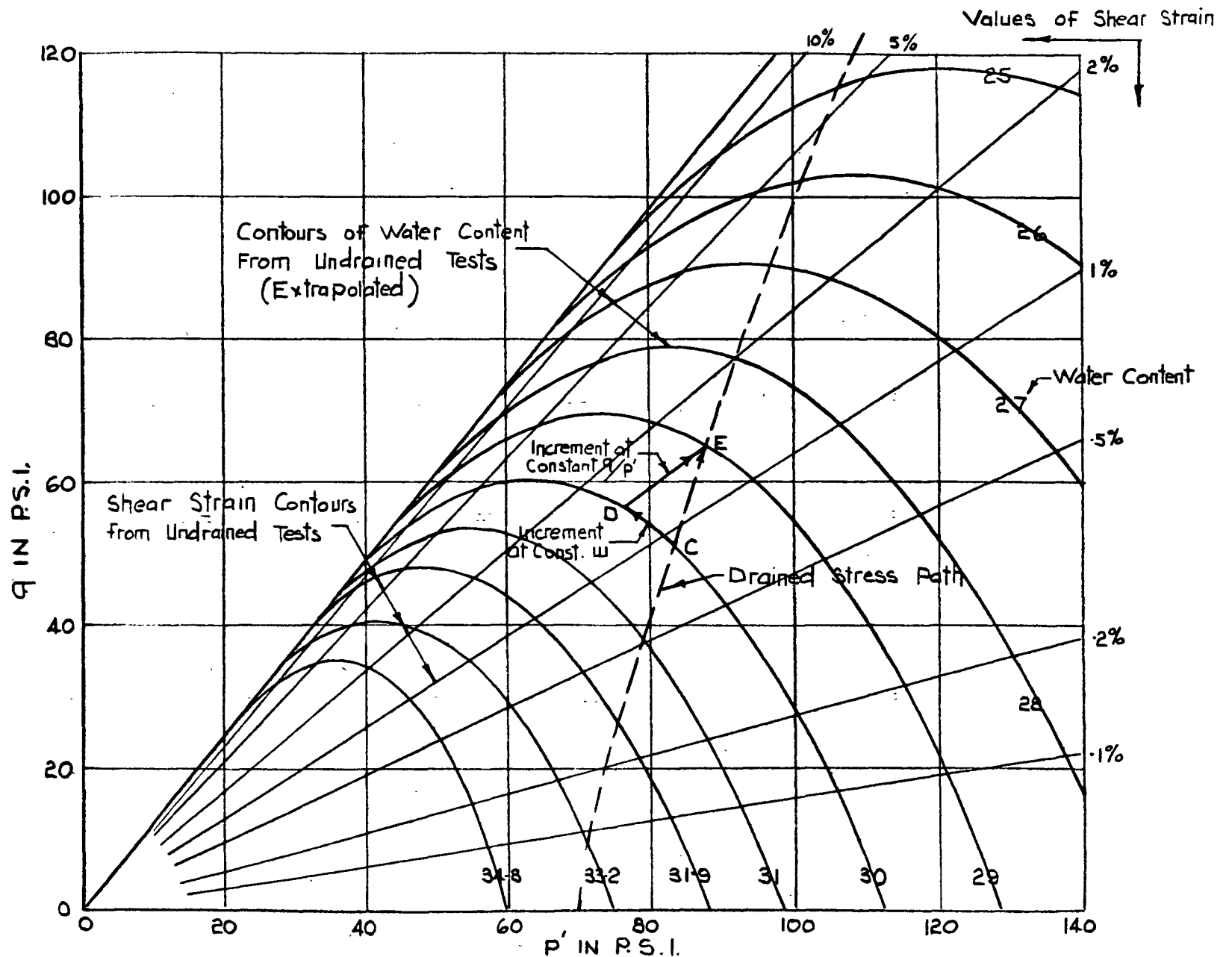


Figure 43 - Contours of Water Content and Strain From Undrained Tests on Haney Clay

$\delta\xi$ = shear strain increment.

The values of M, K and η have already been determined and when substituted in (19) yield

$$\delta\xi = \frac{.78\delta V}{1.27-\eta} \quad \text{---- (20)}$$

and
$$\delta V = \frac{\delta e}{1+e_0} = \frac{2.80\delta w}{1.94} \quad \text{---- (21)}$$

$\delta\xi$ and δV are increments of natural strain, however, since engineering strain was desired, it was assumed that equation (20) also held for engineering strain. For an increment of stress at constant q/p , η is constant and equals 0.737 for the increment DE shown. $\delta V = 1.44$ for this increment, from which the shear strain due to volume change from equation 20 is 2.7 per cent. The total shear strain increment due to the increment CE is the sum of the strain increments at constant volume and constant η and equals 3.2 per cent. By summation of such increments the stress-strain relation was calculated and is shown in Figure 44 along with the measured stress-strain relation. It is seen that although the predicted stress-strain relationship is of approximately the same shape as the measured relation, the correlation could not be considered as satisfactory. Since strains due to volume changes account for the major portion of the calculated strains, stress-strain relations for drained tests cannot be predicted from undrained tests unless contours of water content are independent of stress path.

Roscoe and Schofield (1963) presented an equation from which stress-strain and pore pressure-strain relations can be predicted

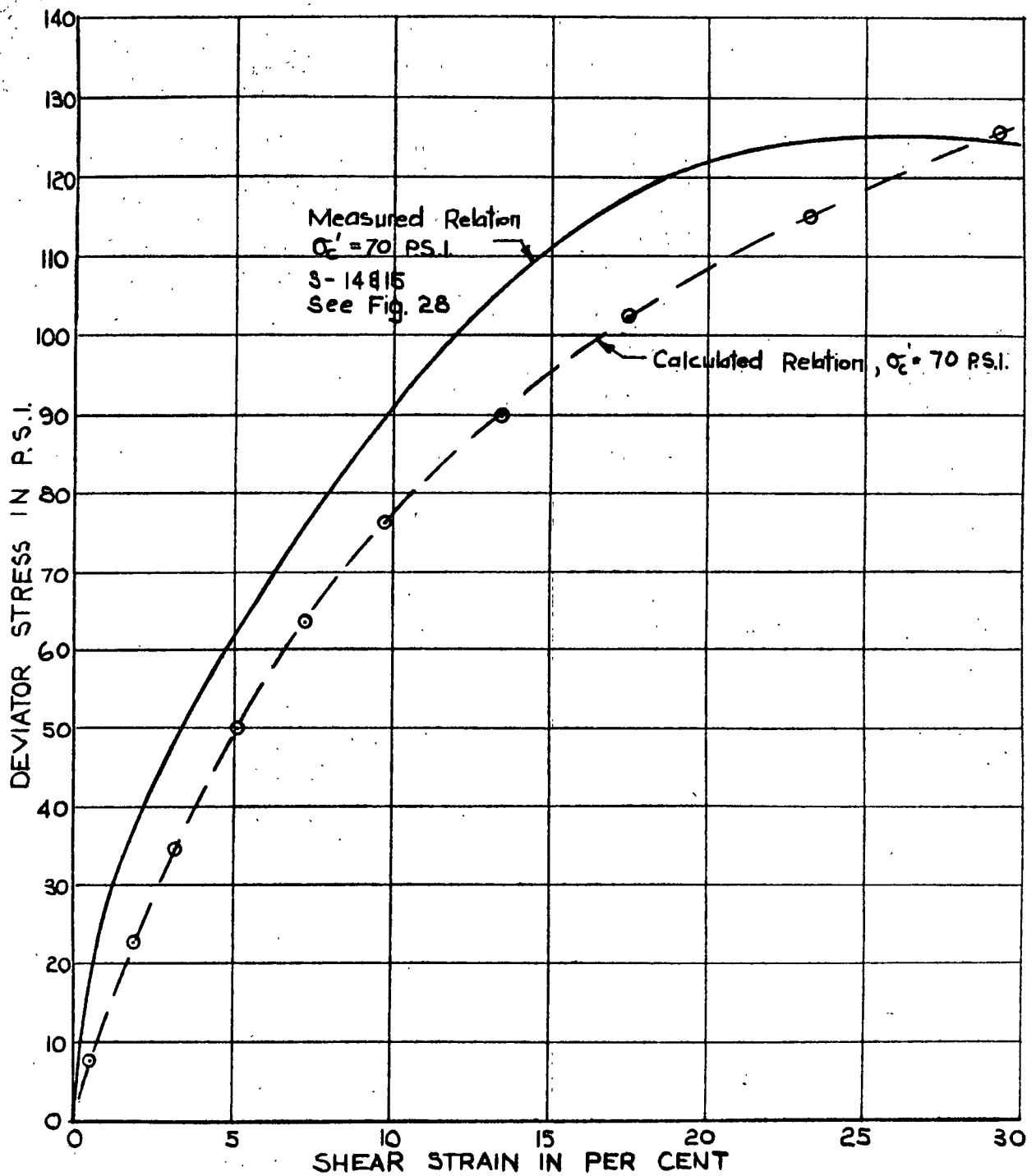


Figure 44-Comparison of Measured and Calculated Stress-strain Relations for Drained Tests on Honey Clay

for undrained tests in terms of K/λ and M . However, the relation is based on the validity of their equation for the state boundary surface. The Roscoe state boundary surface for $M = 1.27$ and $K/\lambda = 0.22$ is shown on the two dimensional Burland plot in Figure 45. It is seen to differ from both the drained and undrained state boundary surfaces. Burland (1965) proposed a variation on the Roscoe state boundary surface and his equation is also shown. It is seen that the undrained state boundary surface lies reasonably close to the Roscoe surface, while the drained lies closer to Burland's surface. Since the Roscoe equation for the state boundary surface was not considered to be in satisfactory agreement with the measured relation, no stress-strain predictions were made.

Landanyi, La Rochelle and Tanguay (1965) presented a method for predicting shear strains in undrained tests from the results of drained tests. This method was discussed in Chapter 2. It appeared to predict that if the relationship between stresses and water content was unique, then the shear strains would also be unique, which is not in agreement with Henkel (1960) and Roscoe. However, since it was found that the stress-water content relationship is not unique for Haney clay, Landanyi's concept was further examined. The method assumes that the relationship between σ'_1/σ'_3 , ξ and σ'_3 form a three dimensional surface which is unique for both drained and undrained paths and paths between these limits. However, Figure 31, Section 7.2 indicates that for drained tests σ'_1/σ'_3 is essentially independent of σ'_3 (apart from an initial kink for samples consolidated to 40 lbs./sq.in.). Therefore, the 3 dimensional surface would reduce to a line, and drained and undrained tests should have the same σ'_1/σ'_3 versus strain relation.

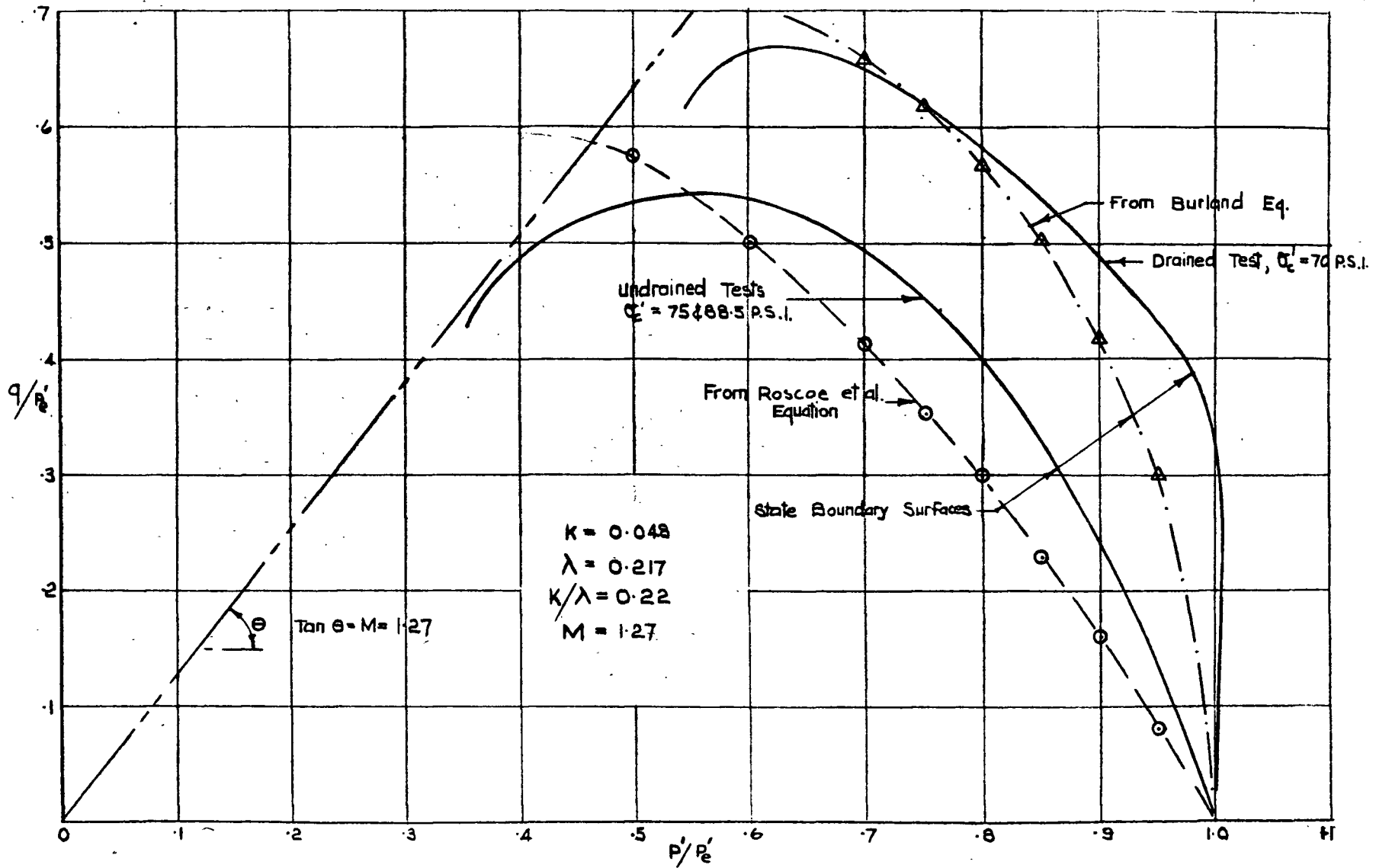


Figure 45 - Comparison of Theoretical and Experimental State Boundary Surfaces (Burland Plot)

It is seen from Figure 32 that drained and undrained tests have quite different σ'_1/σ'_3 versus strain relation. Therefore there is not a unique relation between σ'_1/σ'_3 , ϵ and σ'_3 and Landanyi's concept does not apply to Haney clay.

7.6 Effect of strain rate on drained tests

Since two additional drained tests were performed at one quarter the normal strain rate, but with drainage from one end only as discussed in Chapter 6, the effect of rate of testing on the drained characteristics of Haney clay can be examined. In Chapter 6 it was shown that residual pore pressures are approximately the same for these tests as for those performed at the normal rate but with drainage top and bottom. Deviator and principal stress ratio versus strain relationships for the normal and slow rates are compared in Figures 46 and 47. It is seen that both the deviator stress and the principal stress ratio are slightly higher for tests conducted at the slower rate. The water content versus strain curves shown in Figure 48 indicate that the slow tests drained more due to additional time for secondary compression and this probably accounts for their higher strength. It is generally considered that faster testing rates give higher strength, yet here it appears that slower rates give higher strength. However, undrained tests are usually being considered. In undrained tests it is likely that slower rates would give reduced strength, because the additional time would lead to higher pore pressures due to the tendency for secondary compression.

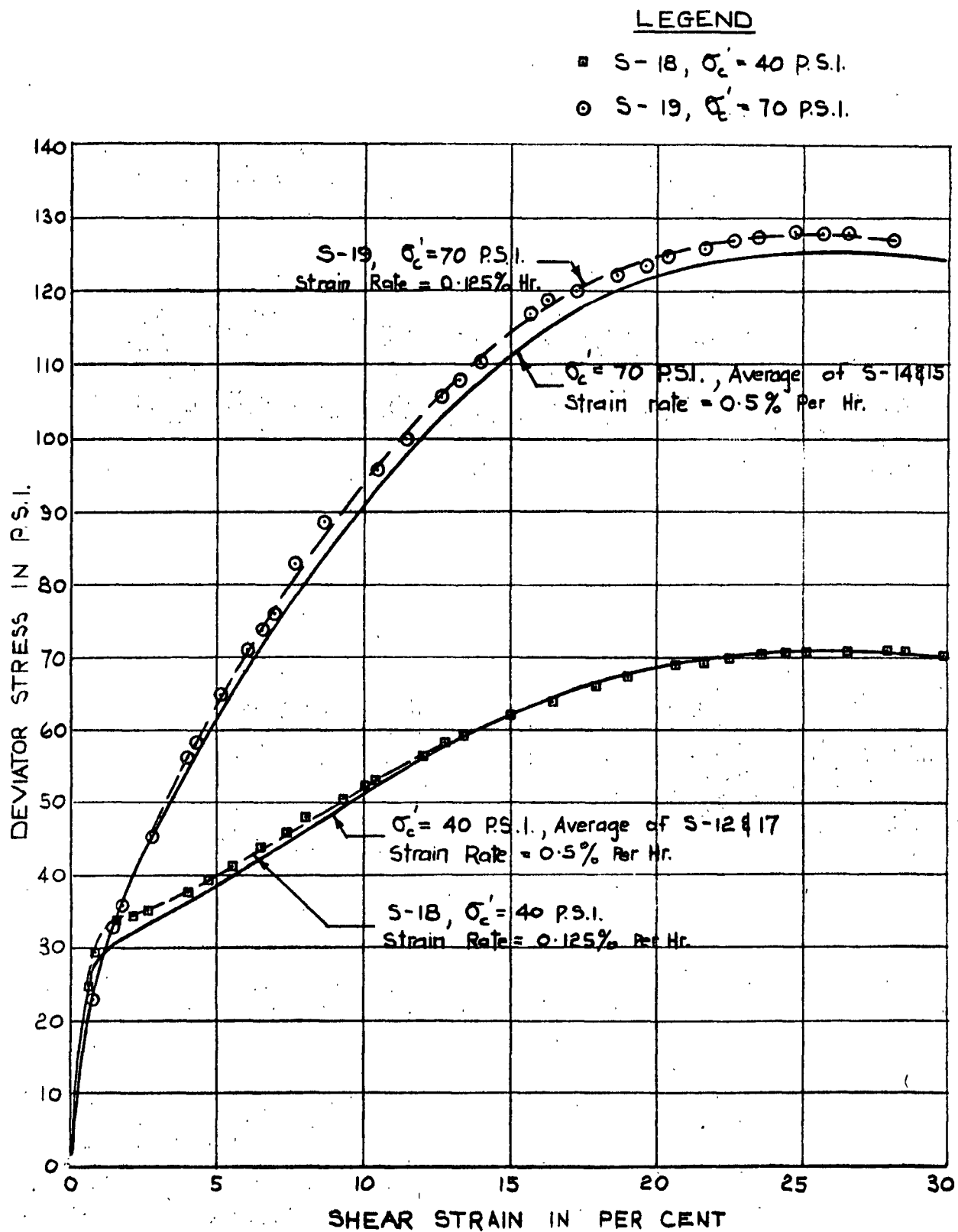


Figure 46-Effect of Strain Rate on the Stress-Strain Relations from Drained Tests on Honey Clay

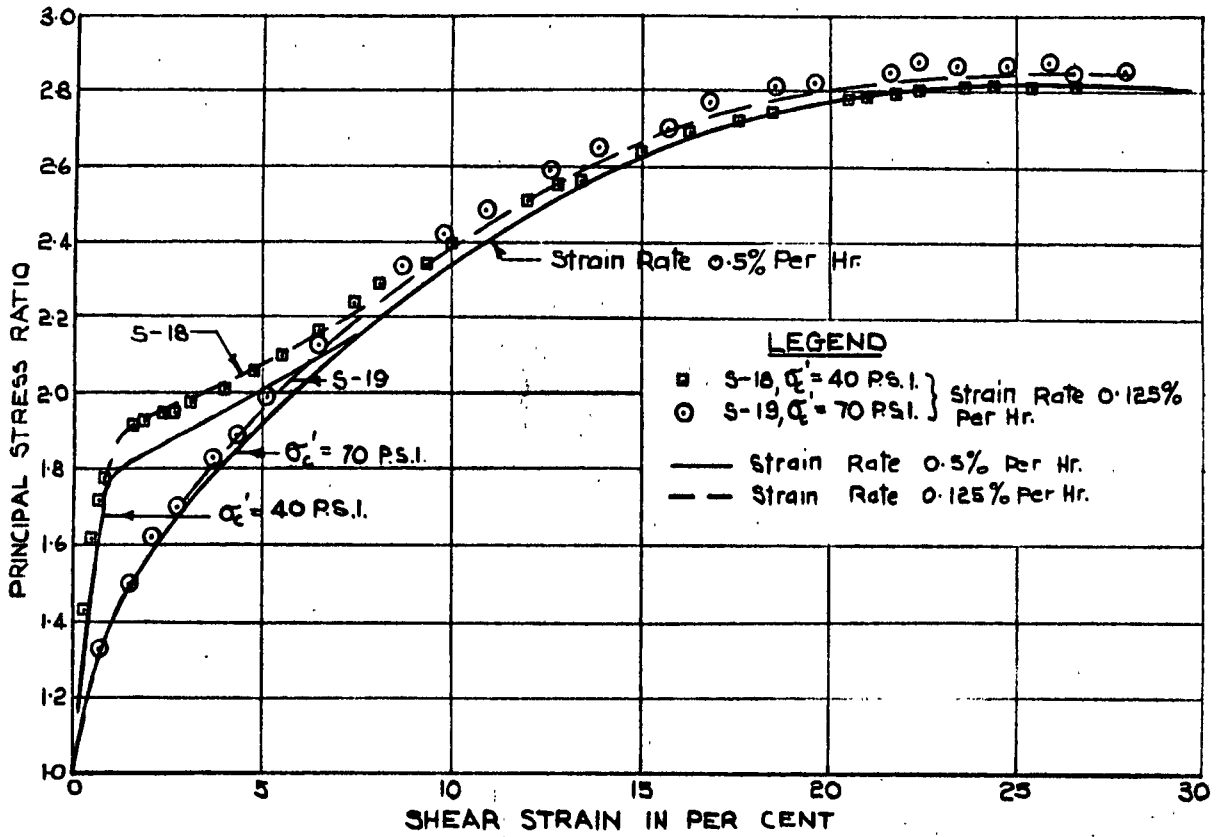


Figure 47- Effect of Strain Rate on the Principal Stress Ratio Vs. Strain Relations for Drained Tests on Honey Clay

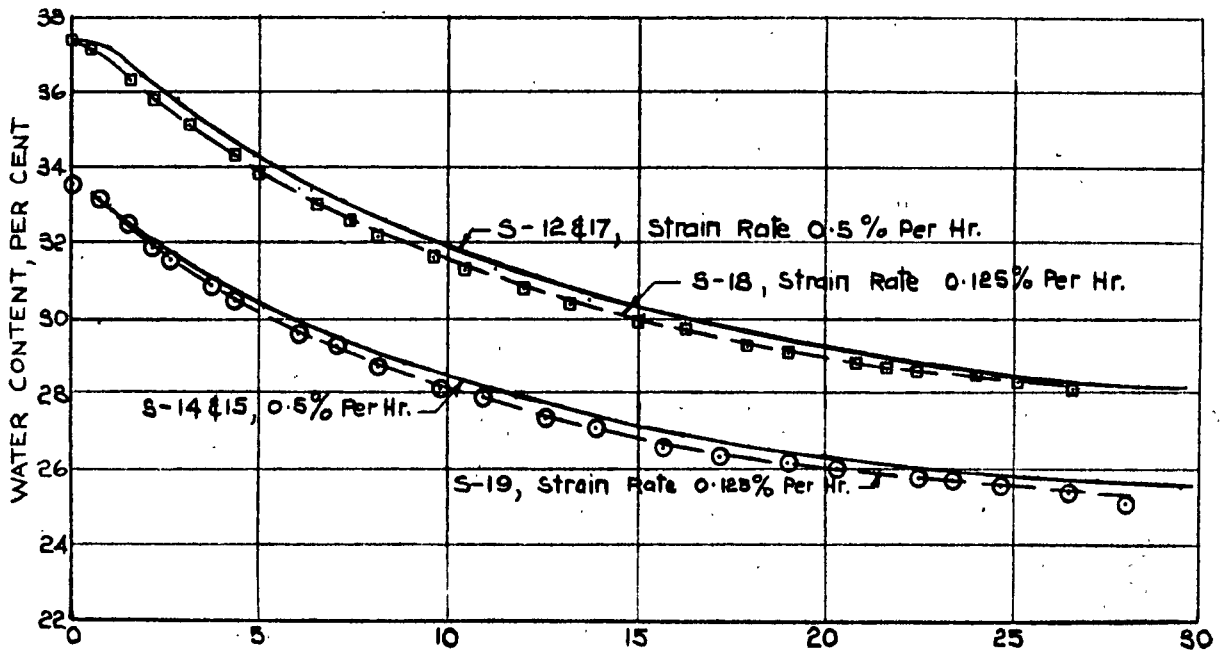


Figure 48- Effect of Strain Rate on the Water Content Vs. Strain Relations for Drained Tests on Honey Clay

CHAPTER 8

CONCLUSIONS AND SUGGESTIONS FOR FURTHER RESEARCH

8.1 CONCLUSIONS

Test results presented in the previous chapter lead to the following conclusions:

1. For sensitive clay, there is not a unique relationship between effective stresses and water content which is independent of stress path, or alternatively, there is not a unique state boundary surface for normally loaded sensitive clay. Henkel (1960) suggested that the relationship for sensitive clays might be more complex than the simple relation proposed for remolded soil.

2. The Roscoe energy equation appears to apply quite well to Haney clay. The equation implies that whenever plastic deformation of soil is occurring, the relationship between the mean normal effective stress and the deviator stress corrected for both energy due to volume change and internal energy is a constant, M . This was found to be approximately true for drained and undrained strain controlled tests as well as creep tests, and for strains varying from one to thirty per cent. This suggests the possibility that the Hvorslev effective friction and effective cohesion parameters and the Schmertmann "Dependent" and "Independent" parameters arise from neglect of internal energy changes and that, in fact, there is only one fundamental strength parameter, M , which corresponds to a friction component, and is independent of both strain and strain rate.

The Roscoe equation further implies that, since M does not depend on strain, it is also independent of particle orientation

or structure. However, the uncorrected deviator stress which is of interest in practical problems is very much dependent on soil structure, since it is soil structure that determines internal energy changes.

3. The Roscoe method for predicting stress-strain relations cannot be applied to a sensitive clay as it does not have a unique state boundary surface.

4. The Landanyi method for predicting stress-strain relations does not apply to a sensitive clay.

5. Stress-strain relations for drained samples of Haney clay with approximately the same degree of residual pore pressure dissipation are only slightly altered by decreased strain rate. Decreased strain rates allow greater time for secondary compression and result in slightly higher strength at all strains.

8.2 Suggestions for further research

During the course of the testing program and the subsequent preparation of this thesis interest developed in the following topics:

1. It was suggested in this thesis that the Roscoe M is a fundamental strength parameter. This concept could be checked by triaxial tests on both overconsolidated undisturbed and remolded samples of Haney clay.
2. In Chapter 6 it was shown that the average permeability of a triaxial specimen at all stages of a drained test, for which the maximum excess pore pressure has been measured, can be calculated.

Since permeability at any given void ratio is also a measure of soil structure, it is felt that very useful information with regard to soil structure could be obtained from void ratio versus permeability plots determined from normally loaded and overconsolidated tests on undisturbed and remolded samples of the same clay. The Hvorslev concept of samples at the same void ratio having the same structure could be checked in this manner.

LIST OF SYMBOLS

a_m	- area of mineral to mineral contact
A	- pore pressure parameter
A	- stress due to electrical attractive forces between particles
B	- pore pressure parameter
c_v	- coefficient of consolidation
c'	- effective cohesion parameter
c_e'	- Hvorslev cohesion parameter
C_c	- compression index
C_e	- expansion index
C-U	- consolidated undrained test
e	- void ratio
h	- half height of sample
J_1'	- first stress invariant
k	- permeability
m_v	- coefficient of unit volume decrease
M	- soil strength parameter
p'	- mean normal effective stress
p_e'	- effective stress on isotropic consolidation
$\delta p'$	- increment of mean normal effective stress
q	- deviator stress
q_R	- deviator stress corrected for energy
q_w	- deviator stress corrected for energy
δq	- increment of deviator stress
R	- stress due to electrical repulsive forces between particles

R	- rate of drainage
t	- time
t_{90}	- time for 90 per cent primary consolidation
t_f	- time to failure
T	- time factor
u	- pore pressure
u_e	- residual pore pressure
Δu	- change in pore pressure
U	- average degree of consolidation
V	- volume of sample
ΔV	- volumetric strain
δV	- change in volumetric strain
w	- water content
δW	- change in energy
Δx	- small change in level of null point
z	- length
γ_w	- unit weight of water
Γ	- critical void ratio when mean normal effective stress equals unity
ε	- shear strain
ε_1	- axial strain
$\delta\varepsilon$	- increment of shear strain
η	- factor depicting boundary drainage condition
η	- ratio of deviator stress to mean normal stress
K	- slope of void ratio versus natural logarithm of pressure during rebound

- λ - slope of void ratio versus natural logarithm of pressure during virgin consolidation
- σ - total stress
- σ' - effective stress
- σ'_a - axial effective stress
- σ'_c - effective consolidation pressure
- σ'_f - effective stress on failure plane
- $\sigma_{1,2,3}$ - principal total stresses
- $\sigma'_{1,2,3}$ - principal effective stresses

- ARMSTRONG, J.E., 1957. "Surficial Geology of New Westminster Map-Area, British Columbia." Geological Survey of Canada, paper 57-5, 25 pp.
- BARRON, R.A., 1960. "Prestress Effects on the Strength of Clays." Proc. Am. Soc. Civil Eng., Research Conference on Shear Strength of Cohesive Soils, Boulder Colo., 1960, pp. 163-168.
- BISHOP, A.W., 1954. Correspondence on a paper by A.D.M. Penman, Geotechnique, Vol. 4, pp. 43-45.
- BISHOP, A.W., 1964. Correspondence on a paper by P.W. Rowe, L. Barden, and I.K. Lee, Geotechnique, Vol. 14, sec., 1964, pp. 370-371.
- BISHOP, A.W., BLIGHT, G.E., and DONALD, I.B., 1960. Discussion, Proc. Am. Soc. Civil Eng., Research Conference on Shear Strength of Cohesive Soils, Boulder, Colo., 1960, pp. 1027-1042.
- BISHOP, A.W., and GIBSON, R.E., 1963. "The Influence of the Provision of Boundary Drainage on the Shear Strength and Consolidation Characteristics of Soil Measured in the Triaxial Apparatus." Proc. NRC/ASTM Symposium on Laboratory Shear Testing, Ottawa, 1963.
- BISHOP, A.W., and HENKEL, D.J., 1962. "The Measurement of Soil Properties in the Triaxial Test." Edward Arnold Ltd., 200 pp.
- BLIGHT, G.E., 1963. "The Effect of Non-uniform Pore Pressures on Laboratory Measurements of the Shear Strength of Soils." Proc. NRC/ASTM Symposium on Laboratory Shear Testing, Ottawa, 1963, pp. 173-184.
- BJERRUM, L., 1954. "Theoretical and Experimental Investigations on the Shear Strength of Soils." Norwegian Geotechnical Institute, Oslo, Bulletin No. 5, 112 pp.
- BJERRUM, L., and SIMONS, N.E., 1960. "Comparison of Shear Strength Characteristics of Normally Consolidated Clays." Proc. Am. Soc. Civil Eng., Research Conference on Shear Strength of Cohesive Soils, Boulder, Colo., 1960, pp. 711-726.
- BURLAND, J.B., 1965. Correspondence, Geotechnique, Vol. 15, June, 1965.
- CAMPANELLA, R.G., 1965. "Effect of Temperature and Stress on the Time-Deformation Behaviour of Saturated Clay." Ph. D. Thesis, University of California, Berkeley.
- CASAGRANDE, A., and WILSON, S.D., 1953. "Prestress Induced in Consolidated Quick Triaxial Tests." Proc. Third Int. Conference on Soil Mech. and Found. Eng., Zurich, 1953, Vol. 1, pp. 106-110.

CASAGRANDE, A., and WILSON, S.D., 1960. Moderators' Report, Proc. Am. Soc. Civil Eng., Research Conference on Shear Strength of Cohesive Soil, Boulder, Colo., 1960, pp. 1123-1130.

CRAWFORD, C.B., 1963a. "Pore Pressures within Soil Specimens in Triaxial Compression". Proc. NRC/ASTM Symposium on Laboratory Shear Testing, Ottawa, 1963, pp. 192-199.

CRAWFORD, C.B., 1963b. Discussion of paper by C.B. Crawford. Proc. NRC/ASTM Symposium on Laboratory Shear Testing, Ottawa, 1963, pp. 209-211.

GIBSON, R.E., 1953. "Experimental Determination of the True Cohesion and True Angle of Internal Friction in Clays." Proc. Third Int. Conference on Soil Mech. and Found. Eng., Zurich, 1953, Vol. 1, pp. 126-130.

GIBSON, R.E., and HENKEL, D.J., 1954. Influence of Duration of Tests at Constant Rate of Strain on Measured Drained Strength." Geotechnique, Vol. 4, 1954, pp. 6-15.

HENKEL, D.J., 1958. The Correlation between Deformation, Pore Water Pressure and Strength Characteristics of Saturated Clays." Thesis, University of London, April 1958.

HENKEL, D.J., 1959. "The Relationships Between Strength, Pore Water Pressure and Volume Change of Saturated Clays." Geotechnique, Vol. 9, pp. 119-135.

HENKEL, D.J., 1960. "The Shear Strength of Saturated Remolded Clays." Proc. Am. Soc. Civil Eng., Research Conference on Shear Strength of Cohesive Soils, Boulder, Colo. 1960, pp. 535-554.

HENKEL, D.J., and SOWA, V.A., 1963. Proc. NRC/ASTM Symposium on Laboratory Shear Testing, Ottawa, 1963, pp. 280-291.

HIRST, T.J., 1966. "Triaxial Compression Tests on an Undisturbed Sensitive Clay." M.A. Sc. Thesis, University of British Columbia, Canada.

KENNEY, T.C., 1959. Discussion on a paper by C.B. Crawford. ASTM Spec. Tech. Publ. No. 254, pp. 49-58.

LAMBE, T.W., 1958. "Soil Testing for Engineers." John Wiley and Sons, Inc., 150 pp.

LAMBE, T.W., 1960. "A Mechanistic Picture of Shear Strength in Clay." Proc. Am. Soc. Civil Eng., Research Conference on Shear Strength of Cohesive Soils, Boulder, Colo., 1960.

LANDANYI, B., La ROCHELLE, P., and TANQUAY, L., 1965. "Some Factors Controlling the Predictability of Stress-Strain Behaviour of Clay.", Canadian Geot. Jour., Vol. 2, May, 1965.

- NOORANY, I., and SEED, H.B., 1965. "A New Experimental Method for the Determination of Hvorslev Strength Parameters for Sensitive Clays." Proc. Sixth Int. Conf. Soil Mech. and Found. Eng., Canada, 1965, pp. 318-322.
- POOROOSHASB, H.B., and ROSCOE, K.H., 1961. "The Correlation of the Results of Shear Tests with Varying Degrees of Dilation." Proc. Fifth Int. Conf. Soil Mech., Vol. 1, pp. 297-304.
- POOROOSHASB, H.B., and ROSCOE, K.H., 1963. "A Graphical Approach to the Stress-Strain Relationships of Normally Consolidated Clays." Proc. NRC/ASTM Symposium on Laboratory Shear Testing, Ottawa, 1963.
- POULOS, S.J., 1964. "Report on Control of Leakage in the Triaxial Test." Harvard Soil Mechanics Series No. 71, Cambridge, Mass., 230 pp.
- RENDULIC, L., 1936. "Relation Between Void Ratio and Effective Principal Stresses for a Remolded Silty Clay." Proc. First Int. Conference Soil Mech. Found. Eng., Cambridge, Vol. 3, pp. 48-51.
- RENDULIC, L., 1937. "Ein Grundgesetz der Tonmechanik und Sein Experimenteller Beweiss." Der Bauingenieur, Vol. 18, pp. 459-467.
- ROSCOE, K.H., SCHOFIELD, A.N., and WROTH, C.P., 1958. "On the Yielding of Soils." Geotechnique, Vol. 8, pp. 22-53.
- ROSCOE, K.H., and SCHOFIELD, A.M., 1963. "Mechanical Behaviour of an Idealized 'Wet-Clay'." European Conf. Soil Mech. and Found. Eng., Vol. 1, pp. 47-54.
- ROSCOE, K.H., SCHOFIELD, A.N., and THURAIRAJAH, A., 1963. "Yielding of Clays in States Wetter than Critical." Geotechnique, Vol. 8:3, Sept., 1963.
- ROSCOE, K.H., SCHOFIELD, A.N., and THURAIRAJAH, A., 1963. "An Evaluation of Test Data for Selecting a Yield Criterion for Soils." Proc. NRC/ASTM Symposium on Laboratory Shear Testing, Ottawa, 1963.
- ROWE, P.W., OATES, D.B., and SKERMER, N.A., 1963. Proc. NRC/ASTM Symposium on Laboratory Shear Testing, Ottawa, 1963.
- SCOTT, R.F., 1963. "Principles of Soil Mechanics." Addison-Wesley Publishing Co. Inc., 550 pp.
- SEED, H.B., MITCHELL, J.K., and CHAN, C.K., 1960. "The Strength of Compacted Soil." Proc. Am. Soc. Civil Eng., Research Conference on Shear Strength of Cohesive Soils, Boulder, Colo., 1960, pp. 887-964.
- SCHMERTMANN, J.H., 1963. "Generalizing and Measuring the Hvorslev Effective Components of Shear Resistance." Proc. NRC/ASTM Symposium on Laboratory Shear Testing, Ottawa, 1963.

- SIMONS, N.E., 1960. "Comprehensive Investigation of the Shear Strength of an Undisturbed Dramman Clay." Proc. Am. Soc. Civil Eng., Research Conference on Shear Strength of Cohesive Soils, Boulder, Colo., 1960.
- SIMONS, N.E., 1963. "The Influence of Stress Path on Triaxial Test Results." Proc. NRC/ASTM Symposium on Laboratory Shear Testing, Ottawa, 1963.
- TAYLOR, D.W., 1948. "Fundamentals of Soil Mechanics." John Wiley and Sons, New York, 700 pp.
- TERZAGHI, K. 1943. "Theoretical Soil Mechanics." John Wiley and Sons Inc., 510 pp.
- WHITMAN, R.V., 1960. "Some Considerations and Data Regarding the Shear Strength of Clays." Proc. Am. Soc. Civil Eng., Research Conference on Shear Strength of Cohesive Soils, Boulder, Colo., 1960, pp. 581-614.
- WHITMAN, R.V., LADD, C.C., and PAULO da CRUZ., 1960, Discussion, Session 3. Proc. Am. Soc. Civil Eng., Research Conference on Shear Strength of Cohesive Soils, Boulder, Colo., 1960, pp. 1049-1056.

APPENDIX 1

RESIDUAL PORE PRESSURES IN DRAINED TESTS, METHOD 1

This method is based on the superposition of pore pressures (Terzaghi, 1943, p. 286). The deviator stress will be some function (t) of time as shown in Figure 49. It is assumed to be applied in instantaneous increments $\Delta\sigma_i$ at times $\frac{1}{2}(t_i + t_{i-1})$ where the subscript (i) refers to a particular increment, so that the assumed $\sigma(t)$ is the dashed line shown on Figure 49. The change in pore pressure Δu_i due to an instantaneous increment of deviator stress $\Delta\sigma_i$ can be obtained from the Skempton equation for change in pore pressure under undrained conditions

$$\Delta u_i = B (\Delta\sigma_3 + A\Delta\sigma_i)$$

Since $B = 1$ for saturated soil and σ_3 does not change in the standard drained test, $\Delta\sigma_3 = 0$

$$\text{therefore } \Delta u_i = A\Delta\sigma_i \quad \text{---- (22)}$$

It is assumed that Δu_i dissipates independently of other pore pressure increments and in accordance with the one dimensional consolidation equation, so that at time t_j where $j \geq i$, the average pore pressure due to Δu_i is Δu_{ij} where

$$\Delta u_{ij} = \Delta u_i (1 - U_{ij})$$

and U_{ij} is the average degree of consolidation after a time $t_{ij} = t_j - \frac{1}{2}(t_i + t_{i-1})$ as shown in Figure 49. By the principle of superposition the average pore pressure at time t_j is the sum of the average partially dissipated incremental pore pressures at time t_j caused by all the increments prior to t_j

$$\text{therefore } u_j = \sum_{i=1}^j \Delta u_i (1 - U_{ij}) \quad \text{---- (23)}$$

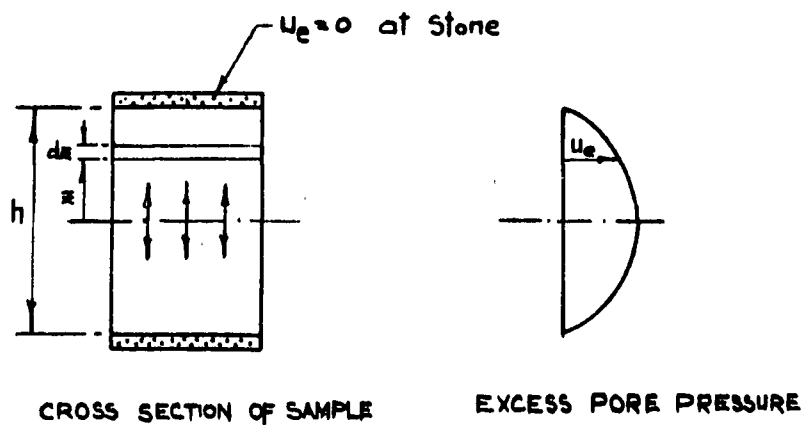


Fig. 49a

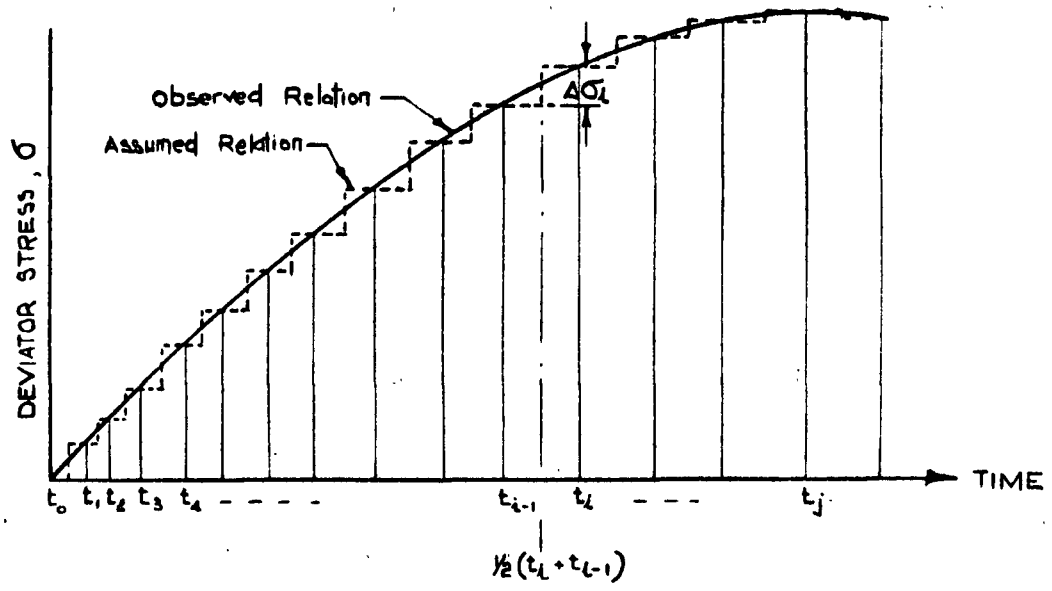


Fig. 49b

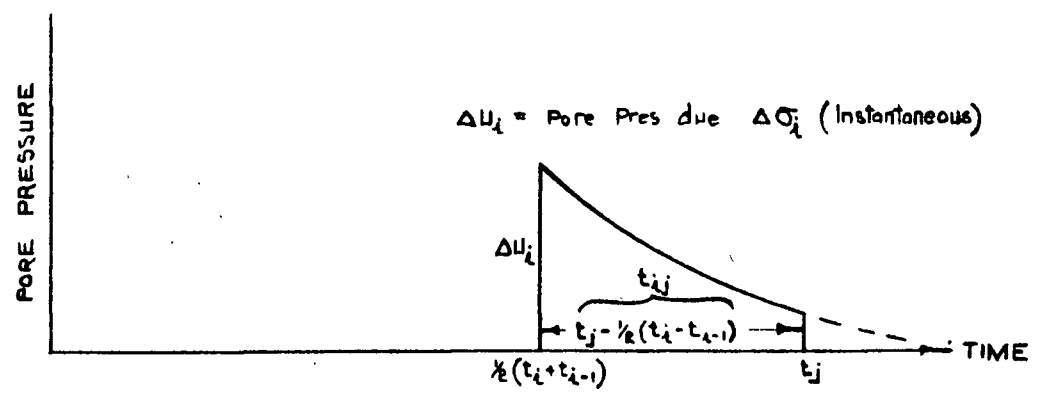


Fig. 49c

Figure 49—Diagrams Showing Assumptions of Method 1

The average degree of consolidation U is a function of the time factor T and is usually determined from a plot of T versus U . However, since a numerical procedure was required the following relations were used (Taylor 1948, p. 234).

$$(1 - U) = 1 - \sqrt{\frac{4T}{\pi}} \quad T < .283 \quad \text{---- (24)}$$

$$(1 - U) = 10 \left(\frac{T + .0851}{.9332} \right) \quad T > .283 \quad \text{---- (25)}$$

where $T = \frac{c_v t}{h^2}$

$$\text{therefore } 1 - U_{ij} = f(T_{ij}) = f\left(\frac{c_v t_{ij}}{h^2}\right) \quad \text{---- (26)}$$

where $f(T)$ may be obtained from equation (24) or (25) depending on the value of T calculated. Combining equations (22), (23) and (26) the complete solution for the average excess pore pressure at any time t_j is:

$$u_j = \sum_{i=1}^j A \Delta \sigma_i f\left(\frac{c_v t_{ij}}{h^2}\right) \quad \text{---- (27)}$$

This expression can be readily programmed for the computer. However, A , c_v and h will vary throughout the test, therefore some assumptions must be made with regard to their values.

The Skempton A used here is an incremental A rather than the A usually calculated. It was at first thought it could be estimated from the results of undrained tests by taking the ratios of increments of pore pressure to increments of deviator stress and possibly expressing A as a function of strain. Typical deviator stress and pore pressure versus strain relationships for undrained tests are shown in Figure 50a. The incremental A values

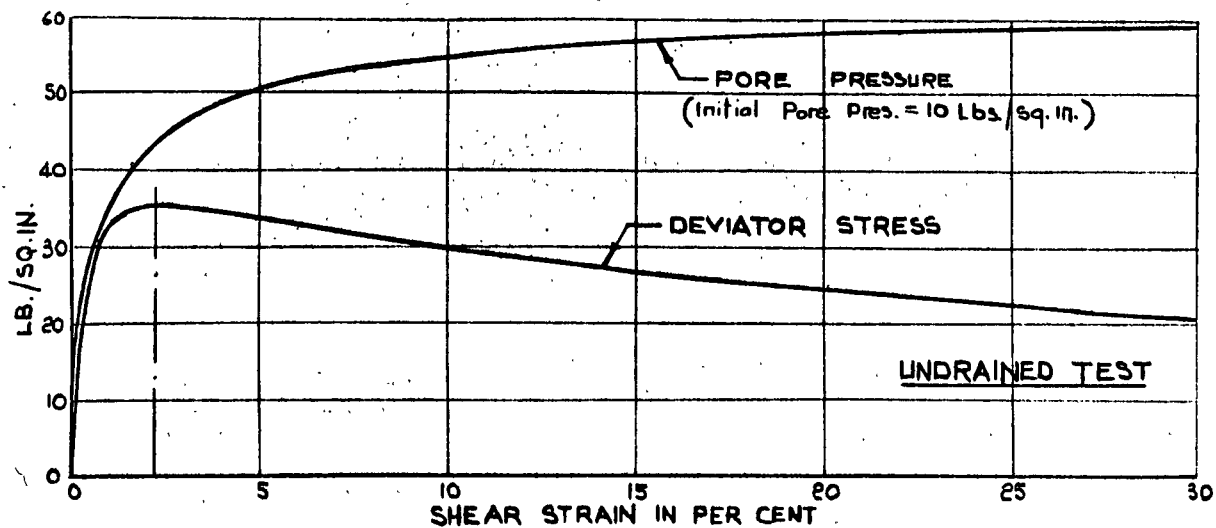


Fig. 50a

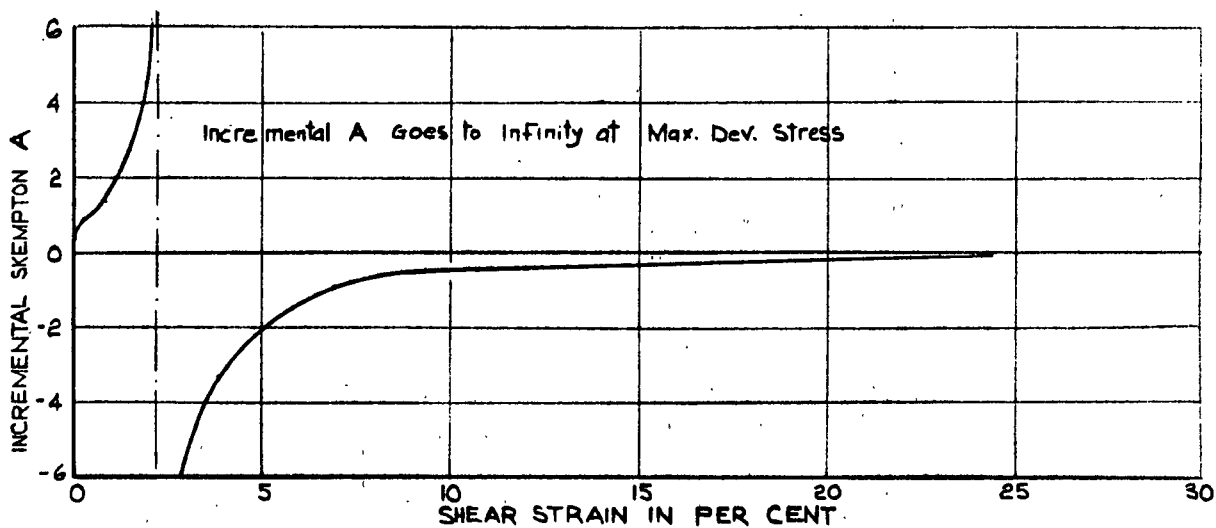


Fig. 50b

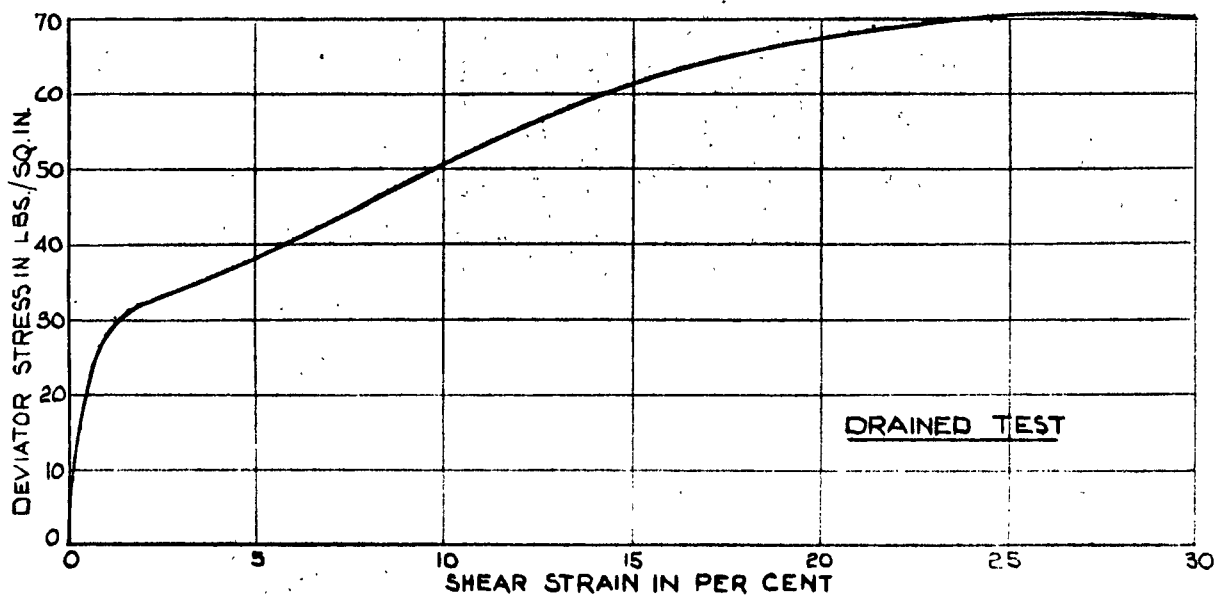


Figure 50 - Stress-Strain Characteristics of Honey Clay

calculated from Figure 50a are shown in Figure 50b. It is seen that at maximum deviator stress, since the rate of change of deviator stress is zero $A = \frac{\Delta u}{\Delta \sigma}$ goes to infinity. After maximum deviator stress, pore pressures continue to increase resulting in negative incremental A values. Increasing pore pressures after maximum deviator stress are caused by distortion, despite falling deviator stress, rather than because of falling deviator stress. A typical deviator stress versus strain curve for a drained test is also shown in Figure 50. It is seen that the shape is quite different from the undrained test with maximum deviator stress occurring at high strain and therefore the incremental A values from undrained tests could not be used. It might be expected that the incremental A would increase with strain from approximately 1/3 at low strain where elastic behaviour might occur to infinity at high strain as maximum deviator stress is approached. However, no logical basis for varying A could be determined and so a constant value of $A = 1$ was chosen.

The coefficient of consolidation, c_v , varies during a test due to change in structure and change in void ratio. Values of c_v determined from both preliminary consolidation prior to shearing and from oedometer tests are plotted versus the average pressure $p' = 1/3 (\sigma'_1 + 2\sigma'_3)$ and shown on Figure 51. For oedometer tests it was assumed that k_0 was 0.75. The range of p' for all drained tests was from 40 to 110 lbs./sq.in. and the relation between p' and c_v in this area was approximated by the straight line on the semi-log plot shown, from which

$$c_v = .0051 - .00243 \log_{10} p' \quad \text{cm}^2/\text{sec.} \quad \text{---- (28)}$$

LEGEND

- Undrained Tests, Preliminary Consolidation
- ◆ Undrained Test, Consolidation After Shearing
- ⊙ Drained Tests, Preliminary Consolidation
- + Oedometer Tests

NOTE:

1. C_v Plotted Versus Average effective Stress For Load Increment.
2. $K_0 = 0.8$ Assumed for Oedometer Tests.

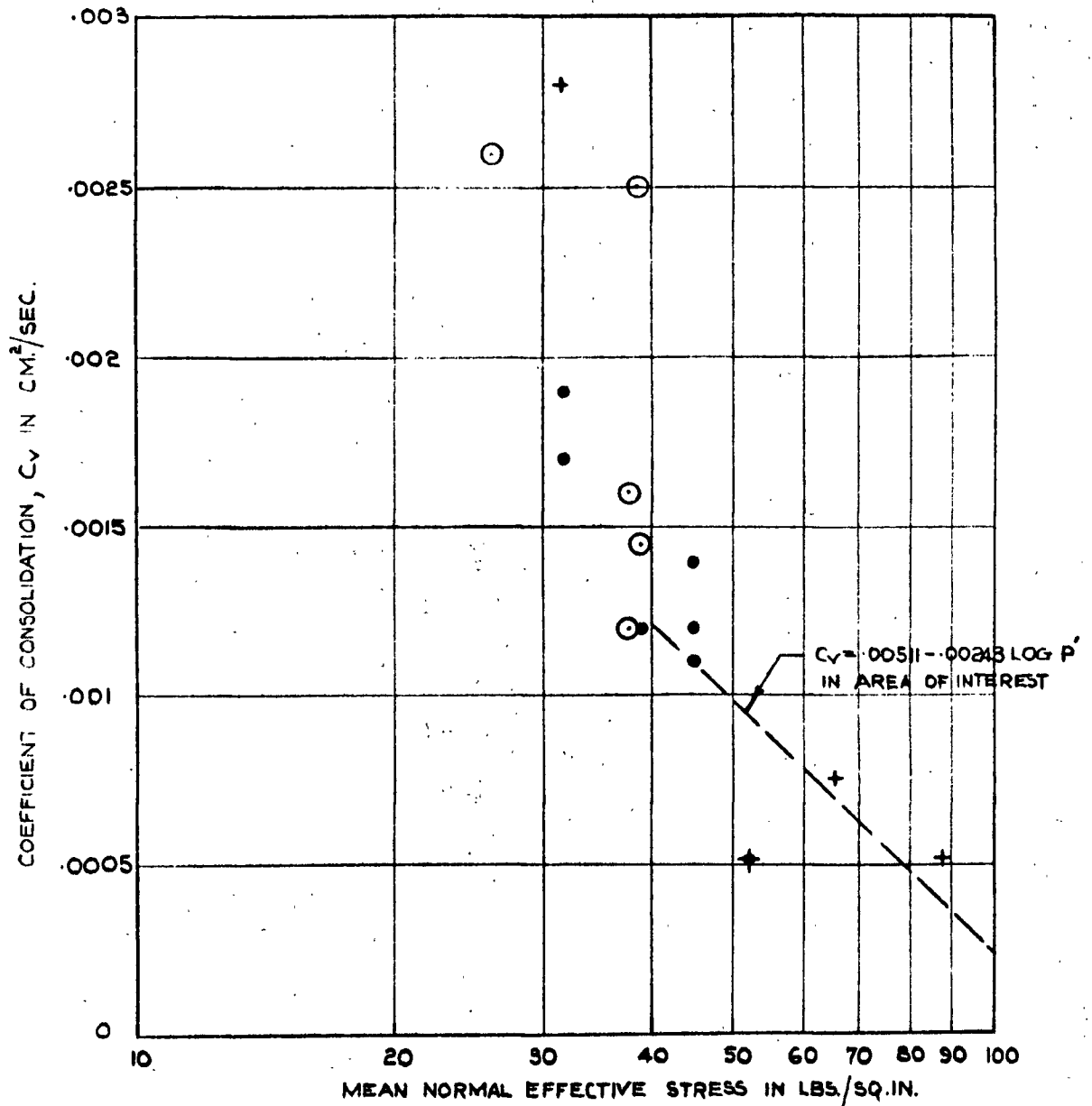


Figure 51 — Relationship Between Coefficient of Consolidation and Effective Stress for Honey Clay.

It appears from Figure 51 that c_v in the area of interest is lower than the figure of 2×10^{-3} cm²/sec. used in the previous chapter to determine testing rates. However, it is understood from Bishop and Henkel (1962) that the c_v mentioned in their expressions is the c_v obtained during the preliminary consolidation prior to shearing and not the c_v that exists at the final consolidation pressure. The c_v values shown in Figure 51 are plotted at the average p' during the consolidation increment. c_v 's obtained from triaxial consolidation vary between 1×10^{-3} cm²/sec. and 3×10^{-3} cm²/sec. and hence the figure of 2×10^{-3} cm²/sec. was chosen.

The height of the sample also varies throughout a test and since axial strain at failure was about 30 per cent, this could not be neglected. The height of the sample was known at all times that readings were taken. It was assumed that at any time t_j the pore pressures due to all prior increments dissipated under the constant sample height and coefficient of consolidation existing at that time. In actual fact pore pressures due to earlier increments would have been dissipating under a gradually reducing height and coefficient of consolidation. However, pore pressures due to earlier increments will be very small and the height and coefficient of consolidation will be essentially correct for those increments applied immediately prior to the time of interest and which undoubtedly cause the major portion of the pore pressure.

APPENDIX II

TRIAxIAL COMPRESSION TEST

SOIL SAMPLE : Honey Clay
 SPECIFIC GRAVITY : 2.80
 TEST TYPE : Consolidated Undrained

TEST NO.: 2
 DATE : July 19, '65
 TESTED BY: P.M.B.

INITIAL MEASURED DIMENSIONS

	Circ. in Cm.	Dia. in Cm.	Area in Cm ²
Top	11.43	3.635	10.38
Centre	11.40	3.625	10.33
Bottom	11.38	3.620	10.30

Height of Sample = 7.05 Cm. = 2.775 In.

Area = $\frac{A_t + 2A_c + A_b}{4} = \frac{10.34 \text{ Cm}^2}{4} = \underline{1.605 \text{ In.}^2}$

Volume (V_t) = 73.0 Cm³, $V_s = \frac{W_s}{G_s} = \underline{32.75 \text{ Cm.}^3}$

Average $w\%$ (Side Trimmings) = 42.5, $e = \frac{V_s - V_a}{V_a} = \underline{1.198}$

Degree of Saturation $S = \frac{wG_s}{e} = \underline{99.3 \text{ Per Cent}}$

AFTER CONSOLIDATION

Change in Vol. = 6.15 cc, Change in Water Content = $\frac{\Delta V}{V_0} = \underline{6.7\%}$, $w\% = \underline{35.8}$

Change in Ht. = 0.14 Cm., Consolidated Ht. = 6.91 Cm. = 2.72 In.

Consolidated Area = $\frac{V - \Delta V}{H_c} = \underline{9.68 \text{ Cm}^2} = \underline{1.50 \text{ In.}^2}$

WATER CONTENTS

Specimen Location	Side	Side	Side	Side	Top	Bottom	Whole Sa. Initially	Whole Sa. Finally
Container No.	1	2	3	4	5	6		
Wt. Container & Wet Soil	39.83	34.11	42.76	44.37	40.49	43.50	133.88	179.79
Wt. Container & Dry Soil	33.19	29.16	35.11	36.30	34.18	36.03	94.32	144.78
Wt. Water in gms.	6.64	4.95	7.65	8.07	6.13	7.47	39.56	35.01
Wt. Container in gms.	17.46	17.53	17.17	17.29	18.56	17.47	3.02	53.48
Wt. Dry Soil in gms	15.73	11.63	17.94	19.01	15.62	18.56	<u>91.30</u>	<u>91.30</u>
Water Content (w) %	42.15	42.50	42.70	42.80	40.4	40.2	43.2	<u>38.3</u>

WATER CONTENT CHECK

Vol. Drained During Consolidation = 6.15 cc, Initial $w\%$ (Side Trimmings) = 42.5
 Vol. Drained During Shear = — cc, Initial $w\%$ from Initial wt.
 Vol. Back Drained = 1.80 cc, & Final Dry Wt. = 43.2
 Total Vol. Change = 4.35 cc, Initial $w\%$ from Final $w\%$
 Change in Water Content = 4.8 %, and Change in $w\%$ = 43.1

REMARKS

Side Trimmings Not Further Trimmed to Allow for Top & Bottom Trimming.

APPLICATION OF CHAMBER PRESSURE
UNDRAINED CONDITIONS

TEST NO.: 2

DATE: July 19, 1965

TESTED BY: P.M.B.

TIME HRS.	ELAPSED TIME MIN.	CHAMBER GAUGE P.S.I.	CHAMBER COR. P.S.I.	CHAMBER PRES. P.S.I.	PORE PR. GAUGE P.S.I.	PORE PR. COR. P.S.I.	PORE PRES. P.S.I.	SKEMPT -ON B
14:51	0	10	0	10	8.5	-4.4	4.1	
				<u>9.9</u>			<u>8.3</u>	<u>0.84</u>
	4	20	-0.1	19.9	17.0	-4.6	12.4	
				<u>10.0</u>			<u>11.1</u>	<u>1.11</u>
	8	30	-0.1	29.9	28.2	-4.7	23.5	
				<u>9.9</u>			<u>10.5</u>	<u>1.06</u>
	12	40	-0.2	39.8	38.7	-4.7	34.0	
				<u>9.9</u>			<u>10.0</u>	<u>1.01</u>
	16	50	-0.2	49.8	48.8	-4.8	44.0	
				<u>10.0</u>			<u>9.8</u>	<u>0.98</u>
	20	60	-0.2	59.8	58.7	-4.9	53.8	
				<u>11.4</u>			<u>11.5</u>	<u>1.01</u>
	24	71.3	-0.1	71.2	70.3	-5.0	65.3	

$$\text{OVER ALL } B = \frac{61.2}{61.2} = 1.00$$

REMARKS: Thermostat stuck Before Commencing and this
May Account For The Variation in B

CONSOLIDATED TRIAXIAL TEST
PRELIMINARY CONSOLIDATION

CHAMBER PRES. GAUGE = 71.3 P.S.I.

TEST NO: 2

GAUGE CORRECTION = -0.1 P.S.I.

DATE: JULY 19, 1965

ELEVATION CORRECTION = -1.2 P.S.I.

TESTED BY: P.M.B

CHAMBER PRESSURE = 70.0 P.S.I.

BACK PRES. = 10.0 P.S.I.

EFFECTIVE STRESS CHANGE 4.7 TO 60.0 P.S.I.

DATE	TIME HRS	ELAPSED TIME MIN.	TIME	DIAL RD. IN.	BUR. RD. CC	TEMP °C
JULY 19 '65	15:25	0:00	0:00	0.9400	9.71	24
		0:04	0:25		9.55	
		0:15	0:50		9.48	
		0:34	0:75		9.38	
		1:00	1:00		9.28	
		1:34	1:25			
		2:15	1:50		9.06	
		3:04	1:75	0.9228	8.95	
		4:00	2:00		8.85	
		6:15	2:50		8.64	
		9:00	3:00		8.43	
		12:15	3:50			
		16:00	4:00		8.00	
		25:00	5:00		7.58	
		36:00	6:00	0.8970	7.20	
		49:00	7:00		6.88	
		65:00	8:05		6.55	
		81:00	9:00		6.29	
		100:00	10:00		6.03	
		120:00	10:35	0.8927	5.80	
		131:00	11:42		5.68	
July 20 '65	15:25			0.8835	3.56	

$\Delta V = 6.15$ C.C.

CONSOLIDATED UNDRAINED TRIAXIAL TEST

Consolidated Area = 1.50 In.² , Proving Ring No.

Test No: 2

Consolidated Length = 2.72 In. , Calibration Factor = .3167 ,

Date: July 20/65

Chamber Pressure = 70.0 Ps.i. , Temp. = 24 °C

Tested By: P.M.B.

Time Hr.	Pore Pres. Gauge	Gauge Cor.	Pore Pres. Ps.i.	Vertical Dial In.	Proving Dial	Time Hr.	Pore Pres. Gauge	Gauge Cor.	Pore Pres. Ps.i.	Vertical Dial In.	Proving Dial
15:583	14.6	-4.6	10.0	.8835	42.5	23:58	54.0	-4.8	49.2	.7783	207.3
15:633	15.6	-4.6	11.0	.8832	50.0	25:10	55.7	-4.8	50.9	.7557	206.3
15:717	16.6	-4.6	12.0	.8826	61.0	25:48	55.9	-4.8	51.1	.7414	204.7
15:833	17.7	-4.6	13.1	.8822	70.0	28:28	58.3	-4.9	53.4	.7057	201.7
15:940	18.8	-4.7	14.1	.8815	80.0	30:45	59.5	-4.9	54.6	.6676	198.4
16:08	20.6	-4.7	15.9	.8807	91.0	33:00	60.2	-4.9	55.3	.6340	196.5
16:18	22.0	-4.7	17.3	.8800	100.0	35:42	60.8	-4.9	55.9	.5967	194.7
16:32	23.4	-4.7	18.7	.8791	111.0	37:33	61.2	-4.9	56.3	.5663	193.2
16:47	25.3	-4.7	21.6	.8778	121.0	38:50	61.2	-4.9	56.3	.5488	191.7
16:60	26.8	-4.7	22.1	.8767	130.5	40:50	61.7	-4.9	56.8	.5195	190.0
16:78	28.6	-4.7	23.9	.8750	140.7	41:0	61.7	-4.9	56.8	.5116	190.0
16:96	30.2	-4.7	25.5	.8733	150.2	47:08	62.7	-4.9	57.8	.4174	187.5
17:17	31.7	-4.7	27.0	.8710	160.0	47:50	62.7	-4.9	57.8	.4114	187.3
17:42	33.9	-4.7	29.2	.8682	170.0	57:50	63.0	-4.9	58.1	.2600	183.3
17:75	36.3	-4.7	31.6	.8643	180.2	60:17	63.8	-4.9	58.9	.2188	182.3
18:17	39.8	-4.7	35.1	.8590	190.0	62:90	64.0	-4.9	59.1	.1765	180.7
18:77	42.5	-4.7	37.8	.8509	199.2	65:00	64.2	-4.9	59.3	.1453	178.6
19:33	44.5	-4.7	39.8	.8428	205.0	72:45	64.2	-4.9	59.3	.0307	177.7
20:38	47.6	-4.8	42.8	.8266	209.3						
21:22	50.5	-4.8	45.7	.8136	210.0						
21:70	51.3	-4.8	46.5	.8062	209.6						

CONSOLIDATED UNDRAINED TRIAXIAL TEST

ELAPSED TIME HOURS	STRAIN PER CENT	DEFORMATION IN. PER DAY	SIGMA 1 EFF PSI	ROOT 2 EFF	SIGMA 3 IN. PSI	DEVIATOR STRESS PSI	PRINCIPAL STRESS RATIO	SKEMPTON A	PORE PRESSURE PSI
-0.00	0.00	-0.000	60.0		84.8	-0.0	1.00	0.00	10.0
0.05	0.01	0.144	60.6		83.4	1.6	1.03	0.63	11.0
0.13	0.03	0.161	61.9		82.0	3.9	1.07	0.51	12.0
0.25	0.05	0.125	62.7		80.5	5.8	1.10	0.53	13.1
0.36	0.07	0.134	63.8		79.0	7.9	1.14	0.52	14.1
0.50	0.10	0.135	64.3		76.5	10.2	1.19	0.58	15.9
0.60	0.13	0.141	64.8		74.5	12.1	1.23	0.60	17.3
0.73	0.16	0.144	65.7		72.5	14.4	1.28	0.60	18.7
0.89	0.21	0.154	64.9		68.4	16.5	1.34	0.70	21.6
1.02	0.25	0.160	66.4		67.7	18.5	1.39	0.65	22.1
1.20	0.31	0.170	66.8		65.2	20.7	1.45	0.67	23.9
1.38	0.38	0.178	67.2		62.9	22.7	1.51	0.68	25.5
1.58	0.46	0.190	67.7		60.8	24.7	1.57	0.69	27.0
1.84	0.56	0.200	67.6		57.7	26.8	1.66	0.72	29.2
2.17	0.71	0.213	67.3		54.3	28.9	1.75	0.75	31.6
2.59	0.90	0.227	65.8		49.3	30.9	1.88	0.81	35.1
3.19	1.20	0.245	64.9		45.5	32.7	2.02	0.85	37.8
3.75	1.50	0.261	64.0		42.7	33.8	2.12	0.88	39.8
4.80	2.09	0.285	61.7		38.5	34.5	2.27	0.95	42.8
5.64	2.57	0.298	58.8		34.4	34.5	2.42	1.04	45.7
6.12	2.84	0.303	57.8		33.2	34.3	2.46	1.06	46.5
7.25	3.46	0.312	56.0		31.4	33.8	2.52	1.12	47.8
8.00	3.87	0.316	54.2		29.4	33.4	2.61	1.17	49.2
9.52	4.70	0.322	52.0		27.0	32.9	2.72	1.24	50.9
10.40	5.22	0.328	51.4		26.7	32.5	2.72	1.27	51.1
12.70	6.54	0.336	48.0		23.5	31.4	2.89	1.38	53.4
14.87	7.94	0.349	45.7		21.8	30.3	2.97	1.47	54.6
17.42	9.17	0.344	44.2		20.8	29.5	3.01	1.53	55.3
19.84	10.54	0.347	42.8		19.9	28.7	3.04	1.60	55.9
21.75	11.66	0.350	41.8		19.4	28.1	3.05	1.65	56.3
22.92	12.31	0.351	41.3		19.4	27.6	3.02	1.68	56.3
24.92	13.38	0.351	40.2		18.7	27.0	3.04	1.73	56.8
25.42	13.67	0.351	40.1		18.7	26.9	3.04	1.74	56.8
31.50	17.14	0.355	37.6		17.3	25.4	3.08	1.88	57.8
31.92	17.36	0.355	37.5		17.3	25.3	3.07	1.89	57.8
41.92	22.92	0.357	34.8		16.8	22.9	2.93	2.10	58.1
44.58	24.44	0.358	33.4		15.7	22.3	3.01	2.19	58.9
47.32	25.99	0.359	32.5		15.4	21.6	2.98	2.27	59.1
49.42	27.14	0.359	31.6		15.1	20.9	2.96	2.35	59.3
56.87	31.35	0.360	30.3		15.1	19.6	2.83	2.52	59.3

CONSOLIDATED UNDRAINED TRIAXIAL TEST

TEST NO. 2
CONSOLIDATION PRES. = 60.0

STRAIN PER CENT	P EFFECTIVE	Q	QW	M	CONSOLIDATION PRES. = 60.0	
	ROSCOE PSI	ROSCOE PSI	ROSCOE PSI	ROSCOE	UNIT P ROSCOE	UNIT Q ROSCOE
0.00	60.0	-0.0	0.0	0.00	1.00	-0.00
0.01	59.5	1.6	77.8	1.31	0.99	0.03
0.03	59.3	3.9	59.1	1.00	0.99	0.07
0.05	58.8	5.8	64.0	1.09	0.98	0.10
0.07	58.5	7.9	61.4	1.05	0.98	0.13
0.10	57.5	10.2	87.0	1.51	0.96	0.17
0.13	56.7	12.1	71.9	1.27	0.95	0.20
0.16	56.1	14.4	85.9	1.53	0.94	0.24
0.21	53.9	16.5	61.5	1.14	0.90	0.28
0.25	54.1	18.5	28.9	0.53	0.90	0.31
0.31	53.0	20.7	59.2	1.12	0.88	0.34
0.38	52.1	22.7	52.9	1.02	0.87	0.38
0.46	51.2	24.7	53.0	1.03	0.85	0.41
0.56	49.7	26.8	58.7	1.18	0.83	0.45
0.71	48.0	28.9	59.6	1.24	0.80	0.48
0.90	45.2	30.9	58.2	1.29	0.75	0.51
1.20	43.1	32.7	47.4	1.10	0.72	0.54
1.50	41.5	33.8	46.0	1.11	0.69	0.56
2.09	38.7	34.5	47.2	1.22	0.64	0.57
2.57	35.8	34.5	44.3	1.24	0.60	0.57
2.84	34.9	34.3	41.0	1.17	0.58	0.57
3.46	33.5	33.8	41.1	1.23	0.56	0.56
3.87	31.9	33.4	40.9	1.28	0.53	0.56
4.70	30.1	32.9	35.8	1.19	0.50	0.55
5.22	29.7	32.5	34.8	1.17	0.50	0.54
6.54	27.1	31.4	35.0	1.29	0.45	0.52
7.94	25.5	30.3	32.4	1.27	0.43	0.51
9.17	24.5	29.5	31.1	1.27	0.41	0.49
10.54	23.7	28.7	30.0	1.27	0.39	0.48
11.66	23.1	28.1	28.9	1.25	0.38	0.47
12.31	22.9	27.6	28.5	1.24	0.38	0.46
13.38	22.2	27.0	27.4	1.24	0.37	0.45
13.67	22.2	26.9	27.1	1.23	0.37	0.45
17.14	20.7	25.4	25.7	1.24	0.34	0.42
17.36	20.6	25.3	25.6	1.24	0.34	0.42
22.92	19.5	22.9	23.9	1.23	0.33	0.38
24.44	18.5	22.3	23.2	1.25	0.31	0.37
25.99	18.1	21.6	22.2	1.23	0.30	0.36
27.14	17.7	20.9	21.5	1.21	0.29	0.35
31.35	17.2	19.6	0.0	0.00	0.29	0.33

TEST NO.17
CONSOLIDATION PRES.= 40.0

CONSOLIDATED DRAINED TRIAXIAL TEST

NO ALLOWANCE MADE FOR RESIDUAL PORE PRESSURE							ALLOWANCE MADE FOR RESIDUAL PORE PRESSURE					
SHEAR STRAIN	AXIAL STRAIN	DEFORMATION IN. PER DAY	WATER CONTENT PER CENT	DEVIATOR STRESS PSI	SIGMA 1 EFF. PSI	PRINCIPAL STRESS RATIO	PORE PRES. PSI	SIGMA 3 EFF. PSI	ROOT 2 SIGMA 3 EFF. PSI	SIGMA 1 EFF. PSI	PRINCIPAL STRESS RATIO	
-0.00	-0.00	-0.000	37.9	0.0	40.0	1.00	0.0	40.0	56.6	40.0	1.00	
0.04	0.05	0.146	37.9	4.1	44.1	1.10	0.5	39.5	55.9	43.6	1.10	
0.13	0.16	0.172	37.8	9.2	49.2	1.23	0.8	39.2	55.4	48.4	1.23	
0.18	0.23	0.182	37.8	11.9	51.9	1.30	0.9	39.1	55.3	51.0	1.30	
0.25	0.31	0.191	37.8	14.7	54.7	1.37	1.0	39.0	55.1	53.7	1.38	
0.35	0.45	0.211	37.7	17.9	57.9	1.45	1.4	38.6	54.6	56.5	1.46	
0.46	0.59	0.224	37.6	20.8	60.8	1.52	1.3	38.7	54.7	59.4	1.54	
0.57	0.74	0.235	37.5	23.5	63.5	1.59	1.5	38.5	54.5	62.0	1.61	
0.73	0.97	0.248	37.4	26.6	66.6	1.67	1.6	38.4	54.3	65.0	1.69	
0.93	1.23	0.264	37.3	28.6	68.6	1.72	1.8	38.2	54.0	66.8	1.75	
1.12	1.50	0.277	37.1	29.9	69.9	1.75	2.1	37.9	53.6	67.7	1.79	
1.42	1.92	0.288	36.8	30.8	70.8	1.77	2.0	38.0	53.7	68.7	1.81	
1.85	2.51	0.298	36.4	31.5	71.5	1.79	2.2	37.8	53.5	69.3	1.83	
2.61	3.57	0.312	35.8	33.2	73.2	1.83	2.3	37.7	53.4	70.9	1.88	
3.40	4.60	0.321	35.2	34.6	74.6	1.87	2.4	37.6	53.2	72.3	1.92	
3.87	5.21	0.326	34.9	35.7	75.7	1.89	2.5	37.5	53.0	73.2	1.95	
4.29	5.77	0.330	34.6	36.8	76.8	1.92	2.5	37.5	53.0	74.2	1.98	
4.77	6.40	0.331	34.3	37.7	77.7	1.94	2.5	37.5	53.0	75.2	2.00	
5.25	7.03	0.331	34.0	38.8	78.8	1.97	2.5	37.5	53.1	76.3	2.03	
8.07	10.50	0.338	32.5	46.9	86.9	2.17	2.3	37.7	53.3	84.6	2.24	
8.72	11.28	0.338	32.2	48.3	88.3	2.21	2.3	37.7	53.3	86.0	2.28	
9.34	12.03	0.338	32.0	50.4	90.4	2.26	2.4	37.6	53.2	88.0	2.34	
10.50	13.39	0.339	31.5	53.3	93.3	2.33	2.2	37.8	53.4	91.1	2.41	
11.22	14.21	0.341	31.3	54.8	94.8	2.37	2.2	37.8	53.4	92.6	2.45	
11.91	15.02	0.342	31.0	56.2	96.2	2.40	2.2	37.8	53.5	94.0	2.49	
12.38	15.56	0.341	30.9	57.0	97.0	2.42	2.1	37.9	53.6	94.9	2.50	
12.95	16.21	0.341	30.7	58.6	98.6	2.46	2.1	37.9	53.6	96.4	2.55	
13.69	17.05	0.341	30.5	60.2	100.2	2.51	1.8	38.2	54.0	98.4	2.58	
14.16	17.58	0.342	30.4	61.1	101.1	2.53	1.7	38.3	54.1	99.4	2.60	
14.68	18.14	0.343	30.2	62.1	102.1	2.55	1.8	38.2	54.0	100.3	2.63	
15.20	18.72	0.344	30.1	62.8	102.8	2.57	1.8	38.2	54.0	101.0	2.64	
19.29	23.20	0.345	29.3	68.3	108.3	2.71	1.5	38.5	54.4	106.7	2.77	
20.04	24.01	0.345	29.1	68.8	108.8	2.72	1.4	38.6	54.6	107.5	2.78	
20.78	24.81	0.344	29.0	69.9	109.9	2.75	1.2	38.8	54.9	108.7	2.80	
21.93	26.03	0.345	28.8	70.5	110.5	2.76	1.1	38.9	55.0	109.4	2.81	
22.70	26.84	0.346	28.7	71.0	111.0	2.78	1.3	38.7	54.7	109.7	2.84	
23.26	27.44	0.346	28.6	71.3	111.3	2.78	1.1	38.9	55.1	110.2	2.83	
23.59	27.79	0.346	28.6	71.3	111.3	2.78	0.9	39.1	55.3	110.4	2.82	
24.25	28.49	0.346	28.5	71.3	111.3	2.78	1.0	39.0	55.2	110.4	2.83	
25.05	29.33	0.345	28.4	71.8	111.8	2.80	1.0	39.0	55.2	110.8	2.84	
25.42	29.72	0.346	28.4	71.9	111.9	2.80	1.0	39.0	55.1	110.9	2.85	
25.96	30.29	0.346	28.3	72.0	112.0	2.80	0.7	39.3	55.5	111.2	2.83	
26.55	30.90	0.347	28.3	72.0	112.0	2.80	0.7	39.3	55.6	111.3	2.83	
27.17	31.54	0.347	28.2	72.0	112.0	2.80	0.7	39.3	55.6	111.3	2.83	
27.69	32.08	0.348	28.2	71.9	111.9	2.80	0.7	39.3	55.5	111.1	2.83	
28.03	32.44	0.348	28.2	71.6	111.6	2.79	0.8	39.2	55.4	110.8	2.83	
28.77	33.20	0.347	28.1	71.4	111.4	2.79	0.6	39.4	55.7	110.8	2.81	
29.62	34.08	0.347	28.0	71.8	111.8	2.79	0.5	39.5	55.9	111.3	2.82	
30.65	35.13	0.348	28.0	71.7	111.7	2.79	0.0	40.0	56.6	111.7	2.79	

CONSOLIDATION PRES.= 40.0
 TEST NO.17

SHEAR STRAIN	P PSI	P MINUS PP. PSI	Q PSI	QW PSI	QW(PP) PSI	M	M(PP)	P/PE	P/PE (PP)	Q/PE
-0.00	40.0	40.0	0.0	-49.7	28.1	-1.24	0.70	1.00	1.00	0.00
0.04	41.3	40.8	4.1	-36.8	30.0	-0.89	0.73	1.03	1.02	0.10
0.13	43.0	42.2	9.2	-0.8	47.9	-0.02	1.14	1.07	1.05	0.23
0.18	43.9	43.1	11.9	4.8	46.0	0.11	1.07	1.09	1.07	0.29
0.25	44.9	43.8	14.7	22.1	56.1	0.49	1.28	1.11	1.08	0.36
0.35	45.9	44.5	17.9	36.9	63.8	0.80	1.43	1.12	1.08	0.44
0.46	46.9	45.5	20.8	42.2	64.4	0.90	1.42	1.13	1.10	0.50
0.57	47.8	46.3	23.5	55.0	73.6	1.15	1.59	1.14	1.10	0.56
0.73	48.8	47.2	26.6	59.8	72.9	1.23	1.54	1.14	1.10	0.62
0.93	49.5	47.7	28.6	76.1	83.6	1.54	1.75	1.14	1.10	0.66
1.12	49.9	47.8	29.9	81.1	85.5	1.63	1.79	1.12	1.07	0.67
1.42	50.2	48.2	30.8	85.2	87.4	1.70	1.81	1.09	1.04	0.67
1.85	50.4	48.3	31.5	86.3	87.4	1.71	1.81	1.04	1.00	0.65
2.61	51.0	48.7	33.2	84.4	84.6	1.66	1.74	0.97	0.93	0.63
3.40	51.5	49.1	34.6	82.4	82.1	1.60	1.67	0.91	0.87	0.61
3.87	51.8	49.4	35.7	83.1	82.7	1.60	1.68	0.88	0.83	0.60
4.29	52.2	49.7	36.8	84.8	84.1	1.62	1.69	0.85	0.81	0.60
4.77	52.5	50.0	37.7	84.1	83.6	1.60	1.67	0.82	0.78	0.59
5.25	52.9	50.4	38.8	83.7	83.3	1.58	1.65	0.79	0.75	0.58
8.07	55.6	53.3	46.9	79.7	79.9	1.43	1.50	0.68	0.66	0.58
8.72	56.0	53.7	48.3	80.1	80.8	1.43	1.50	0.67	0.64	0.57
9.34	56.7	54.4	50.4	80.4	81.1	1.42	1.49	0.65	0.62	0.58
10.50	57.7	55.5	53.3	78.9	79.6	1.37	1.43	0.62	0.60	0.58
11.22	58.2	56.0	54.8	80.0	80.6	1.37	1.44	0.61	0.59	0.57
11.91	58.7	56.5	56.2	80.8	81.2	1.38	1.44	0.59	0.57	0.57
12.38	58.9	56.8	57.0	80.9	81.6	1.37	1.44	0.59	0.56	0.57
12.95	59.5	57.3	58.6	81.3	82.0	1.37	1.43	0.58	0.56	0.57
13.69	60.0	58.2	60.2	78.6	79.4	1.31	1.37	0.56	0.55	0.57
14.16	60.3	58.6	61.1	78.2	79.1	1.30	1.35	0.56	0.54	0.57
14.68	60.6	58.9	62.1	78.6	79.3	1.30	1.35	0.55	0.54	0.57
15.20	60.9	59.1	62.8	79.2	79.8	1.30	1.35	0.55	0.53	0.56
19.29	62.7	61.2	68.3	82.8	83.0	1.32	1.36	0.50	0.49	0.55
20.04	62.9	61.5	68.8	81.9	82.4	1.30	1.34	0.49	0.48	0.54
20.78	63.2	62.0	69.9	81.4	81.8	1.29	1.32	0.49	0.48	0.54
21.93	63.4	62.3	70.5	80.3	80.6	1.27	1.29	0.48	0.47	0.53
22.70	63.6	62.3	71.0	82.0	82.2	1.29	1.32	0.48	0.47	0.53
23.26	63.7	62.6	71.3	79.6	79.7	1.25	1.27	0.47	0.46	0.53
23.59	63.7	62.8	71.3	80.3	80.3	1.26	1.28	0.47	0.46	0.53
24.25	63.7	62.8	71.3	79.5	79.6	1.25	1.27	0.46	0.46	0.52
25.05	63.9	62.9	71.8	79.7	79.8	1.25	1.27	0.46	0.45	0.52
25.42	63.9	62.9	71.9	79.9	80.0	1.25	1.27	0.46	0.45	0.51
25.96	63.9	63.2	72.0	77.9	78.0	1.22	1.23	0.45	0.45	0.51
26.55	63.9	63.3	72.0	78.6	78.5	1.23	1.24	0.45	0.45	0.51
27.17	63.9	63.2	72.0	77.4	77.2	1.21	1.22	0.45	0.44	0.50
27.69	63.9	63.1	71.9	79.2	78.8	1.24	1.25	0.45	0.44	0.50
28.03	63.8	63.0	71.6	78.2	77.9	1.23	1.24	0.44	0.44	0.50
28.77	63.7	63.1	71.4	77.5	77.4	1.22	1.23	0.44	0.43	0.49
29.62	63.9	63.4	71.8	76.0	76.0	1.19	1.20	0.44	0.43	0.49
30.65	63.9	63.9	71.7	0.0	0.0	0.00	0.00	0.43	0.43	0.49

TEST NO.17
 CONSOLIDATION PRES.= 40.0

SHEAR STRAIN	PORE PRESSURE		
	CV, H, A CONSTANT	A CONSTANT CV, H VARY	K, H VARY
-0.00	0.0	0.0	0.0
0.04	3.2	3.2	0.5
0.13	5.8	5.9	0.8
0.18	6.7	6.9	0.9
0.25	7.4	7.8	1.0
0.35	7.8	8.4	1.4
0.46	7.8	8.6	1.3
0.57	7.7	8.7	1.5
0.73	7.0	8.2	1.6
0.93	5.8	7.1	1.8
1.12	4.5	5.8	2.1
1.42	2.7	3.7	2.0
1.85	1.3	1.9	2.2
2.61	0.8	1.1	2.3
3.40	0.6	0.8	2.4
3.87	0.8	0.9	2.5
4.29	0.9	1.0	2.5
4.77	0.7	0.9	2.5
5.25	0.7	0.9	2.5
8.07	0.4	0.5	2.3
8.72	0.7	0.8	2.3
9.34	1.1	1.2	2.4
10.50	0.9	1.0	2.2
11.22	0.9	1.0	2.2
11.91	0.8	0.9	2.2
12.38	0.7	0.8	2.1
12.95	0.9	1.0	2.1
13.69	0.9	1.0	1.8
14.16	0.9	0.9	1.7
14.68	0.9	0.9	1.8
15.20	0.7	0.8	1.8
19.29	0.1	0.1	1.5
20.04	0.2	0.2	1.4
20.78	0.5	0.4	1.2
21.93	0.3	0.2	1.1
22.70	0.3	0.3	1.3
23.26	0.2	0.2	1.1
23.59	0.2	0.1	0.9
24.25	0.1	0.0	1.0
25.05	0.2	0.2	1.0
25.42	0.2	0.2	1.0
25.96	0.1	0.1	0.7
26.55	0.1	0.0	0.7
27.17	0.0	0.0	0.7
27.69	-0.1	-0.1	0.7
28.03	-0.2	-0.2	0.8
28.77	-0.1	-0.1	0.6
29.62	0.1	0.1	0.5
30.65	0.0	0.0	0.0